UNIVERSITY *of the*
WESTERN CAPE

Some New Bimetallic Nickel and Palladium Complexes for Catalysis Applications

By

Shane Cedrick Van Wyk

A thesis submitted in partial fulfillment of the requirements for the degree of

Magister Scientiae in Chemistry

Faculty of Science

University of the Western Cape

Cape Town, South Africa

Supervisor: Assoc. Prof. Martin O. Onani

November 2015

DECLARATION

I declare that *Some New Bimetallic Nickel And Palladium Complexes For Catalysis Applications* is my own work, that it has not been submitted for any degree or examination in any other university, and that all the sources I have used or quoted have been indicated and acknowledged by complete references.

Shane Cedrick Van Wyk November 2015

Signature.....

DEDICATION

I would like to dedicate this thesis to my family for their unconditional love and support, especially my parents Annie Van Wyk and Frederick Van Wyk.

I would also like to dedicate this to the members of the Old Apostolic Church, especially the communities of Eastridge, Beacon Valley and Roodebloem for all the support, encouragement and prayers. Without those, I do not think I would make it this far.

ACKNOWLEDGEMENTS

I wish to acknowledge the contributions of my supervisor, Prof. Martin Onani for the academic and emotional support, your support is truly appreciated. I would also like to thank my supervisor while I was in Sweden, Prof. Ebbe Nordlander for the valuable advice and knowledge that you passed down to me during my stay and also during your visits to South Africa. I would also like to thank Prof. James Darkwa for the research advice given during the initial phase of my masters.

I also want to thank the organizations that funded me during my degree namely the National Research Foundation (NRF) and EUROSA.

I also want to show my appreciation to the Inorganic Chemistry group of Lund University. This is for all the chemistry knowledge, for helping me adapt to living in a foreign land as well as making me feel part of the team. I am eternally grateful for what you've done.

The chemistry department technical staff namely: Timothy Lesch; Ben de Wet; and Andile Mantyi for providing appropriate technical assistance when it was needed. I would also like to thank the mass-spectrometry technician of the University of Bologna; Mr Yunus Kippie of the School of Pharmacy (University of the Western Cape) for assisting with the TGA; Dr Masikini (University of the Western Cape) for assisting with the UV-Vis; Dr Edith Beukes (University of the Western Cape) for assisting with the NMR; lastly the group of Dr Stephen Ojwach (University of Kwazulu Natal) for carrying out the catalysis reactions.

Last, but definitely not least I would like to thank the Organometallics and Nanomaterials Research Group for all the support, advice and encouragement given throughout my postgraduate career. I would especially like to thank the following people: Paul Mushonga and Linda Ouma for helping me adapt to working in the research group during the initial

phase of my masters; Mduduzi Radebe, Garvin Allard, Kiplagat Ayabei and Asanda Busa for the advice you have given me and for making the lab environment more fun; Leandre Brandt for organizing functions to help keep the balance of the academic and social aspects of our group; lastly Leoni Swartz for the emotional support, encouraging me, keeping me focused and being like a sister to me. Having you guys around is like having a whole new family.

ABSTRACT

This thesis reports on the syntheses of new bimetallic iminopyridyl nickel(II) and palladium(II) complexes as catalyst precursors for ethylene oligomerization/polymerization. Tetrahydrophenyl-linked iminopyridyl ligands, pyridin-2-ylmethyl-{4-[(pyridin-2-ylmethylimino)-methyl]-benzylidene}-amine (**L1**) and (2-pyridin-2-yl-ethyl)-{4-[(2-pyridin-2-yl-ethylimino)-methyl]-benzylidene}-amine (**L2**) were prepared via condensation from terephthaldehyde and 2 molar equivalents of a primary pyridylamine. Alkyl-linked iminopyridyl ligands N,N'-bis-pyridin-2-ylmethylene-propane-1,3-diamine (**L3**), N,N'-bis-pyridin-2-ylmethylene-butane-1,4-diamine (**L4**) and N,N'-bis-pyridin-2-ylmethylene-pentane-1,5-diamine (**L5**) were prepared by condensation of 2 equivalents of 2-pyridinecarboxaldehyde and a primary diamine. The ligands were obtained as either red oils or orange solids.

These ligands were characterized using Fourier-transform infrared spectroscopy (FTIR), nuclear magnetic resonance spectroscopy (NMR), mass spectrometry (MS), elemental analysis (EA), ultraviolet-visible spectrophotometry (UV-Vis) and thermal gravimetric analysis (TGA) where applicable.

The tetrahydrophenyl-linked iminopyridyl ligands were subsequently used to prepare their corresponding homobimetallic palladium(II) and nickel(II) complexes. A 1:2 reaction of the ligands with $PdCl_2$(COD), $NiCl_2$(DME) and $NiBr_2$(DME) gave palladium(II) and nickel(II) complexes **C1**-**C6** in moderate to very good yields (58-94%). The palladium(II) complexes were found to be stable, but light-sensitive solids while the nickel(II) complexes were found to be stable, but light and air sensitive solids. These complexes were characterized using FTIR, NMR, EA, MS, UV-Vis and TGA.

These complexes were then tested for catalytic activity of ethylene oligomerization. It was found that complexes **C1** and **C5** were highly active when activated by the cocatalysts methylaluminoxane (MAO) as well as ethyl aluminium dichloride (EADC). It was found that EADC gave the highest activity so the remaining catalysts (**C3** and **C6**) were tested exclusively with EADC. All four complexes were active for ethylene oligomerization with yields of between 2.7-6.5 g, with **C5** providing the highest activity and **C1** the lowest. These catalysts were highly selective towards C_4 oligomers with percentages ranging from 71-81%. Optimization studies were then carried out with **C3** by varying the pressure and Al:Ni ratio.

PUBLICATION AND CONFERENCE CONTRIBUTIONS

1. Shane C. Van Wyk, Martin O. Onani, Ebbe Nordlander, Synthesis of Bimetallic Nickel and Palladium Complexes for Catalysis Applications, Young Chemists' Symposium, University of Cape Town, South-Africa, 23 Oct 2014, Poster presentation

2. Shane C. Van Wyk, Martin O. Onani, Ebbe Nordlander, Bimetallic Nickel and Palladium Complexes for Catalysis Applications, CATSA Annual Conference, St George Hotel, Pretoria, South- Africa. 9 - 12 Nov 2014, Poster presentation.

3. Shane C. Van Wyk, Martin O. Onani, Ebbe Nordlander, Bimetallic Nickel and Palladium Complexes for Catalysis Applications, CATSA Annual Conference, Arabella Hotel and Spa, Hermanus, South- Africa. 15 - 18 Nov 2015, Oral presentation.

4. Shane C. Van Wyk, Martin O. Onani, Ebbe Nordlander, Bimetallic Nickel and Palladium Complexes for Catalysis Applications, Chemical Papers, Accepted 2015, manuscript number 0221-15.

TABLE OF CONTENTS

Content	**Page**
Title Page	
Declaration	i
Dedication	ii
Acknowledgements	iii
Abstract	v
Publication and conference contributions	vi
Table of contents	vii
List of figures	xii
List of schemes	xv
List of tables	xvi
Abbreviations and symbols	xviii
CHAPTER 1	**1**
1. Literature Review	**1**
1.1 Introduction to Homogeneous Catalysis	1
1.2 Iminopyridines [N,N]-systems	4
1.3 Iminopyridyl Complexes	8
1.4 Ethylene Polymerization	18
1.5 Conclusions and Future Prospects	24

1.6 Aims and objectives of this study 27

1.7 References 28

CHAPTER 2 **38**

2. Experimental Section **38**

2.1 General Remarks 38

2.2 Instrumentation 39

2.3 Alkene Oligomerization 41

2.3.1 Ethylene Oligomerization 41

2.4 Synthesis of Iminopyridyl Ligands 42

2.4.1 Pyridin-2-ylmethyl-{4-[(pyridin-2-ylmethylimino)-methyl]-benzylidene}-amine (L1) 42

2.4.2 (2-Pyridin-2-yl-ethyl)-{4-[(2-pyridin-2-yl-ethylimino)-methyl]-benzylidene}-amine (L2) 42

2.4.3 N,N'-Bis-pyridin-2-ylmethylene-propane-1,3-diamine (L3) 43

2.4.4 N,N'-Bis-pyridin-2-ylmethylene-butane-1,4-diamine (L4) 43

2.4.5 N,N'-Bis-pyridin-2-ylmethylene-pentane-1,5-diamine (L5) 44

2.5 Synthesis of Iminopyridyl Complexes 44

2.5.1 Tetrachloro-[pyridin-2-ylmethyl-{4-[(pyridin-2-ylmethylimino)-methyl]- 44

benzylidene}-amine]dipalladium(II) (C1)

2.5.2 Tetrachloro-[(2-Pyridin-2-yl-ethyl)-{4-[(2-pyridin-2-yl-ethylimino)-methyl]-benzylidene}-amine]dipalladium(II) (C2) 45

2.5.3 Tetrachloro-[pyridin-2-ylmethyl-{4-[(pyridin-2-ylmethylimino)-methyl]-benzylidene}-amine]dinickel(II) (C3) 46

2.5.4 Tetrachloro-[(2-Pyridin-2-yl-ethyl)-{4-[(2-pyridin-2-yl-ethylimino)-methyl]-benzylidene}-amine]dinickel(II) (C4) 46

2.5.5 Tetrabromo-[pyridin-2-ylmethyl-{4-[(pyridin-2-ylmethylimino)-methyl]-benzylidene}-amine]dinickel(II) (C5) 47

2.5.6 Tetrabromo-[(2-Pyridin-2-yl-ethyl)-{4-[(2-pyridin-2-yl-ethylimino)-methyl]-benzylidene}-amine]dinickel(II) (C6) 47

2.6 References 48

CHAPTER 3 **49**

3. Results and Discussion **49**

3.1 Iminopyridyl Ligands 49

3.1.1 General 49

3.2.1 FTIR Studies of iminopyridyl ligands 52

3.2.2 ^{1}H NMR studies of iminopyridyl ligands 55

3.2.2.1 Tetrahydrophenyl-linked iminopyridines 55

3.2.2.2 Alkyl-linked iminopyridyl ligands 58

3.2.3 ^{13}C NMR studies of iminopyridyl ligands 60

3.2.3.1 Tetrahydrophenyl-linked iminopyridyl ligands 60

3.2.3.2 Alkyl-linked iminopyridyl ligands 62

3.2.4 UV-Vis studies of iminopyridyl ligands 65

3.2.5 TGA studies of iminopyridyl ligands 68

3.2.6 Mass spectroscopic analysis of iminopyridyl ligands 71

3.3 Iminopyridyl complexes 73

3.3.1 Bimetallic Iminopyridyl Pd(II) complexes 73

3.3.1.1 FTIR studies of bimetallic iminopyridyl Pd(II) complexes 74

3.3.1.2 ^{1}H and ^{13}C NMR studies of bimetallic Pd(II) complexes 76

3.3.1.3 UV-Vis Studies of bimetallic Pd(II) complexes 80

3.3.1.4 TGA Studies of bimetallic Pd(II) complexes 82

3.3.1.5 Mass spectroscopic analysis of iminopyridyl palladium(II) complexes 84

3.3.2 Bimetallic Iminopyridyl Ni(II) complexes 87

3.3.2.1 IR studies of Bimetallic Iminopyridyl Ni(II) complexes 88

3.3.2.2 UV-Vis Studies of bimetallic Ni(II) complexes 90

3.3.2.4 Mass spectroscopic analysis of iminopyridyl nickel(II) complexes 91

3.4 References 94

CHAPTER 4 **96**

4. Catalytic Application of the Iminopyridyl Complexes **96**

4.1 Ethylene Oligomerization/Polymerization Reactions 96

4.1.1 Background 96

4.1.2 Mechanism of ethylene oligomerization/polymerization reaction 99

4.2 Palladium(II) and Nickel(II) Iminopyridyl catalyzed ethylene oligomerization reactions 100

4.3 References 113

CHAPTER 5 **115**

5. Conclusion and recommendations **115**

5.1 Conclusion 115

5.2 Recommendations 117

APPENDIX **118**

LIST OF FIGURES

Figure		Page
1.1	Examples of Ziegler-Natta Catalysts ($TiCl_4$ derivatives and methylzirconocene)	2
1.2	General structure of α-diimine metal complexes (where M is a late transition metal and L_n is a ligand)	3
1.3	General structure of porphyrinphenanthroline heterobimetallic palladium complex (where M=Co, Ni, Zn, Cu or Mg and Ar is an aryl group)	17
3.1	IR spectrum for Pyridin-2-ylmethyl-{4-[(pyridin-2-ylmethylimino)-methyl]-benzylidene}-amine **L2**.	52
3.2	Numbered structure for tetrahydrophenyl-linked iminopyridyl ligand **L1** for chemical shifts assignment	55
3.3	^{1}H NMR Spectrum of (2-Pyridin-2-yl-ethyl)-{4-[(2-pyridin-2-yl-ethylimino)-methyl]-benzylidene}-amine **(L2)**	56
3.4	Alkyl-linked iminopyridyl ligands that will be discussed	58
3.5	^{1}H NMR of N,N'-bis-pyridin-2-ylmethylene-butane-1,4-diamine **(L4)**	58
3.6	^{13}C NMR of (2-pyridin-2-yl-ethyl)-{4-[(2-pyridin-2-yl-ethylimino)-methyl]-benzylidene}-amine **L2**	61
3.7	^{13}C NMR of N,N'-bis-pyridin-2-ylmethylene-butane-1,4-diamine **L4**	63
3.8	UV-Vis spectrum of (2-pyridin-2-yl-ethyl)-{4-[(2-pyridin-2-yl-ethylimino)-	65

methyl]-benzylidene}-amine **L2**

3.9 UV-Vis spectrum of N,N'-Bis-pyridin-2-ylmethylene-propane-1,3-diamine **(L3)** 66

3.10 TGA spectrum of Pyridin-2-ylmethyl-{4-[(pyridin-2-ylmethylimino)-methyl]-benzylidene}-amine (**L1**) 68

3.11 TGA spectrum of (2-pyridin-2-yl-ethyl)-{4-[(2-pyridin-2-yl-ethylimino)-methyl]-benzylidene}-amine (**L2**) 69

3.12 ESI-MS spectrum of Pyridin-2-ylmethyl-{4-[(pyridin-2-ylmethylimino)-methyl]-benzylidene}-amine (**L1**) 71

3.13 IR spectrum of complex **C2** 74

3.14 ^{1}H NMR spectrum of Tetrachloro-[pyridin-2-ylmethyl-{4-[(pyridin-2-ylmethylimino)-methyl]-benzylidene}-amine]dipalladium(II) (**C1**) 76

3.15 ^{13}C NMR spectrum of tetrachloro-[pyridin-2-ylmethyl-{4-[(pyridin-2-ylmethylimino)-methyl]-benzylidene}-amine]dipalladium(II) (**C1**) 78

3.16 UV-Vis Spectrum of tetrachloro-[(2-Pyridin-2-yl-ethyl)-{4-[(2-pyridin-2-yl-ethylimino)-methyl]-benzylidene}-amine]dipalladium(II) (**C2**) 80

3.17 TGA Spectrum of tetrachloro-[(2-Pyridin-2-yl-ethyl)-{4-[(2-pyridin-2-yl-ethylimino)-methyl]-benzylidene}-amine]dipalladium(II) (**C2**) 82

3.18 ESI-MS spectra of complex **C2** 85

3.19 IR spectrum of complex **C4** 88

3.20	UV-Vis Spectrum of tetrachloro-[(2-Pyridin-2-yl-ethyl)-{4-[(2-pyridin-2-yl-ethylimino)-methyl]-benzylidene}-amine]dinickel(II) (**C4**)	90
3.21	ESI-MS Spectra of **C6**	92
4.1	% distribution of processes of polyethylene for HDPE and LLDPE/LDPE	97
4.2	Bimetallic tetrahydrophenyl linked iminopyridyl Pd(II) and Ni(II) complexes	100
4.3	Activities of trial reactions involving **C1** and **C5** where EADC and MAO were used as cocatalysts	102
4.4	Oligomer selectivities of trial reactions involving **C1** and **C5** where EADC and MAO were used as cocatalysts	102
4.5	Bar graph of oligomerization activity when $EtAlCl_2$ (EADC) is used as the cocatalyst	103
4.6	GC-MS spectrum of the product formed using catalyst **5** at 30 °C and 20 bar for 1 h confirming the formation of octene.	105
4.7	Graph of oligomer selectivity for **C1**, **C3**, **C5** and **C6** when EADC is used	106
4.8	Catalytic activity of **C3** at various pressures	108
4.9	Oligomer selectivities resulting from **C3** at various pressures	109
4.10	Catalytic activity of **C3** at various Al:Ni ratios	111
4.11	Oligomer selectivities resulting from **C3** at various Al:Ni ratios	112

Scheme **LIST OF SCHEMES** Page

1.1	Synthesis of diamine precursor	6
1.2	Synthesis of diiminopyridyl ligand	6
1.3	Synthesis of diimine ligand	7
1.4	General scheme for synthesis of monometallic α-diimine nickel(II) complexes	8
1.5	General scheme for synthesis of bimetallic α-diimine nickel(II) complexes	12
1.6	General equation for ethylene oligomerization/polymerization (where n=1, 2, 3…)	18
1.7	Proposed mechanism for ethylene oligomerization/polymerization using a late transition metal catalyst	24
2.1	General equation for ethylene oligomerization	41
3.1	Condensation reaction of terephthaldehyde with corresponding primary amine.	50
3.2	Condensation reaction of 2-pyridinecarboxaldehyde and a primary diamine	52
3.3	Synthesis of tetrahydrophenyl-linked iminopyridyl palladium(II) complexes	73
3.4	Possible fragmentation pattern for **C2**	86
3.5	Synthesis of tetrahydrophenyl-linked iminopyridyl nickel(II) complexes	87
3.6	Possible fragmentation pattern of **C6**	93
4.1	Scheme for ethylene oligomerization reaction using nickel and palladium	97

bimetallic precatalysts

LIST OF TABLES

Table		Page
3.1	Summary of IR data and yields for ligands **L1-L5**	54
3.2	Summary of ^{1}H NMR data for ligands **L1-L2**	56
3.3	Summary of ^{1}H NMR data for ligand **L3-L5**	59
3.4	Summary of ^{13}C NMR data for ligands **L1-L2**	61
3.5	Summary of ^{13}C NMR data for ligands **L3-L5**	63
3.6	λ_{max} for ligands **L1** and **L2**	65
3.7	λ_{max} for ligands **L3-L5**	66
3.8	Summary of the ESI-MS data of ligands **L1** and **L2**	71
3.9	FTIR Data of complexes of **C1** and **C2**	74
3.10	^{1}H NMR data of complexes **C1** and **C2**	77
3.11	^{13}C NMR data of complexes **C1** and **C2**	78
3.12	Summary of UV-Vis data for ligands **C1** and **C2**	80
3.13	FTIR data of complexes **C3-C6**	88
3.14	Summary of UV-Vis Data for **C3** and **C4**	90
4.1	Main uses of polyethylene by type	98

4.2 Ethylene oligomerization data for complexes **C1, C3, C5** and **C6**[a] 101

4.3 Ethylene oligomerization selectivity data for complexes **C1, C3, C5** and **C6**[a] 105

4.4 Activity and oligomer selectivities for at various pressures[a] 108

4.5 Activity and oligomer selectivities for **C3** at various Al:Ni ratios[a] 110

ABBREVIATIONS AND SYMBOLS

°C	Degrees Celsius
$^{-}$OTf	Triflate
$(TBA)^{+}$	tetrabutylammonium
Ar	aryl group
C	Complex
CCD	Charged-coupled device
C-C	Carbon-carbon
cat.	Catalysts
COD	1,5-cyclooctadiene
d	Doublet
DCM	dichloromethane
DEAC	diethylaluminium chloride
DFT	density functional theory
DME	1,2-dimethoxyethane
DMF	N,N-dimethylformamide
DMSO	dimethyl sulfoxide
DNA	deoxyribonucleic acid

dt	Doublet of Triplets
EADC	ethyl aluminium dichloride
EASC	ethyl aluminium sesquichloride
EDG	electron donating groups
ESI-MS	electron spray ionization mass spectrometry
eq.	molar equivalents
EtOH	Ethanol
EWG	electron withdrawing group
Fig.	Figure
FTIR	Fourier transform infrared
GC	gas chromatography
h	Hour
H^+	Proton
HCl	hydrochloric acid
HDPE	high density polyethylene
*i*Pr	*iso*-propyl
KBr	Potassium bromide
kg	Kilogram

L	Ligand
LDPE	low density polyethylene
$LiAlH_4$	lithium aluminium hydride
LLDPE	linear low density polyethylene
L_n	General term for a ligand
M	late transition metal
m	Multiplet
MADC	methyl aluminium dichloride
MAO	Methylaluminoxane
Me	Methyl
MeOH	Methanol
$MgSO_4$	magnesium sulphate
MHz	Megahertz
min	Minute
mL	millilitre
mmol	Millimoles
mol	Mole
mp	melting point

n-BuOH	n-butanol
NaCl	sodium chloride
NaOH	Sodium hydroxide
NMR	nuclear magnetic resonance
p-TsOH	*para*-tosic acid
PDI	polymer dispersion index
PE	Polyethylene
Ph	Phenyl
PPh_3	triphenylphosphine
ppm	parts per million
q	Quartet
quin	Quintet
RT	Room temperature
s	Singlet
TBAB	tetra-*n*-butylammonium bromide
TGA	Thermal gravimetric analysis
TLS	turnover limiting step
TMS	tetramethylsilane

UV-Vis	Ultraviolet-visible spectroscopy
X	Halide
XRD	x-ray diffraction

Chapter 1

1.1 **Introduction to Homogeneous Catalysis**

Organometallic chemistry is the study of chemical compounds containing bonds between carbon and a metal [1]. An alternative definition could also include bonds between a metal and an element with a largely covalent character [1]. Numerous researches have been carried out on organometallic complexes. This is mainly due to their vast applications in catalysis [2-4] as well as biological studies [5-12]. Catalytic studies were first carried out for the early transition metals such as titanium in the form of heterogeneous catalysts [2, 13-14]. Later work emphasized the importance of late transition metals such as copper [3] and iron [4], but also nickel and palladium, especially in ethylene polymerization [15, 16 - 22]. Other applications for nickel and palladium complexes include magnetic susceptibility [12, 23-25] and electrochemical studies [12, 23, 26-28]. The successful application of these late transition metals in catalysis is due to their lower oxophilicity compared to the early transition metals, which also allows copolymerization of ethylene and polar monomers [29-30]. When a cocatalyst such as MAO (methylaluminoxane) was used in ethylene polymerization, α-olefins were obtained [15]. In mineral rich countries such as South Africa, catalytic transformations of carbon-carbon double bonds have been a very successful industry.

Further studies have shown that the homobimetallic complexes for both nickel and palladium have superior catalytic activity of ethylene polymerization than their mononuclear analogues [26, 31-36]. This was likely due to the cooperative effect of the two metals [31]. This is achieved because the two metal centres are brought into closer proximity to each other by using an appropriate ligand system. For nickel bimetallic complexes, there are many types of

ligand systems which have been used as backbones. Such systems include [N,N] (such as α-diimines, β-diimines or iminopyridyls), [N,O] (such as salicyldiaminito) [15, 37-39], [P,N] and [P,P] bidentate ligands [40-43]. For palladium bimetallic complexes, the tetradentate bis(dithiolene) and bis(phosphino)pyrazole ligand systems were found to be suitable for catalysis [36].

Olefin polymerization has been commercialized for over 60 years. The olefin polymerization has three major classes, namely: HDPE (high density polyethylene); LLDPE (linear low density polyethylene) and LDPE (low density polyethylene). HDPEs are linear, semi-crystalline ethylene polymers, LLDPEs are random copolymers of ethylene and α-olefins (e.g. 1-butene, 1-hexene or 1-octene) and LDPEs are branched ethylene homopolymers prepared in a high temperature and high pressure free-radical process [44].

The catalytic systems used for ethylene oligomerization/polymerization started with Ziegler-Natta catalysts. The homogeneous based catalysts involve the metallocenes (**Fig. 1.1**) [45] which are usually used in combination with a cocatalyst such as MAO while the heterogeneous based catalysts (**Fig. 1.1**) had titanium compounds and were used in conjunction with a cocatalyst, organoaluminium compounds e.g. triethylaluminium [46]. Of these two classes, the former is less dominant and catalyzes the formation of LLDPEs while the latter catalyzes the formation of HDPEs.

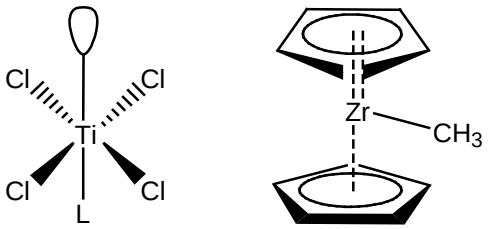

Figure 1.1: Examples of Ziegler-Natta Catalysts ($TiCl_4$ derivatives and methylzirconocene)

Recently a new family of catalysts has been brought to the fore. These are late transition metal complexes consisting of various nitrogen (**Fig. 1.2.**) and oxygen donor ligands [47]. The most successful of these were the α-diimines and iminopyridyls. These were used for various late transition metals such as iron, cobalt, nickel and palladium [48-49].

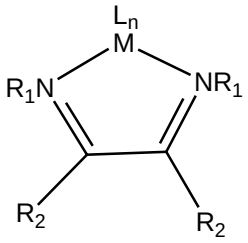

M = metal
L_n = ligand
R = alkyl group

Figure 1.2: General structure of α-diimine metal complexes

The following section will discuss the ligand systems individually

1.2 Iminopyridines [N,N Systems]

An iminopyridine is a class of ligand which is pyridine derivative with an imine sidearm appended to the 2, 3 or 4-position. The two nitrogen centres can bind metals in a bidentate fashion. They are best formed by the Schiff-base condensation reactions.

The Schiff bases are compounds with a functional group that contains a carbon-nitrogen double bond with the nitrogen atom connected to an aryl or alkyl group. These are usually formed via a condensation reaction of an aldehyde/ketone with a primary amine [50]. The use of Schiff base ligands have increased over the years and further research has been carried out to utilize their properties, especially when synthetic organometallic complexes are involved [49]. Much focus was placed on various ligands with multiple imine bonds due to chelating properties with transition metals. This was especially true for α-diimine and β-diimine ligands which are used in stabilizing nickel(II) and palladium(II) complexes [48].

In 2001, Simion *et al.* used a vastly different method for synthesizing imines. They repeatedly combined various carbonyl compounds with primary imines using water as the solvent and still obtained good yields for the various imines, diimines and macrocyclic diimines that were reported [51]. This opened a new chapter for a “greener” method for the synthesis of the Schiff bases that questioned the rationale of using the more expensive organic solvents when water would suffice.

Apart from catalysis, some of these ligands have been applied to the biological and electrochemical applications. Saedifar *et al.* showed that one can synthesize glycine derivatives of bipyridine ligands by simply reacting piperidine and morpholine with bromoacetic acid in the presence of sodium hydroxide [52]. The palladium complexes that

were synthesized from these ligands were then used for cytotoxic assays and DNA-binding studies [52]. Another example was reported by Shaban *et al.* where they showed how bis(imino)pyridyl ligands were synthesized with their subsequent copper(II) complexes and were used for oxidative catalysis as catecholase analogues [3].

Various electron donating and electron withdrawing groups were incorporated into the iminopyridyl ligands. One such example is a report by Kuwabara *et al.* where either a hydroxymethyl or an acrylate group was used as a pendant [53]. The coordination of these ligands to various metals such as cobalt, iron and nickel was studied [53]. It was found that when an acrylate was incorporated only cobalt interacted with it and this was a weak interaction [53]. It was concluded that this could be due to a 7-member metallacycle that formed, which is very unfavourable [53]. When a hydroxy group was used as a pendant, it coordinated to nickel in an N,N′,O-tridentate fashion [53] . Due to the Br ligand being dissociated by the aqua group in the presence of the hydroxyl, it was speculated that the hydroxy group coordinates more strongly to nickel than the Br group [53]. This is likely due to the chelate effect [53].

One can also synthesize disubstituted iminopyridyl ligands either by reacting a dialdehyde with a pyridylamine or a diamine with pyridinecarboxaldehyde. Two examples of the latter can be found in reports by Bahuleyan [31,36]. In both cases the ligands required two steps to be synthesized. The diamine was first synthesized using benzaldehyde and a substituted aniline using an earlier procedure that Bahuleyan *et al.* reported (as shown in **Scheme 1.1)** [36].

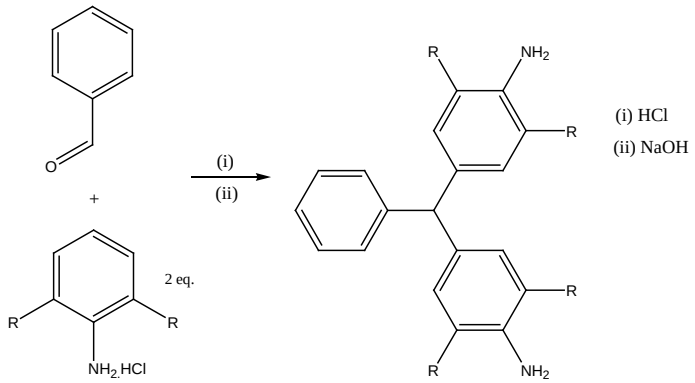

Scheme 1.1: Synthesis of diamine

The resulting diamine was dissolved in methanol and then reacted with 2-pyridine carboxaldehyde to form the disubstituted iminopyridyl ligand (as shown in **Scheme 1.2**) [36].

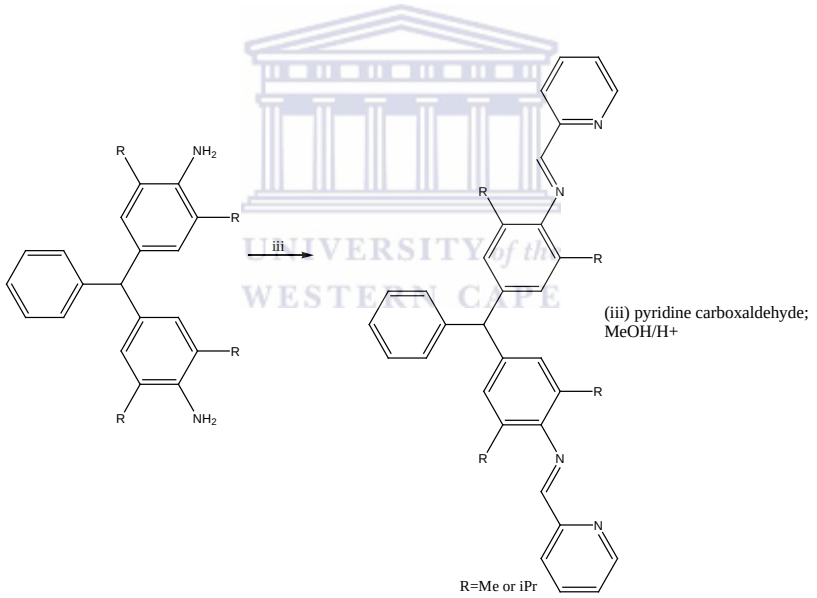

Scheme 1.2 Synthesis of diiminopyridyl ligand

Another example is explained by Pelletier *et al.* where both symmetrical and unsymmetrical tetramethylphenyl-linked iminopyridines were synthesized [35]. Synthesis for the symmetrical iminopyridine was carried out by reacting 1,4-$(NH_2)_2$-2,3,5,6-Me_4C_6 with two equivalents of either 2-pyridine carboxaldehyde in ethanol at room temperature or with 2-

acetylpyridine in n-butanol at 90 °C in the presence of a catalytic amount of formic acid (as shown in **Scheme 1.3**)

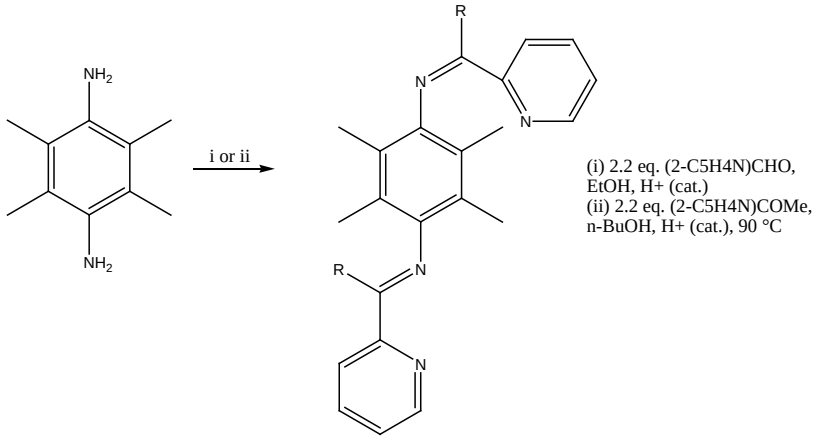

Scheme 1.3 Synthesis of diimine ligand

Other heterocycles can be incorporated into the iminopyridyl ligands as well. One example of this is a report by Motswainyana *et al.* [54]. They added a thiophene moiety to these ligands. What resulted were more stable ligands with very good yields (92-93%) [54].

Sometimes it is not the iminopyridines alone that can be useful as ligands. They can be reduced to pyridine-amines and the complexes that formed were still active as catalysts for ethylene polymerization as was reported by Zai *et al.* [19]. One contrast that these ligands have compared to their iminopyridyl counterparts as that when bulky substituents are incorporated at the 2 and 6-positions the activity decreases for their respective nickel complexes [19].

Iminopyridyl ligands have also been used as part of dendrimer chemistry. One example can be found in a report by Benito *et al.* [16]. In this case carbinosilane dendrimers were used and the resulting nickel complexes were found to be active for ethylene polymerization [16].

1.3 Iminopyridyl Complexes

Synthesizing α-diimine complexes usually require an α-diimine ligand and a metal precursor. For example a nickel based product is shown below in **Scheme 1.4**.

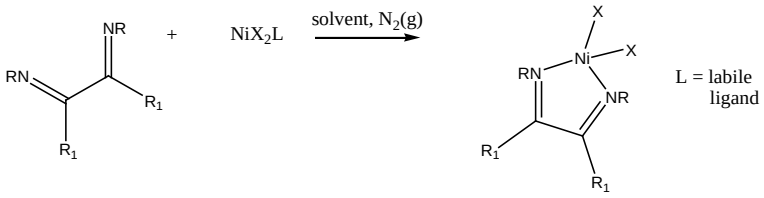

Scheme 1.4: General scheme for synthesis of monometallic α-diimine nickel(II) complexes

An example of similar types of complexes can be found in a procedure described by Bahuleyan *et al.*. This work also reported the steric and electronic effects of various ligands in catalysis [31].

Zai *et al.* carried out a study on how altering the substituents of pyridine-amine nickel catalyst precursors specifically affect ethylene polymerization [19]. They observed that varying the pyridine amine framework had a decisive effect on ethylene polymerization. Introduction of bulky aryls to the pyridine moiety on amine-pyridine nickel led to significantly lower activities and molecular weights of the polyethylenes. Increasing the steric hindrance of the amine moiety led to significantly lower activities and higher molecular weight for the polyethylenes. This also led to a narrower polydispersity. Introducing an electron donating group to the amine moiety led to the formation of higher molecular weight polymers with enhanced activity. Transition metal catalysts offer a means to control the structural variations in the molecular architecture of polyolefin materials [30, 48, 55-56].

A procedure reported by Gates *et al.* uses a ketone of acenaphthenequinone with various anilines in toluene as the solvent followed by an addition of a catalytic amount of sulphuric acid to generate the α-diimine [18]. These diimines were reacted with nickel(II) dibromide and the resulting mononuclear complexes were used for ethylene polymerization [18]. The α-diimine nickel(II) complexes could also be synthesized in a one-pot reaction as described by Maldanis *et al.* where the acenaphthoquinone was reacted with an excess of a trisubstituted aniline and refluxed in glacial acetic acid for 4 hours followed by an addition of the nickel(II) bromide in the same vessel and the reflux was allowed to continue for a further 16 hours to give the product [57]. In the very same report another route where the α-diimine was separately synthesized and later used in the reaction with the nickel precursor is reported. Again this was done by reacting acenaphthoquinone with the aniline in methanol with formic acid as a catalyst. This reaction was carried out for 16 hours and the complexation was carried out for 3 days, both at room temperature. The two-step reaction resulted in slightly better yields for the complex compared to the one-pot synthesis of the complexes chosen. The individual steps for the two-step reaction were also performed under less harsh conditions compared to the one-pot reaction. Based on the evidence, the two-step reaction was found to be superior. The resulting complexes were then evaluated for catalytic activity at which it polymerized ethylenes using different types of cocatalyst. Each of these catalytic complexes was found to be active, where the use of DEAC (diethylaluminium chloride) as a cocatalyst gave the highest activity.

A range of the pyridine-amine nickel complexes were synthesized reported on a variety of functional group substitutions. The catalytic activities of varying the bulk of the pyridine scaffold, bridge carbon and amine scaffold were studied systematically as well as the electronic effects of the amine scaffold [19]. It was determined that the alteration of the

pyridine-amine moiety does indeed have a conclusive effect on the polymerization activities. Bringing in bulky aryls on the pyridine scaffold on amine-pyridine led to a noticeable lowering in the activity and molecular mass of the polyethylene, while the opposite happens when the bulk of the bridge carbon increases [19]. In the case of an amine scaffold, elevating the steric hindrance resulted in a lower activity [19]. This also led to a large polyethylene with a narrower polymer distribution [19]. The introduction of EDGs (electron donating groups) led to the production of large polyethylenes with an increased catalytic activity.

These reactions need to be under inert conditions since it is well-known that Ni(II) can easily bind to water and form an octahedral complex [58]. Also oxidation could occur and a Ni(III) complex would form. For all of the previously mentioned products, it was found that nickel α-diimine complexes usually had poor solubility in the organic solvents. These complexes have also been found to be paramagnetic. Due to these factors, NMR spectroscopy is not always an immediate choice for characterization of nickel complexes.

The *N,N* chelating systems have also worked for palladium(II) complexes, mainly in the form of α- and β-diimines. The β-diimines have been studied more often as Heck, Suzuki and Hiyama coupling catalysts while the α-diimines have more often been studied as catalyst for ethylene oligomerization/polymerization among others [47].

An example of where β-diimine complexes are used for C-C cross coupling reactions can be found in a study carried out by Domin *et al.* [9]. Here new sterically demanding β-diimine ligands were used to synthesize nickel(II) and palladium(II) complexes. These complexes were then used as catalysts for Heck, Suzuki and Hiyama reactions [47].

In the above reaction the β-diimine ligands were synthesized using a four-step process. Firstly the diesters were synthesized by reacting diethyl malonate with various terminal dibromoalkanes with sodium ethoxylate being used as the base. The esters were then reduced

to alcohols using $LiAlH_4$. These alcohols would then undergo a Swern oxidation to form dialdehydes. These dialdehydes were then reacted with various amines in the presence of *p*-TsOH to form the β-diimines. The $PdCl_2(CH_3CN)$ was then treated with these ligands in boiling acetonitrile to form the β-diimine palladium(II) complexes as the final products [47].

In the catalytic testing of these complexes, for the Suzuki reactions various aryl halides were coupled to arylboronic acids. In the Heck reactions, these halides were coupled to methyl acrylate, while for the Hiyama reactions, they were coupled to phenyltrimethoxysilane [47].

Feldman *et al.* synthesized above similar complexes and then compared their catalytic activity to those of their previously reported α-diimine analogues. It was found that the β-diimine palladium(II) complexes indeed had lower catalytic activity than their α-diimine counterparts [17].

The procedure for synthesizing monometallic palladium(II) complexes are similar to the nickel analogue, except the metal precursor used is $PdCl_2$(COD) giving the product with a metal centre that is square planar. It was also more soluble in organic solvents than the nickel analogues. These complexes are also diamagnetic, so the NMR spectroscopy was found to be a suitable characterization technique in this case. Examples of these types of complexes were studied by Pascu *et al.* [59], Motswainyana *et al.* [60] and Pan *et al.* [61]. Whereas Pascu delved mainly into the synthetic procedures for synthesizing α-diimine nickel(II) and palladium(II) complexes with chlorinated backbones, Motswainyana *et al.* studied how these complexes could be used for Heck and Suzuki coupling [59-60].

Pan *et al.* studied how these complexes could be used as catalysts for copolymerization of ethylene with functionalized olefins [61]. There have also been many reviews written about these complexes, the most notable being one written by Ittel *et al.* [48].

A bimetallic complex is a metal complex consisting of two metal centres. A typical example would be a complex consisting of two nickel centres where each metal is bound to a bidentate [N,N] system. These bimetallic nickel complexes are synthesized using the same procedure as the monometallic complex, except two equivalents of nickel precursor with one equivalent of disubstituted α-diimine ligand are used [31]. The product is usually a dinuclear nickel(II) complex with a tetrahedral metal centre and poor solubility in the organic solvents. This also leads to the complex being paramagnetic hence solution NMR (nuclear magnetic resonance) would not be a suitable characterization technique. The XRD (x-ray diffraction) has also shown a decrease in the bond length between the metal and the nitrogen donors in comparison to the monometallic analogue [31]. This has been attributed to the cooperative effect between the metal centres. These types of complexes usually have the following general scheme as shown in Scheme 1.5.

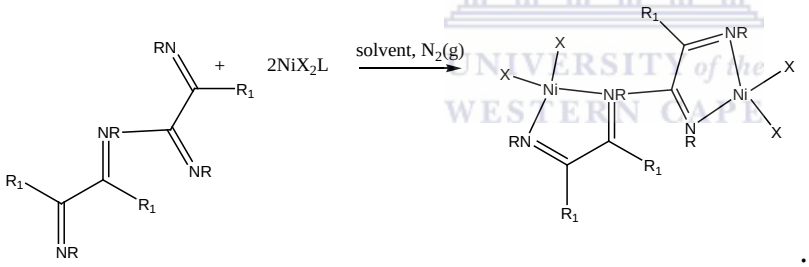

Scheme 1.5: General scheme for synthesis of bimetallic α-diimine nickel(II) complexes

Caris *et al.* reported on the synthesis and structural characterization of a series of mono- and bimetallic nickel bromide complexes bearing azolate-imine ligands [26]. This was carried out to determine what effect the ligands would have on coordination and ultimately ethylene polymerization. As far as the crystal structure was concerned, the most noticeable feature of this structure is an unexpected bimetallic, non-centrosymmetric ligand arrangement around the two nickel centres.

Bahuleyan *et al.* investigated the polymerization and oligomerization of an ethylene gas using a collection of iminopyridyl Ni(II) bimetallic catalysts. The complexes were modified electronically as well as in their steric bulk to optimize their catalytic activity. The binuclear early transition metal showed very few characteristics of the cooperative effect other than much lower polymerization activities and broadened polymer distributions [31]. Most recently, a range of sterically structured complexes of dinuclear nickel have been used in ethylene polymerization studies [62-64]. The intent was to force the late metal centres closer to each other, spatially restricted M_2 centres on bulky aryl-bridged pyridyl-imine partitioned ligands have been studied for ethylene oligomerization, yielding small oligomers with moderate activity when combined with cocatalyst MAO [65].

Neutral iminopyridyl ligands which can be modified electronically and sterically were targeted as possible supports for homobimetallic nickel(II) complexes.

Pelletier *et al.* reported the synthesis and structure of a series of symmetrical and asymmetrical bimetallic nickel complexes having aryl-linked iminopyridines. Recently investigations have been conducted within the bidentate *N,N*-chelating ligand frame, including alteration in the steric/electronic features found in the *N*-aryl group, the imino-carbon substituent and the pyridyl substituents and their influence on the catalytic activity [35]. In contrast, bringing in two pyridyl-imine binding modes into a binucleating ligand has received much lower recognition [65]. For example bimetallic nickel catalysts supported by methylene-linked pyridylimine was recently reported to exhibit high activities [66]. The rationale behind that was to bring the nickel centres closer together using aryl-linked pyridylimines [67], and particularly the bulkier tetramethylphenyl-linked derivative [68]. There was also an interest in the probing of the effect of how slight changes to two pyridyl-imine binding domains have on catalytic activity. Specifically, the nature of the two imino-

carbon substituents was systematically altered to bring in symmetrical aldimine-aldimine and ketimine-ketimine combinations as well as the asymmetrical analogue.

Tetramethylphenyl-linked iminopyridines have been reported as supports for the nickel central metal which are the active centres for the polymerization process. The complexes comprising the combinations of aldimine/aldimine, ketimine/ketimine and aldimine/ketimine when reacted with the co-catalyst, MAO are efficient for ethylene polymerization yielding preferable low molecular weight polyethylene polymer.

There are few literature articles available on the syntheses of heterobimetallic nickel(II) complexes, let alone their catalytic applications. Roth *et al.* have successfully synthesized a complex consisting of a nickel(II) and zinc(II) metal centre. This was achieved by synthesizing benzoic acid[1-(3-){[2-(bispyridin-2-ylmethylamino)ethylimino]methyl}-2-hydroxy-5-methylphenyl)methylidene]hydrazide (H_2bpampbh) as the ligand. This ligand consists of a planar tridentate [ONO] and a pentadentate [ON_4] compartment which bind to the zinc(II) and nickel(II) centre respectively. This complex was synthesized in good yield(71%). Their overall objective was to use these complexes for biological applications such as testing their reactivity with superoxide radicals [69].

Research for these bimetallic palladium(II) complexes have not been as well-explored as that for bimetallic α-diimine nickel(II) complexes, but the procedure for synthesizing the palladium complexes should be the same as for the bimetallic nickel analogue. So far the only catalytic applications successfully studied were terminal olefin epoxidation [70], Suzuki-Miyaura reactions [71], Mizoroki-Heck reactions and norbornene polymerization [72]. There were also other approaches to the synthesis and applications these bimetallic complexes which will be described in greater detail later.

However one notable feature from the limited literature available was evidence of the cooperative effect being cited. This was reported by Döring *et al.* who used the NCN pincer ligands [73]. The phenomenon was evidenced by a decrease in the bond length between the metal centres and the nitrogen donors as compared to the monometallic analogue. These complexes were also found to be soluble in organic solvents and have metal centres with square planar geometry. They were also found to be diamagnetic thus making them suitable for the NMR characterization technique.

As far as synthesis is concerned, there will be two approaches that will be discussed in detail. One of them was discovered by Pop *et al.* and the other by Taher *et al.*. Pop *et al.'s* approach consists of combining a bis(dithiolene) with a palladium(II) precursor consisting of triphenylphosphines to increase lability. Yields were very low for these bimetallic complexes(5%) [36]. Taher *et al.* described the synthesis of rigid-rod structured homobimetallic palladium complex in which the transition metals were linked by a π-conjugated organic unit. The first step was to perform an oxidative addition of $Pd(PPh_3)_4$ to diiodobenzene, followed by incorporating $^{-}$OTf (triflate) ions via AgOTf to substitute the iodine that was bonded to the palladium. The weakly bound triflate was then substituted with a stronger base such as a dicyano π-conjugated organic species. In this communication two products formed, a divalent bimetallic palladium(II) cationic complexes where the metals were bridged by two iodines and the other was bridged by the π-conjugated organic species. The yields for these complexes were still low but still much higher than the bis(dithiolene) approach [74].

Although there is not much literature on the catalytic applications of bimetallic palladium complexes, the work done still shows some promise due to the variety of applications studied so far. One example of this is where Hamed *et al.* use chiral bimetallic palladium(II) complexes to catalytically oxidize ketones to form asymmetric α-hydroxyketones [75].

Netalkar *et al.* successfully used bimetallic palladium(II) complexes to catalytically epoxidize 1-octene as well as styrene. In this work, conversion was much better for 1-octene than styrene [70].

Of the four complexes that were synthesized by Sachse *et al.*, all of them were catalytically active producing polynorbornene within one minute. One of these complexes was chosen to optimize the reaction conditions of polymerization [72].

There was also work done on the synthesis as well as the catalytic applications of heterobimetallic palladium(II) complexes. Firstly, Rivera *et al.* designed syntheses of four complexes consisting of a palladium(II) and platinum(II) metal centre. Both metals were bound to a 1,2-bis(diphenylphosphino)ethane (dppe) moiety and were connected with two fluorobenzenethiolate bridges. These complexes were synthesized in NMR tubes without further isolation. As a result, a mixture of three complexes was present namely: the homobimetallic palladium(II) and platinum(II) analogues as well as the intended heterobimetallic complex [76].

In another report by Lin *et al.*, various heterobimetallic palladium(II) complexes were synthesized using porphyrinphenanthroline and then studied for catalytic activity of Mizoroki-Heck coupling reactions.

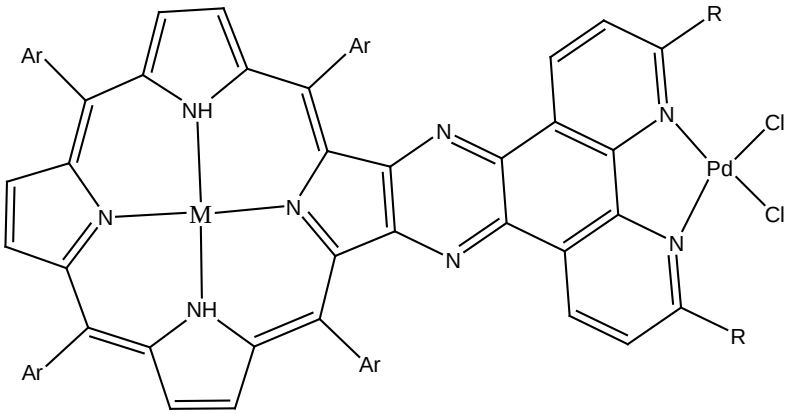

Figure 1.3: General structure of porphyrinphenanthroline heterobimetallic palladium complex (where M=Co, Ni, Zn, Cu or Mg and Ar is an aryl group)

The porphyrinphenanthroline ligand consists of tetradentate [N,N,N,N] system and a bidentate [N,N] system which were chelated to the other metal(Co, Ni, Zn, Cu or Mg in this case) and Pd respectively. Firstly the other metal was added to porphyrin ring to form a monometallic complex, then the palladium(II) was added to the [N,N] system. These were tested for catalytic activity of Mizoroki-Heck coupling reactions using iodobenzene and butyl acrylate as substrates. After optimizing the reaction conditions it was found that the Pd/Zn complex was the most active. The Pd/Ni, Pd/Cu and Pd/Mg complexes had very similar activities while the Pd/Co complex was inactive [77].

1.4 Ethylene Polymerization

Ethylene oligomerization/polymerization can be defined by the following equation.

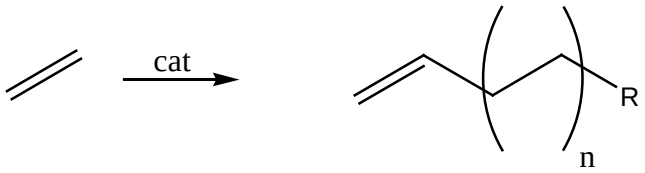

Scheme 1.6: General equation for ethylene oligomerization/polymerization (where n=1, 2, 3…)

The research area of ethylene polymerization has evolved over the last 60 years. It started with the heterogeneous Ziegler-Natta catalysts [78-80]. Then metallocenes that were used consisted of group IVB, VB and VIB transition metal atoms [48]. This was lastly followed by the α-diimine complexes which used the group VIII, IX, IB and IIB transition metals [81-84]. The initial work on these complexes was reviewed by Ittel *et al.* [48]. It was found that the most effective of the late transition metals are nickel and palladium [48].

As far as nickel is concerned, various donor systems such as N,N [26, 85] or N,O [86] can be used. It started with the monometallic system [87, 88], then moved on to a bimetallic system [31, 33]. An example of a bimetallic nickel being used was that used by Zhang *et al.*, when trimethyl phenyl linked salicylaldimine ligands were used [49]. The electronic effects were studied. When a *tert*-butyl group was incorporated on the side rings, the catalytic activity was 3.7 x 10^4 PE mol^{-1} Ni h^{-1}, but when a more electron withdrawing phenyl group was incorporated the activity increased to 1.1 x 10^5 PE mol^{-1} Ni h^{-1} which was consistent with the electronic effect of mononuclear Grubbs catalysts [17, 37, 89].

Caris *et al.* reported on the use of mono- and bimetallic nickel azolate-imine complexes as catalysts for ethylene polymerization. Synthetic control and tailoring of bulk polyolefin properties is a major focus of academic and industrial research groups. Advance in the design

of single site catalysts provided many options for combining ligands with their respective metal, therefore increasing the number of catalysts available for ethylene polymerization [90]. General trends have emerged in the design of catalyst structure, which allows for the production of a specific polymer configuration, bulk properties as well as catalyst design. Aspects that one would look at when it comes to designing a catalyst are namely: the steric bulk of the catalyst as this would affect how linear or branched the polyethylene is; electronic effects of the catalyst which is likely to affect the activity of polymerization.

Catalyst systems containing one active site have had a major influence on the commercial processes that produce commodities [30, 48, 91]. Examples of these vary from the early transition metals such as molybdenum [92] and titanium [93-95], to the group IX-XII metals such as nickel [56] and palladium [55]. This is based largely on their lower oxophilicity and the ease with which large ligands and catalysts can be synthesized. One could prepare polyolefinic materials under gentle conditions, but also novel compounds with well-defined chemical properties, including a plethora of possible chemical substitutions [51, 96-101]. These systems are built on catalytic oligomerization processes, in which nickel or palladium centres chelated by P,N or P,P are used [40-42].

The sterics and structure of the ligands could alter the PDI (polymer dispersion index) to afford heavier polymers. In the case of N,N or N,O coordination modes [38-39, 102], the sterics of the aromatic substituents on the imine or imide and carboxamide nitrogens would affect the donors it would bind to (i.e., N,N versus N,O) [38, 103-104], the reaction rate and the propagation and termination ratio, allowing access to a vast collection of novel compounds. A lot of work has been carried out on studying the co-activators. Lewis acids can be applied to activate the metal centre upon complexation to a basic functionality on the

ligand moiety at a site that is away from the metal centre [26]. This places the Lewis acid away from the site of the monomer insertion and removes the complications that usually occur with using aluminoxanes in which the anion would have needed to be removed for monomer insertion to take place [105]. The bidentate ligand scaffolds which have an additional peripheral heteroaromatic substituent have been discussed, particularly the *N*-heteroaryl 1,2-diimine [106]. This type of ligand is reported to facilely coordinate to the appropriate transition metal halide but the impact of the heteroaromatic substituent on the reaction rate and polymers properties were not discussed.

The molecular masses of the polymers drop as polymerization temperatures rise. The mononuclear complex gives a product with branching. An explanation for this is that the catalyst system has undergone prolonged chainwalking with β-hydride transfer occurring afterwards [48]. The highly branched structure and relatively low molecular mass of the polymers are in agreement with the previous work on nickel transition metal ethene polymerization catalysts [107]. The complex with the less crowded nickel centre has a higher polymerization activity and generates low molecular weight materials. The resulting materials are waxes, all of which are oligomers. This is in agreement with the presence of only one active metal site. To corroborate this point, the complex was shown to be effective in the oligomerization of higher alkenes to high molecular masses with narrow polymer distributions.

Netalkar *et al.* used bis-α-diimine ligands when synthesizing nickel bimetallic complexes. These complexes were sterically tuned in the *ortho* position and their activities were studied. The alkyl groups that were used were methyl, ethyl and *iso*-propyl. The activities were 662.2 kg-oligomer mol-Ni^{-1} bar^{-1} h^{-1}, 889.6 kg-oligomer mol-Ni^{-1} bar^{-1} h^{-1} and 1123.4 kg-oligomer mol-Ni^{-1} bar^{-1} h^{-1} respectively which indicates that an increase in steric bulk increases the activity of oligomerization. It was mainly oligomers that formed with the vast majority of

them consisting of 4 carbons. This is consistent with nickel alkyls being the active centre where fast β-hydrogen elimination is likely to occur [108].

Kong *et al.* used methylene bridged mono- and bimetallic nickel complexes where effects of the various cocatalysts were studied. These complexes were also sterically tuned. During optimization it was found that Et_2AlCl (diethyl aluminium chloride) was most effective in a 500:1 Al/Ni ratio with activities in the range of 5.42-7.29 x 10^6 PE (mol Ni)$^{-1}$ h^{-1} for the bimetallic compared to the lower activity range of 3.85-5.43 x 10^6 PE (mol Ni)$^{-1}$ h^{-1} for their respective monometallic analogues. It was determined that catalytic activities could be enhanced by using less bulky *ortho* substituents or by having an additional *para*-methyl substituent present. There was also a higher molecular weight and broader PDI for the bimetallic complexes compared to their monometallic analogues which suggests a positive synergistic effect under these conditions. When MAO was used as the cocatalyst it was most effective in a 2000:1 Al/Ni ratio with activities in the range of 9.07-15.99 x 10^6 PE (mol Ni)$^{-1}$ h^{-1} for the bimetallic complex which was more than double the activity of their monometallic counterparts which was in a range of 3.84-7.15 x 10^6 PE (mol Ni)$^{-1}$ h^{-1}. There was also a higher molecular weight and broader PDI for the bimetallic complexes under these conditions. This was consistent with the notion that bimetallic complex pre-catalysts promote chain propagation which resulted in a higher molecular weight [109].

Bahuleyan *et al.* used iminopyridyl bimetallic nickel complexes as catalysts for ethylene polymerization. Again the steric, electronic, cocatalytic, temperature and cooperative effects were studied. The steric effects were studied by varying the alkyl substituent *ortho* to the pyridine ring and it was found that the catalytic activity decreased with increasing steric bulk with activities as high as 17.18 x 10^5 g-product/(mol-Ni h bar) then decreasing to 1.68 x 10^5 g-product/(mol-Ni h bar) [31]. There was no clear explanation for this but a possible explanation given by the researchers was that severe interference from the protruding alkyl

group obstructs one of the equatorial coordination sites which could be the cause of the lower catalytic activity [110]. When the electronic effects were studied, it was found that having an EDG as a substituent resulted in a higher activity than the EWG. When the cocatalytic effects were studied, first the type of cocatalyst was varied namely EASC, MAO and MADC (methylaluminium dichloride), this was followed by optimizing the reaction conditions. EASC gave the highest activity (17.18 x 10^5 g-product/(mol-Ni h bar)), followed by MAO (2.24 x 10^5 g-product/(mol-Ni h bar)) and lastly MADC (0.82 x 10^5 g-product/(mol-Ni h bar)). The activity for EASC was further increased to 24.5 x 10^5 g-product/(mol-Ni h bar) when a 500:1 Al/Ni ratio was used. There was also a lower selectivity towards the 4-carbon oligomers from 91.6% (250:1 Al/Ni ratio) to 87.5%. The optimum temperature was found to be 30 °C [31]. To see what possible cooperative effect there is, the activity was studied for the monometallic analogue as well using a known procedure [109, 111]. The activity was found to be 6.13 x 10^5 g-product/(mol-Ni h bar) and C_{12} was the major oligomer fraction. Compared to the monometallic system, there was a high molecular weight and a broad molecular weight distribution which can be attributed to the cooperative effect [31].

All the electronically and sterically modulated catalysts showed significant catalytic activity for ethylene oligomerization/polymerization with various cocatalysts. All catalysts showed good selectivity for C_4, between 72-91% and small amounts of PE (polyethylene) of approximately 1-10%. EASC was the best cocatalyst. The molecular weight of the resulting PE was increased compared to that of the monometallic analogue due to the tandem effect of the iminopyridyl bimetallic nickel system.

Pelletier *et al.* studied the effects of using symmetrical and unsymmetrical bimetallic complexes where ketimine/ketimine, aldimine/aldimine or ketimine/aldimine systems were used as the ligands. The activities fell in a similar range with the ketimine/ketimine system the highest being at 409 g/mmol^{-1} h^{-1} bar^{-1} and the oligomer to polymer ratio ranging from 4:1

for the ketimine/ketimine to 1:4 for the aldimine/aldimine system. All of these systems produced low molecular weight polymers with broad molecular weight distributions. The aldimine/aldimine systems produced the lowest molecular weight polymers and the mixed ketimine/aldimine system afforded the broadest molecular distribution [35].

There was also a study carried out on heterobimetallic nickel and cobalt complexes using an N,N,N,N,N-system. The activities were tested using the heterobimetallic system and comparing it to a mixture of the corresponding monometallic nickel and cobalt complexes as well as comparing it to the sum of the corresponding monometallic complex activities. The mixture resulted in the highest activity while the heterobimetallic complex resulted in the lowest activity [112].

Although there is no literature available on bimetallic palladium catalysts, there are some useful articles on N,N palladium complexes. One example of this is a work by Mkoyi *et al.* They used (pyrazol-1-yl)carbonyl palladium complexes as ethylene polymerization catalysts. Four of the complexes have two phenyl rings with various alkoxy substituents *para* to the carbonyl substituents, two of them have two thiophenyl and another two have two furanyl rings. Of the complexes with the phenyl rings, two of them were active while the other two with the bulkier alkoxy substituents were inactive. The complexes with the thiophenyl and furanyl rings were all active. The activities were generally moderate ranging between 130 and 471 kg mol^{-1} h^{-1}. This was attributed to the higher migratory insertion barriers of the coordinated ethylene [113].

There were also attempts to incorporate dendritic wedges into the complexes. It was found that the complexes were active but only yielded oligomers, and only a small amount at that. The only oligomers that could be obtained were the involatile ones (some C_{10}, C_{12}, all C_{14}+). It was found that the dendritic wedges do not sterically interfere with the cationic metal

centre. It was then suggested that the palladium complexes could be used as a model for the more active (yet more difficult to characterize) nickel analogues [114].

Motswainyana *et al.* used hemi-labile pyridyl-imine palladium complexes where thiophenyls and furanyls were also incorporated. Three of the complexes were tested for catalytic activity with only negligible yields. After carrying out DFT (density functional theory) calculations, it was determined that it is possible that the poor activities could be due to the difficulty of ethylene in displacing the coordinated furan or thiophene groups [54].

In a review written by Ittel *et al.* ethylene polymerization follows this mechanism where TLS is the "turnover limiting step" and M is a late transition metal [48].

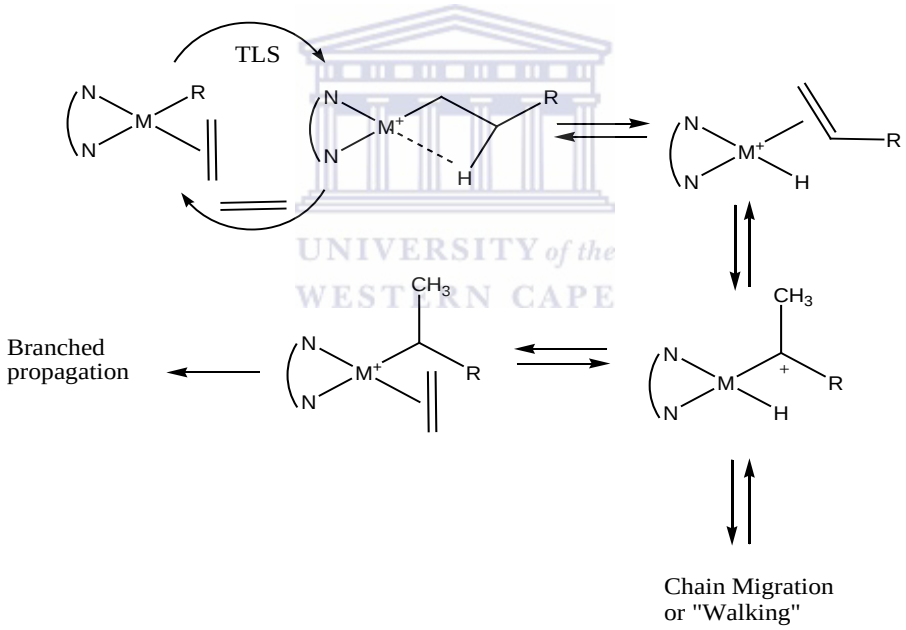

Scheme 1.7: Proposed mechanism for ethylene oligomerization/polymerization using a late transition metal catalyst [48]

1.5 Conclusions and Future Prospects

There is no question that heterogeneous catalysis is the most dominant form of catalysis at the moment, but homogeneous catalysis has been very popular for a very long time and presents a very strong alternative. The applications of diimine complexes have grown over time, especially the iminopyridyls. The ligands were found to be relatively simple to synthesize and characterize. The late transition metals used, especially nickel and palladium were found to coordinate easily, but there are some challenges when it comes to characterizing the nickel complexes due to their paramagnetism and lack of solubility in organic solvents. One way to overcome this issue in the future is to incorporate an anion that can be easily removed such as a triflate or one could bring in bulkier ligands and attach it to the aromatic rings thus forcing a square planar geometry at the metal centre which would lead to a diamagnetic complex.

One area that has not been fully explored is the possibility of using two metals instead of one which would then bring in the cooperative effect. Based on the evidence in earlier papers, this is a worthwhile possibility, especially with the nickel complexes. There was also not much work done on the bimetallic palladium complexes, there is much potential with this metal too, it definitely needs to be explored further, especially in catalysis.

These bimetallic complexes can have many uses in homogeneous catalysis. In Suzuki and Heck coupling, there has been much success with palladium, mono- and bimetallic, not so much with nickel yet, mainly due to not enough work being done on it as yet, but it is improving. In ethylene polymerization, there has been more success with bimetallic nickel complexes than with palladium. In future more research needs to be done on using bimetallic palladium complexes for ethylene polymerization. In addition to being measured for its own

activity, it can also be used as a model for how the nickel complexes will behave (due to nickel complexes being difficult to characterize).

1.6 Aims and objectives of this study

A number of iminopyridyl nickel and palladium complexes based on iminopyridyl ligands were synthesized and used in catalysis of ethylene oligomerization/polymerization, but they were mainly on monometallic complexes [54]. The aim of this study is to synthesize bimetallic iminopyridyl nickel and palladium complexes and test their potential as catalysts for ethylene oligomerization.

The objectives of this study were as follows

- To prepare bifunctional iminopyridyl ligands with either tetrahydrophenyl or alkyl linkers via Schiff base condensation of an appropriate aldehyde and a range of primary amines or diamines.
- To react these ligands with the appropriate nickel or palladium salt to obtain the desired bimetallic complexes
- To characterize the complexes using Fourier transform infrared (FTIR) spectroscopy, nuclear magnetic resonance (NMR) spectroscopy, ultraviolet-visible (UV-Vis) spectrophotometry, thermogravimetric analysis (TGA), electron spray ionization mass spectrometry (ESI-MS) and elemental analysis
- To evaluate these complexes as catalysts for ethylene oligomerization

The remaining chapters report on: the preparation of the ligands and complexes, as well as instrumental information (Chapter 2); synthesis and characterization results (Chapter 3); catalysis results (Chapter 4) as well as the conclusions and recommendations for future research on this topic (Chapter 5).

1.7 References

[1] Crabtree, R. H., *The Organometallic Chemistry of the Transition Metals*, Wiley, New Jersey, 4th edn, 2005, 560

[2] Suttil, J.A., McGuiness, D.S., Gardiner, M.G., Evans, S.J., *Dalton Trans.*, 2013, **42**, 4185 - 4196

[3] Shaban, S., Ramadan, A. M., Van Eldik, R., *J. Coord. Chem.*, 2012, **65**, 2415 - 2431

[4] Small, B.L., Rios, R., Fernandez, E.R., Gerlach, D.L., Halfen, J.A., Carney, M.J., *Organometallics*, 2010, **29**, 6723 - 6731

[5] Shi, D.-H., Cao, Z.-L., Liu, W.-W., Xu, R.-B., Zhang, N., Gao, L.-L., Zhang, Q., *Synth. React. Inorg. Met.-Org. Chem.*, 2012. **42**, 1128 - 1131.

[6] Guha, A., Banu, K.S., Das, S., Chattopadhyay, T., Sanyal, R., Zangrando, E., Das, D., *Polyhedron*, 2013, **52**, 669 - 678

[7] Akita, M., Fujisawa, K., Hikichi, S., Moro-Oka, Y., *Res. Chem. Intermed.*, 1998, **24**, 291 - 307

[8] Green, K.N., Jeffrey, S.P., Reibenspies, J.H., Darensburg, M.Y., *J. Am. Chem. Soc.*, 2006, **128**, 6493 - 6498

[9] Surati, K., *Spectrochimica Acta Part A*, 2011, **79**, 272 - 277

[10] Durg, V., Patel, N., Shivaprasad, K.H., *Int. J. Pharm. Bio. Sci.*, 2011, **2**, 256 - 260

[11] Ghosh, M., Fleck, M., Mahanti, B., Ghosh, A., Pilet, G., Bandyopadhyay, D., *J. Coord. Chem.*, 2012, **65**, 3884 - 3894

[12] Biswas, C., Zhu M., Lu, L., Kaity, S., Das, M., Samanta, A., Naskar, J.P., *Polyhedron*, 2013, **56**, 211 – 220.

[13] Adam, W., Corma, A., Garcia, H., Weichold, O., *J. Catal.*, 2000, **196**, 339 - 344

[14] Mitayake, T., Mizunuma, K., Kakugo, M., *Macromol. Symp.*, 1993, **66**, 203 - 214

[15] Sun, W. -H., Tang, X., Gao, T., Wu, B., Zhang, W., Ma, H., *Organometallics*, 2004, **23**, 5037 - 5047

[16] Benito, J.M., de Jesus, E., de la Mata, F.J., Flores, J.C., Gomez, R., Gómez-Sal, P., *Organometallics*, 2006, **25**, 3876 - 3887

[17] Feldman, J., McLain, S.J., Parthasarathy, A., Marshall, W.J., Calabrese, J.C., Arthur, S. D., *Organometallics*, 1997, **16**, 1514 - 1518

[18] Gates, D.P., Svejda, S.A., Onate, E., Killian, C.M., Johnson, L.K, White, P.S., Brookhart M., *Macromolecules*, 2000, **33**, 2320 - 2334

[19] Zai, S., Gao, H., Huang, Z., Hu H., Wu, H., Wu, Q., *ACS Catal.*, 2012, **2**, 433 - 440

[20] Tang, X., Sun, W.-H., Gao, T., Hou, J., Chen, J., Chen, W., *J. Organomet. Chem.*, 2005, **690**, 1570 - 1580

[21] Zhang, S., Sun, W.-H., Kang, X., Vystorop I., Yi, J., *J. Organomet. Chem.*, 2007, **692**, 5307 - 5316

[22] Smit, T.M., Tomov, A.K., Britovsek, G.J.P., Gibson, V.C., White, A.J.P., Williams, D.J., *Catal. Sci. Tech.*, 2012, **2**, 643 – 655

[23] Mandal, D., Abtab, S.M.T., Audhya, A., Tiekink, E.R.T., Endo, A., Clérac, R., Chaudhury, M., *Polyhedron*, 2013, **52**, 355 – 363

[24] Xiang, J., Zhao, L.-L., Luo, Y., Yan, Z.-H, Wang, C.-H., Zhang, J., Zhou, F., Mei, P., *Inorg. Chem. Commun.*, 2013, **30**, 29 - 33

[25] Talukder, P., Shit, S., Nöth, H., Westerhausen, M., Kneifel, A.N., Mitra, S., *Transition Met. Chem.*, 2012, **37**, 71 - 77

[26] Caris, R., Peoples, B.C., Valderrama, M., Wu G., Rojas, R., *J. Organomet. Chem.*, 2009, **694**, 1795 - 1801

[27] Raebiger, J.W., Turner, J.W., Noll, B.C., Curtis, C.J., Miedaner, A., Cox, B., DuBois, D.L., *Organometallics*, 2006, **25**, 3345 - 3351

[28] Morrin, A., Moutlali, R.M., Killard, A.J., Smyth, M.R., Darkwa, J., Iwuoha, E., *Talanta*, 2004, **64**, 30 - 38

[29] Britovsek, G.J.P., Bruce, M., Gibson, V.C., Kimberley, B.S., Maddox, P.J., Mastroianni, S., McTavish, S.J., Redshaw, C., Solan, G.A., Stromberg, S., White, A.J.P., Williams, D.J., *J. Am. Chem. Soc.*, 1999, **121**, 8728 - 8740

[30] Gibson, V.C., Spitzmesser, S.K., *Chem. Rev.*, 2003, **103**, 283 - 316.

[31] Bahuleyan, B.K., Lee, U., Ha, C.S., Kim, I., *Appl. Catal., A: Gen.*, 2008, **351**, 36 - 44

[32] Bahuleyan, B.K., Lee, K.J., Lee, S.H., Liu, Y., Zhou, W., Kim, I., *Catal. Today*, 2011, **164**, 80 - 87

[33] Zhang, D., Jin, G.X., *Inorg. Chem. Commun.*, 2006, **9**, 1322 - 1325

[34] Bahuleyan, B.K., Kim, J.H., Seo, H.S., Oh, J.M., Ahn, I.Y., Ha, C.-S., Park, D.-W., Kim, I., *Catal. Lett.*, 2008, **126**, 371 - 377

[35] Pelletier, J.D.A., Fawcett, J., Singh, K., Solan, G.A., *J. Organomet. Chem.*, 2008, **693**, 2723 - 2731

[36] Pop, F., Branzea, D.G., Cauchy, T. & Avarvari, N., *C. R. Chim.*, 2012, **15**, 904 - 910

[37] Younkin, T.R., Connor, E.F., Henderson, Friedrich, S.K., Grubbs, R.H., Bansleben, D.A., *Science*, 2000, **287**, 460 - 462

[38] Chen, E.Y.-X., Marks, T.J., *Chem. Rev.*, 2000, **100**, 1391 - 1434

[39] Yang, Q.Z., Kermagoret, A., Agostinho, M., Siri, O., Braunstein, P., *Organometallics*, 2006, **25**, 5518 - 5527

[40] Speiser, F., Braunstein, P., Saussine, L., *Acc. Chem. Res.*, 2005, **38**, 784 - 793

[41] Dennett, J.N.L., Gillon, A.L., Heslop, K., Hyett, D.J., Fleming, J.S., Lloyd-Jones, C.E., Orpen, A.G., Pringle, P.G., Wass, D.F., Scutt, J.N., Weatherhead, R.H., *Organometallics*, 2004, **23**, 6077 - 6079

[42] Albers, I., Alvarez, E., Campora, J., Maya C.M., Palma, P., Sanchez L.J., Passaglia E.J., *J. Organomet. Chem.*, 2004, **689**, 833 - 839

[43] Speiser, F., Braunstein, P., Saussine, L., Welter, R., *Organometallics*, 2004, **23**, 2613 – 2624

[44] Kissen, Y. V., *In Kirk-Othmer Encyclopedia of Chemical Technology*, Wiley-Interscience, New York, 1996, 819.

[45] Elschenbroich, C., *Organometallics*, Wiley-VCH: Weinheim, 2006

[46] Ruokolainen, J., Mezzenga R., Fredrickson, G.H., Kramer E.J., Hustad, P.D., Coates, G.W., *Macromolecules*, 2005, **38**, 851 – 860

[47] Domin, D., Benito-Garagorri, D., Mereiter, K., Frohlich, J., Kirchner, K., *Organometallics*, 2005, **24**, 3957 - 3965

[48] Ittel, S.D., Johnson, L.K., *Ittel*, M., *Chem. Rev.*, 2000, **100**, 1169 - 1204

[49] Zhang, J. Ke, Z. Bao, F. Long, J. Gao, H. Zhu, F., Wu, Q., *J. Mol. Catal. A: Chem.*, 2006, **249**, 31 - 39

[50] Sprung, M.M., *Chem. Rev.*, 1940, **26**, 297 - 338

[51] Simion, A., Simion, C., Kanda, T., Nagashima, S., Mitoma, Y., Yamada, T., Mimura, K., Tashiro, M., *J. Chem. Soc., Perkin Trans. 1*, 2001, **2001**, 2071 - 2078

[52] Saedifar M., Mansuri-Torshizi H., Divsalar A., Saboury, A.A., *J. Iranian Chem. Soc.*, 2013, **10**, 1001 – 1011

[53] Kuwabara, J., Takeuchi, D., Osakada, K., *Polyhedron*, 2009, **28**, 2459 - 2465

[54] Motswainyana, W.M., Ojwach, S.O., Onani, M.O., Iwuoha, E.I., Darkwa, J., *Polyhedron*, 2011, **30**, 2574 – 2580

[55] Mecking, S., *Coord. Chem. Rev.*, 2000, **203**, 325 - 351

[56] Coates, G.W., Hustad, P.D., Reinartz, S., *Angew. Chem. Int. Ed.*, 2002, **41**, 2236 – 2257

[57] Maldanis, R.J., Wood, J.S., Chandrasekran, A., Rausch, M.D., Chien, J.C.W., *J. Organomet. Chem.*, 2002, **645**, 158 - 167

[58] Krayushkina, A.V., Miyulkov, V.A., Sinyashin, O.G., Lönnecke, P., Hey-Hawkins, E., *Russ. Chem. Bull.*, 2014, **63**, 1599 - 1605

[59] Pascu, S.I., Balazs, G., Green, J.C., M. Green, L.H., Vei, I.C., Warren, J.E., Windsor, C., *Inorg. Chim. Acta*, 2010, **363**, 1157 - 1172

[60] Motswainyana, W.M., Onani, M.O., Ojwach, S.O., Omondi, B., *Inorg. Chim. Acta*, 2012, **397**, 93 - 97

[61] Pan, H., Zhu, L., Li, J., Zang, D., Fu, Z., Fan, Z., *J. Mol. Catal. A: Chem.*, 2014, **399**, 1 - 9

[62] Hu, T., Tang, L.M., Li, X.F., Li, Y.S., Hu, N.H., *Organometallics*, 2005, **24**, 2628 - 2632

[63] Zhang, D., Jin, G.X., *Organometallics*, 2003, **22**, 2851 - 2854

[64] Jie, S., Zhang, D., Zhang, T., Sun, W.H., Chen, J., Ren, Q., Liu, D., Zheng, G., Chen, W., *J. Organomet. Chem.*, 2005, **690**, 1739 - 1749

[65] Champouret, Y.D.M., Fawcett, J., Nodes, W.J., Singh, K., Solan, G.A., *Inorg. Chem.*, 2006, **45**, 9890 - 9900

[66] Taquet, J.P., Siri, O., Braunstein, P., *Inorg. Chem.*, 2006, **45**, 4668 - 4676

[67] Singh, A., Chandra, M., Sahay, A.N., Pandey, D.S., Pandey, K.K., Mobin S.M., Puerta, P., Valerga, M.C., *J. Organomet. Chem.*, 2004, **689**, 1821 - 1834

[68] Gibson, V.C., Redshaw, C., Solan, G.A., *Chem. Rev.*, 2007, **107**, 1745 - 1776

[69] Roth, A., Buchholz, A., Rudolph, M., Schütze, E., Kothe, E., Plass, W., *Chem. Eur. J.* 2008, **14**, 1571 - 1583

[70] Netalkar, S.P., Nevrekar, A.A., Revankar, V.K., *Catal. Lett.*, 2014, **144**, 1573 - 1583

[71] Guisado-Barrios, G., Hiller, J., Peris, E., *Chem. Eur. J.*, 2013, **19**, 10405 - 10411

[72] Sachse, A., Demeshko, S., Dechert, S., Daebel, V., Langeb, A., Meyer, F., *Dalton Trans.*, 2010, **39**, 3903 - 3914

[73] Döring, K., Taher, D., Walfort, B., Lutz, M., Spek, A.L., van Klink, G.P.M., van Koten, G., Lang, H., *Inorg. Chim. Acta*, 2008, **361**, 2731 - 2739

[74] Taher, D., Walfort, B., Lang, H., *Inorg. Chem. Commun.*, 2004, **7**, 1006 - 1009

[75] Hamed, O.A., El-Qisairi, A., Qaseer, H., Hamed, E.M., Henry, P.M. & Becker, D.P., *Tetrahedron Lett.*, 2012, **53**, 2699 - 2701

[76] Rivera, G., Bernès, S., Rodríguez de Barbarín, C., Torrens, H., *Inorg. Chim. Acta*, 2009, **362**, 5122 – 5125

[77] Lin, R.S., Li, M.-R., Liu, Y.H., Peng, S.M., Liu, S.T., *Inorg. Chim. Acta*, 2010, **363**, 3523 – 3529

[78] Natta, G., Pino, P., Corradini, P., Danusso, F., Mantica, E., Mazzanti, G., Moraglio, G., *J. Am. Chem. Soc.*, 1955, **77**, 1708 - 1710

[79] Natta, G., Corradini, P., Allegra, G., *J. Polym. Sci., Part A: Polym. Chem.*, 1961, **51**, 399 - 410

[80] Hoff, R. Mathers, R. T., *Handbook of Transition Metal Polymerization*, Catalysts. Eds. John Wiley & Sons, 2010

[81] Mecking, S., Johnson, L.K., Wang, L., *Ittel* M., *J. Am. Chem. Soc.*, 1998, **120**, 888 - 889

[82] Killian, C.M., Tempel, D.J., Johnson, L.K., *Ittel*, M., *J. Am. Chem. Soc.*, 1996, **118**, 11664 – 11665

[83] Johnson, L.K., Killian, C.M., *Ittel*, M., *J. Am. Chem. Soc.*, 1995, **117**, 6414 - 6415

[84] Johnson, L.K., Mecking, S., *Ittel*, M., *J. Am. Chem. Soc.*, 1996, **118**, 267 - 268

[85] Zhang, D., Nadres E.T., *Ittel*, M., Daugulis, O., *Organometallics*, 2013, **32**, 5136 - 5143

[86] Na, S.J., Joe, D.J., Sujith, S., Han, W.S, Kang, S.O., Lee, B.Y., *J. Organomet. Chem.*, 2006, **691**, 611 - 620

[87] Wang, J., Zong, Y., Weib, S., Pan, Y., *Appl. Org. Chem.*, 2014, **28**, 351 - 353

[88] Liu, H.–R., Gomes, P.T., Costa, S.I., Teresa Duarte, M., Branquinho, R., Fernandes, A.C., Chien, J.C.W., Singh, R.P., Marques M.M., *J. Organomet. Chem.*, 2005, **690**, 1314 - 1323

[89] Wang, C., Friedrich S., Younkin, T.R., Li, R.T., Grubbs, R.H., Bansleben. D.A., Day M.W., *Organometallics*, 1998, **17**, 3149 – 3151

[90] Bochmann, M.J., *J. Chem. Soc., Dalton Trans.*, 1996, **3**, 255 - 270

[91] Galli, P., Vecellio, G.J., *J. Polym. Sci., Part A: Polym. Chem.*, 2004, **42**, 396 - 415

[92] Auriemma, F., De Rosa, C., Esposito S., Coates, G.W., Fujita, M., *Macromolecules*, 2005, **38**, 7416 - 7429

[93] Mason, A.F., Coates G.W., *J. Am. Chem. Soc.*, 2004, **126**, 10798 - 10799

[94] Mason, A.F., Coates G.W., *J. Am. Chem. Soc.*, 2004, **126**, 16326 - 16327

[95] Mitani, M., Furuyama, R., Mohri, J.-I., Saito, J., Ishii, S., Terao, H., Nakano, T., Tanaka, H., Fujita, T., *J. Am. Chem. Soc.*, 2003, **125**, 4293 - 4305

[96] Connor, E.F., Younkin, T.R., Henderson, J.I., Hwang S., Grubbs, R.H., Roberts W.P., Litzau, J.J., *J. Polym. Sci., Part A: Polym. Chem.*, 2002, **40**, 2842 - 2854

[97] Benedikt, G.M., Elce, E., Goodall, B.L., Kalamarides, H.A., McIntosh III, L.H., Rhodes, L.F., Selvy, K.T., Andes, C., Oyler, K., Sen, A., *Macromolecules*, 2002, **35**, 8978 - 8988

[98] Chung T.C., *Prog. Polym. Sci.*, 2002, **27**, 39 - 85

[99] Matthew, J.P., Reinmuth, A., Swords, N., Risser, W., *Macromolecules*, 1996, **29**, 2755 - 2763

[100] Goodall, B.L., McIntosh, L.H., Rhodes L.F., *Macromol. Symp.*, 1995, **89**, 421 - 432

[101] Hong, S.C., Jia, S., Teodorescu, M., Kowalewski, T., Matyjaszewski, K., Gottfried, A.C., *Ittel*, M., *J. Polym. Sci., Part A: Polym. Chem.*, 2002, **40**, 2736 - 2739

[102] Yang, W.H., Lee, C.S., Pal, S., Chen, Y.N., Hwang, W.S., Lin, I.J.B., Wang, J.-C., *J. Organomet. Chem.*, 2008, **693**, 3729 - 3740

[103] Rojas, R.S., Wasilke, J.C., Wu, G., Ziller, J.W., Bazan, G.C., *Organometallics*, 2005, **24**, 5644 - 5653

[104] Rojas, R.S., Barrera Galland, G., Wu, G., Bazan, G.C., *Organometallics*, 2007, **26**, 5339 - 5345

[105] Boardman, B.M., Valderrama, J.M., Muñoz, F., Wu, G., Bazan, G.C., Rojas, R., *Organometallics*, 2008, **27**, 1671 - 1674

[106] Chen, Y., Bazan, G.C., Wu, G., *Angew. Chem. Int. Ed.*, **44**, 1108 – 1112

[107] Rose, J.M., Cherian, A.E., Coates, G.W., *J. Am. Chem. Soc.*, 2006, **128**, 4186 - 4187

[108] Netalkar, S.P., Netalkar, P.P., Sathisha, M.P., Budagumpi, S., Revankar, V.K., *Catal. Lett.*, 2014, **144**, 181 - 191

[109] Kong, S., Song, K., Liang, T., Guo, C.-Y., Sun W.–H., Redshaw, C., *Dalton Trans.*, 2013, **42**, 9176 - 9187

[110] Laine, T.V., Lappalainen, K., Liimatta, J., Aitola, E., Lofgren B., Leskela, M., *Macromol. Rapid Commun.*, 1999, **20**. 487 - 491

[111] Britovsek, G.J.P., Baugh, S.P.D., Hoarau, O., Gibson, V.C., Wass, D.F., White, A.J.P., Williams, D.J., *Inorg. Chim. Acta*, 2003, **345**, 279–291

[112] Sun, T., Wang, Q., Fan, Z., *Polymer*, 2010, **51**, 3091 - 3098

[113] Mkoyi, H.D., Ojwach, S.O., Guzei, I.A., Darkwa, J., *J. Organomet. Chem.*, 2013, **724**, 95 - 101

[114] Blom, B., Overett, M.J., Meijboom, R., Moss, J.R., *Inorg. Chim. Acta*, 2005, **358**, 3491 – 3496

Chapter 2: Experimental Section

2.1 General Remarks

All reactions were carried out under oxygen free nitrogen atmosphere using a dual vacuum/nitrogen line and standard Schlenk techniques unless stated otherwise. The solvents used were purified by heating at reflux under nitrogen in the presence of a suitable drying agent and stored with activated molecular sieves in tightly sealed solvent bottles. Dichloromethane was refluxed and distilled over phosphorus (V) oxide, while diethyl ether was dried over sodium wire and benzophenone under nitrogen. Methanol and ethanol were dried from magnesium. $PdCl_2$(COD) [1], $NiBr_2$(DME) [2] and $NiCl_2$(DME) [2] were prepared following literature methods.

2-picolylamine, 2-(2-pyridyl)ethylamine, 2-pyridinecarboxaldehyde, 1,3-diaminopropane, 1,4-diaminobutane, 1,5-diaminopentane, 1,2-dimethoxyethane, 1,5-cyclooctadiene, nickel(II) bromide, nickel(II) chloride and palladium(II) chloride were purchased from Aldrich and were used without any further purification. Anhydrous magnesium sulphate ($MgSO_4$) was used for drying.

2.2 Instrumentation

^{1}H and ^{13}C NMR spectra were recorded on Bruker Avance IIIHD Nanobay 400 MHz spectrometer at room temperature (298K) equipped with a 5 mm BBO probe at the University of the Western Cape (400 MHz for ^{1}H and 100 MHz for ^{13}C) and a Varian Unity Inova 500 MHz spectrometer (500 MHz for ^{1}H and 200 MHz for ^{13}C respectively) at Lund University. Standard 1D and 2D pulse programs were used to acquire the spectra. The ^{1}H spectra were referenced internally using the residual $CDCl_3$ and reported relative to the internal standard tetramethylsilane (TMS). Chemical shift values are given in ppm.

The FTIR spectra in solution were recorded with Perkin-Elmer Spectrum 100 Series FTIR spectrometer using nujol mulls on NaCl plates and KBr pellets for solids at Lund University and the University of the Western Cape.

ESI-MS (ESI+) analyses were performed on a Waters API Q-TOF Ultima instrument by direct injection of sample at the University of Bologna.

Thermal gravimetric analysis (TGA) was carried out using a Perkin Elmer TGA4000 thermogravimetric analyzer from a temperature range of 25 – 900 ˚C at the School of Pharmacy of the University of the Western Cape.

Ultraviolet-visible (UV-Vis) studies were carried out using a Nicolet100 spectrophotometer.

GC-MS was carried out on a GCMS-QP 2010 version 2 gas chromatograph fitted with flame ionization detector and column ZB1, 100% dimethylpolysiloxane with dimensions of 30 m by 0.25 mm at the University of Kwazulu Natal.

Melting point of synthesized compounds was determined using open capillaries using SMP10 melting point apparatus and was reported as uncorrected.

Elemental analysis was performed on Server 1112 Series Elemental Analyzer by the micro-analytical laboratory at the University of Cape Town.

2.3 Alkene Oligomerization

2.3.1 Ethylene Oligomerization

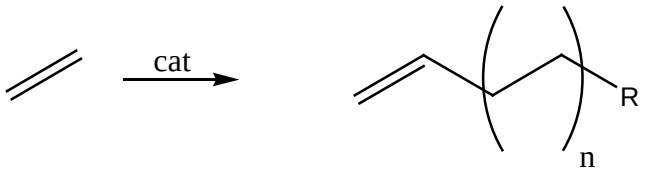

Scheme 2.1: General equation for ethylene oligomerization

Ethylene oligomerization reactions were carried out in a 400 mL stainless steel Parr reactor equipped with a mechanical stirrer, temperature controller and an internal cooling system. In a typical experiment, the reactor was preheated to 100 ˚C *in vacuo* and cooled to room temperature. An appropriate amount of the catalyst precursor (10.0 µmol) was transferred into a dry Schlenk tube under nitrogen and toluene (20 mL) was added using a syringe. The required amount of co-catalyst ($EtAlCl_2$ or MAO) was then injected into the Schlenk tube containing the pre-catalyst, and the resultant solution was transferred *via* cannula into the reactor. An additional 60 mL of toluene solvent was also transferred *via* cannula into the reactor giving a total volume of 80 mL. The reactor was then flushed three times with ethylene and the desired pressure and temperature was set and the reaction started. After the reaction time, the reaction was stopped by cooling the reactor to -20 °C and excess ethylene vented off. An exact amount of heptane (0.1 mL) was added as an internal standard and the mixture was analyzed quantitatively by GC-MS.

2.4 Synthesis of Iminopyridyl Ligands

2.4.1 Pyridin-2-ylmethyl-{4-[(pyridin-2-ylmethylimino)-methyl]-benzylidene}-amine (L1)

A Schlenk tube was charged with 80 ml absolute ethanol and terephthaldehyde(0.6198 g, 4.621 mmol). 2-Picolylamine(1.0007 g, 9.254 mmol) was added to the resulting solution. When complete dissolution occurred, anhydrous magnesium sulphate(ca. 1 g.) was added. The reaction was allowed to proceed under reflux for two hours. The reaction was monitored by ^{1}H NMR. The absence of the HC=O peak confirmed that the reaction was complete. The yellow mixture was filtered using gravity. The resulting solution was cooled at -4 °C overnight and the solvent was removed under reduced pressure at 40 °C for 2 hours to obtain the desired product which was a white solid. Yield: 1.0035 g, (69%). Melting point: 93 – 94 ˚C. IR (nujol cm^{-1}); ν(C=N) 1642 ^{1}H NMR (400 MHz, CD_3Cl_3): 8.57 (d, J = 4.20, 2H); δ 8.50 (s, 2H); 7.86 (s, 4H); 7.67 (dt, J = 3.42 Hz, 2H); 7.43 (d, J = 7.76, 2H); 7.17 (t, J = 4.04 Hz, 2H); 4.97 (s, 4H); ^{13}C NMR (200 MHz, CD_3Cl_3) δ CH (***imine***) 162.56; CN (***pyridyl***) 159.12; CH (***aromatic***) 149.43; 138.27; 136.62; 128.68; 122.45; 122.20; CH_2(***aliphatic***) 67.02. Elemental analysis for $C_{20}H_{18}N_4$ (314.392 g/mol), Calculated: C, 76.4%; H, 5.77%; N, 17.8%. Found: C, 74.48; H, 5.27; N 16.59. ESI-MS: 315 $[M]^+$.

2.4.2 (2-Pyridin-2-yl-ethyl)-{4-[(2-pyridin-2-yl-ethylimino)-methyl]-benzylidene}-amine (L2)

Condensation reaction was carried out following the procedure used to synthesize ligand **L1**. Terephthaldehyde(0.5477 g, 4.083 mmol) and 2-(2-pyridyl)ethylamine(1.0006 g, 8.190 mmol) were used as starting materials. A yellow or orange solid was obtained and it was treated as in ligand **L1** in section 2.4.1. Yield: 1.2209 g, (87%), IR (nujol cm^{-1}); ν(C=N) 1641; Melting point: 104 – 106 ˚C ^{1}H NMR (400 MHz, CD_3OD): δ 8.46 (d, J = 1.07 Hz, 2H);

8.24 (s, 2H); 7.72 (m, 6H); 7.32 (d, J = 7.84 Hz, 2H); 7.24 (m, 2H); 4.00 (t, J = 3.06 Hz, 4H); 3.17 (t, 7.12 Hz, 4H); ^{13}C NMR (200 MHz, CD_3OD) δ CH (***imine***) 163.79; CN (***iminopyridyl***) 160.47; 160.47; CH (***aromatic***) 149.67; 139.21; 138.47; 138.590; 129.41; 125.44; 123.02; CH_2 (***aliphatic***) 61.79; 39.79; Elemental analysis for $C_{22}H_{22}N_4$ (342.444 g/mol), Calculated: C, 77.2%; H, 6.48%; N, 16.4%. Found: C, 75.9; H, 6.50; N 16.6. ESI-MS: 344 $[M]^+$.

2.4.3 N,N'-Bis-pyridin-2-ylmethylene-propane-1,3-diamine (L3)

In a Schlenk tube filled with dry ethanol (10 ml) under nitrogen atmosphere, 1,3-diamino-propane (0.2634 g, 3.55 mmol) was added whilst stirring giving a light-orange colour solution. Pyridine-2-carboxaldehyde (0.7201 g, 6.72 mmol) was added to the formed solution giving an orange solution. The resulting solution was stirred for 5 minutes followed by the addition of anhydrous magnesium sulphate (~0.8 g, $MgSO_4$) giving a light-orange solution. The solution was stirred for 24 hours under nitrogen atmosphere after which it was filtered to remove the $MgSO_4$. The solvent was removed from the filtrate under high vacuum and the orange oily residue was dissolved in 10 ml dichloromethane and washed with (10 x 40ml) distilled water. The organic layers were combined and dried over 3 g of anhydrous MgSO4 and filtered. The filtrate was evaporated under high vacuum with the product obtained as a red oil, Yield: 0.2252 g, (27%), IR (nujol cm^{-1}); ν(C=N) 1655; ^{1}H NMR (400 MHz, $CDCl_3$) δ 8.59 (d, J = 1.0 Hz, 2H), 8.41 (s, 2H), 8.02 (d, J = 2.0 Hz, 2H), 7.89 (td, J = 2.4 Hz, 2H), 7.46 (t, J = 2.0 Hz, 2H), 3.80 (t, J = 3.0 Hz, 4H), 2.15 (quin, J = 6.9 Hz, 2H); ^{13}C NMR (200 MHz, CD_3OD) δ CH (***imine***) 163.45; CN (***iminopyridyl***) 155.10; CH (***aromatic***) 150.19; 138.60; 126.33; 122.69; (***aliphatic***) 59.75; 32.49;

2.4.4 N,N'-Bis-pyridin-2-ylmethylene-butane-1,4-diamine (L4)

Condensation reaction was carried out following the procedure used to synthesize ligand **L3**. 1,4-diamino-butane (0.2605 g, 2.96 mmol) and pyridine-2-carboxaldehyde (0.6086 g, 5.68

mmol) were used as starting materials. A brown, waxy solid was obtained and it was treated as in ligand **L3** in section 2.4.3. Yield: 0.2002 g, (26%); IR (nujol cm^{-1}); ν(C=N) 1650; Melting point 36-38 °C. ^{1}H NMR (400 MHz, $CDCl_3$) δ 8.62 (d, J = 2.4 Hz, 2H), 8.37 (s, 2H), 7.96 (d, J = 7.9 Hz, 2H), 7.72 (m, J = 3.4 Hz, 2H), 7.29 (m, J = 1.9 Hz, 2H), 3.72 (q, J = 3.8 Hz, 4H), 1.82 (m, J = 3.2 Hz, 4H); ^{13}C NMR (200 MHz, CD_3OD) δ CH (***imine***) 163.20; CN (***pyridyl***) 155.10; CH (***aromatic***) 155.10; 150.22; 138.64; 126.54; 122.67; (***aliphatic***) 61.84; 29.30;

2.4.5 N,N'-Bis-pyridin-2-ylmethylene-pentane-1,5-diamine (L5)

Condensation reaction was carried out following the procedure used to synthesize ligand **L3**. 1,5-diamino-pentane (0.2540 g, 2.49 mmol) and pyridine-2-carboxaldehyde (0.5217 g, 4.87 mmol) were used as starting materials. An orange oil was obtained and it was treated as in ligand **L3** in section 2.4.3 [3]. Yield: 0.3441 g, (50%); IR (nujol cm^{-1}); ν(C=N) 1650; ^{1}H NMR (400 MHz, $CDCl_3$) δ 8.63 (d, J = 4.7 Hz, 2H), 8.36 (s, 2H), 7.96 (d, J = 7.9 Hz, 2H), 7.72 (m, J = 4.2 Hz, 2H), 7.29 (m, J = 3.1 Hz, 2H), 3.72 (t, J = 6.9 Hz, 4H), 1.78 (m, J = 7.4 Hz, 4H), 1.48 (m, J = 3.9 Hz, 2H); ^{13}C NMR (200 MHz, $CDCl_3$) δ CH (***imine***) 161.93; CN (***pyridyl***) 154.70; CH (***aromatic***) 149.52; 136.66; 124.73; 121.35; (***aliphatic***) 61.52; 30.59; 25.18;

2.5 Synthesis of Iminopyridyl Complexes

2.5.1 Tetrachloro-[pyridin-2-ylmethyl-{4-[(pyridin-2-ylmethylimino)-methyl]-benzylidene}-amine]dipalladium(II) (C1)

$PdCl_2$(COD) (0.0888g, 0.3110mmol) was added to a Schlenk tube charged with 10 ml dichloromethane. pyridin-2-ylmethyl-{4-[(pyridin-2-ylmethylimino)-methyl]-benzylidene}-amine (0.0488g, 0.1552mmol) was dissolved separately in 2 ml dichloromethane and the

resulting solution was added slowly to the Schlenk tube. The reaction was allowed to proceed at room temperature, resulting to formation of an orange precipitate. The volume of the mixture was then reduced *in vacuo.* The mixture was then precipitated further using copious amounts of diethyl ether. The precipitate was filtered and the solvent removed under reduced pressure to obtain a light brown solid. Yield: 0.0723g (69%), decomposes at 211 °C, IR (KBr cm^{-1}); ν(C=N) 1618, ^{1}H NMR (400 MHz, DMSO): 8.75 (s); 8.41 (s); 7.61 (d); 7.51 (t); 8.76 (d); 5.61 (s); ^{13}C NMR (200 MHz, DMSO) δ CH (***imine***) 165.62; (***aromatic*)** 148.59, 139.67, 128.31, 123.63, 121.59 CH_2 (***aliphatic***) 51.80; Elemental analysis for $C_{20}H_{18}N_4Cl_4Pd_2$ (669.052 g/mol), Calculated: C, 35.9%; H, 2.71%; N, 8.37%. Found: C, 34.3; H, 3.47; N 7.93. ESI-MS: 670 $[M]^+$.

2.5.2 Tetrachloro-[(2-Pyridin-2-yl-ethyl)-{4-[(2-pyridin-2-yl-ethylimino)-methyl]-benzylidene}-amine]dipalladium(II) (C2)

The complex was prepared analogously to **C1**. $PdCl_2$(COD) (0.1496g, 0.5240mmol) and 2-2yridin-2-ylethyl-{4-[(pyridin-2-ylethylimino)-methyl]-benzylidene}-amine (0.0900g, 0.2628mmol) were used as starting materials. A brown solid was obtained, and it was treated as in **C1**. Yield: 0.1055g (58%), decomposes at 195 °C, IR (KBr cm^{-1}); ν(C=N) 1619, ^{1}H NMR (400 MHz, DMSO): δ 8.91 (s); 8.00 (s); 7.54 (d); 7.44 (dt); 4.94 (s); 3.21 (s); ^{13}C NMR (200 MHz, DMSO) δ CH (***imine***) 158.45; (***aromatic*)** 153.18; 140.34; 139.99; 125.06; 123.05; CH_2 (***aliphatic***) 37.33; 36.43; Elemental analysis for $C_{22}H_{22}N_4Cl_4Pd_2$ (697.104 g/mol), Calculated: C, 37.9%; H, 3.18%; N, 8.04%. Found: C, 31.0%; H, 2.92%; N 8.29%. ESI-MS: 695 $[M]^+$.

2.5.6 Tetrachloro-[pyridin-2-ylmethyl-{4-[(pyridin-2-ylmethylimino)-methyl]-benzylidene}-amine]dinickel(II) (C3)

$NiCl_2$(DME) (0.0582g, 0.2651mmol) was added to a Schlenk tube charged with 10 ml dichloromethane. Pyridin-2-ylmethyl-{4-[(pyridin-2-ylmethylimino)-methyl]-benzylidene}-amine (0.0341g, 0.1085mmol) was dissolved separately in 2 ml dichloromethane and the resulting solution was added slowly to the Schlenk tube. The reaction was allowed to proceed at room temperature, resulting in the formation of a pale green solid. The volume of the mixture was then reduced *in vacuo.* The mixture was then precipitated further using copious amounts of hexane. The supernatant was decanted and the remaining solvent was removed under reduced pressure to obtain a pale blue solid. Yield: 0.0583g (94%), mp: > 300°C, IR (KBr cm^{-1}); ν(C=N) 1614, Elemental analysis for $C_{20}H_{18}N_4Cl_4Ni_2$ (573.572 g/mol), Calculated: C, 41.9%; H, 3.16%; N, 9.77%. Found: C, 26.0%; H, 3.76%; N, 6.90%. ESI-MS: 575 $[M]^+$.

2.5.7 Tetrachloro-[(2-Pyridin-2-yl-ethyl)-{4-[(2-pyridin-2-yl-ethylimino)-methyl]-benzylidene}-amine]dinickel(II) (C4)

The complex was prepared analogously to **C3**. $NiCl_2$(DME) (0.0538g, 0.2451mmol) and pyridin-2-yl-ethyl-{4-[(pyridin-2-ylethylimino)-methyl]-benzylidene}-amine (0.0373g, 0.1089mmol) were the starting materials. A green solid was obtained and it was treated as in **C3**. Yield: 0.0480g (73%); decomposes at 225 °C, IR (KBr cm^{-1}); ν(C=N) 1612, Elemental analysis for $C_{22}H_{22}N_4Cl_4Ni_2$ (601.624 g/mol), Calculated: C, 43.9%; H, 3.69%; N, 9.31%. Found: C, 24.3%; H, 4.32%; N, 5.65%. ESI-MS: 607 $[M]^+$.

2.5.11 Tetrabromo-[pyridin-2-ylmethyl-{4-[(pyridin-2-ylmethylimino)-methyl]-benzylidene}-amine]dinickel(II) (C5)

$NiBr_2$(DME) (0.1008g, 0.3266mmol) was added to a Schlenk tube charged with 10 ml dichloromethane. pyridin-2-ylmethyl-{4-[(pyridin-2-ylmethylimino)-methyl]-benzylidene}-amine (0.0500g, 0.1590mmol) was dissolved separately in 2 ml dichloromethane and the resulting solution was added slowly to the Schlenk tube. The reaction was allowed to proceed at room temperature, resulting to formation of a brown precipitate. The volume of the mixture was then reduced *in vacuo.* The mixture was then precipitated further using copious amounts of hexane. The supernatant was decanted and the remaining solvent was removed under reduced pressure to obtain a brown solid. Yield: 0.0783g (66%), decomposes at 131 °C, IR (KBr cm^{-1}); ν(C=N) 1618, Elemental analysis for $C_{20}H_{18}N_4Br_4Ni_2$ (751.372 g/mol), Calculated: C, 32.0%; H, 2.68%; N, 7.46%. Found: C, 22.9%; H, 2.99%; N, 5.91%. ESI-MS: 751 $[M]^+$.

2.5.12 Tetrabromo-[(2-Pyridin-2-yl-ethyl)-{4-[(2-pyridin-2-yl-ethylimino)-methyl]-benzylidene}-amine]dinickel(II) (C6)

The complex was prepared analogously to **C5**. $NiBr_2$(DME) (0.1026g, 0.3324mmol) and 2-pyridin-2-yl-ethyl-{4-[(pyridin-2-ylethylimino)-methyl]-benzylidene}-amine (0.0526g, 0.1536mmol) were used as starting materials. A yellow-brown solid was obtained and treated as in **C5**. Yield: 0.0729g (61%), decomposes at 105 °C, IR (KBr cm^{-1}); ν(C=N) 1616, Elemental analysis for $C_{22}H_{22}N_4Br_4Ni_2$ (779.424 g/mol), Calculated: C, 33.9%; H, 2.84%; N, 7.19%. Found: C, 31.6%; H, 2.32%; N, 4.71%. ESI-MS: 782 $[M]^+$.

2.6 References

[1] Wiedermann, J., Mereiter, K., Kirchner, K., *J. Mol. Cat. A: Chem*., 2006, **257**, 67-72

[2] Ward, L.G.L., *Inorg. Synth*, 1972, **13**, 154 – 164

[3] Sibanyoni, J. M., Bagihalli, G.B., Mapolie, S.F., *J. Organomet. Chem.*, 2012, **700**, 93-102

CHAPTER 3

3 Results and Discussion

3.1 Iminopyridyl Ligands

3.1.1 General

The iminopyridyl ligands belong to a popular class of N-N ligands, whereby two or more nitrogen atoms are used as donor sites [1]. Most iminopyridyl ligands are prepared via Schiff base condensation reactions of ketones or aldehydes with primary amines. Literature work has revealed that complexes containing the nitrogen based ligands which are phosphine-free. Even though iminopyridyl ligands have been widely used as olefin oligomerization and polymerization catalysts, other applications involved Heck coupling reactions. Few research groups have reportedly synthesized bimetallic iminopyridyl palladium complexes and evaluated their ability as potential ethylene polymerization reaction catalyst precursors.

In this study we report synthesis and characterization of iminopyridyl ligands, which we thought that upon coordination to two palladium and nickel centres may form stable and active complexes for ethylene oligomerization/polymerization reactions in comparison to the literature reports [2-4].

A 1:2 ratio reaction of terephthaldehyde with an appropriate primary amine showed that the reaction went to completion after 2 hrs of stirring in ethanol under reflux (Scheme 3.1) [5-6]. The water by-product was removed with a drying agent anhydrous magnesium sulphate. The reaction was monitored at 1 hour intervals using ^{1}H NMR spectroscopy, and it showed the starting material up to 1 hour. However, there was no evidence of either starting materials at the end of the 2 hrs. The ligands were obtained as light white or pale orange solids having yields as high as 87%. They were observed to be light sensitive but air stable at room

temperature and soluble in common organic solvents, such as dichloromethane, chloroform, ethanol and methanol. The ligands showed some decomposition when left for prolonged periods at room temperature. However there was no decomposition when the ligands were stored at -4 ^{o}C for extended periods.

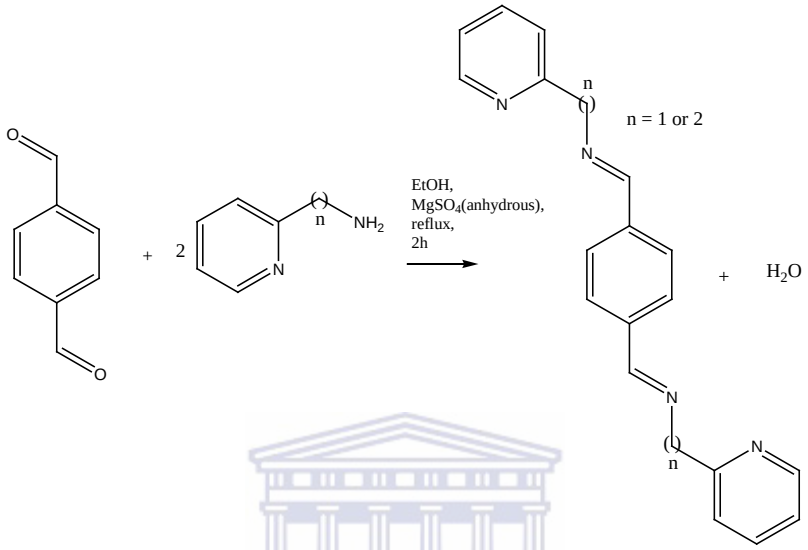

Scheme 3.1: Condensation reaction of terephthaldehyde with corresponding primary amine

A 2:1 ratio of 2-pyridinecarboxaldehyde with a primary diamine showed that the reaction went to completion after 24 hours of stirring in absolute ethanol. To remove excess water anhydrous $MgSO_4$ was used as a dehydrating agent (Scheme 3.2) [7].

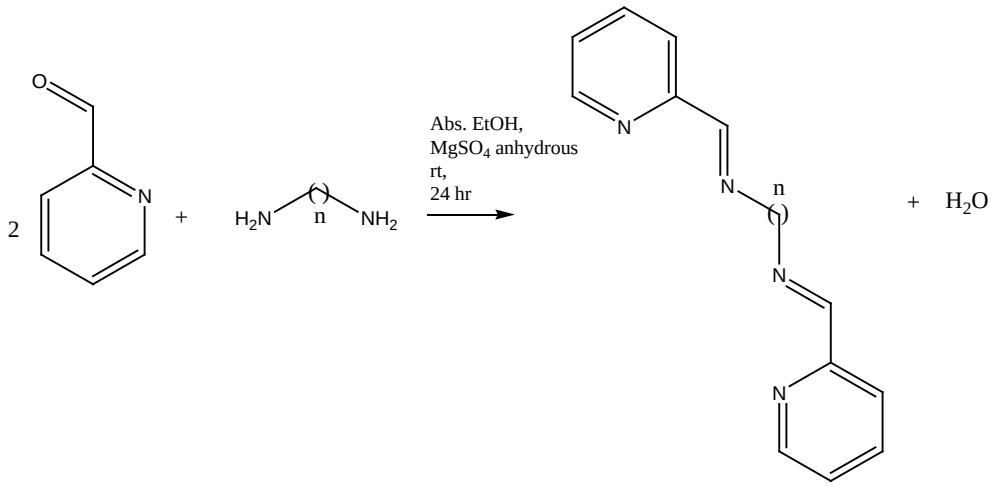

n=3, (**L3**)
n=4, (**L4**)
n=5, (**L5**)

Scheme 3.2: Condensation reaction of 2-pyridinecarboxaldehyde and a primary diamine

These ligands contain weakly coordinated nitrogen donor atoms which are favorable for Pd and Ni complex formation. These ligands were fully characterized by FTIR spectroscopy, ^{1}H and ^{13}C NMR spectroscopy, mass spectroscopy and elemental analysis.

The proposed mechanisms for both reactions reveal the formation of an unstable carbinolamine, which is then followed by the elimination of the water molecule. This is then repeated when an additional one equivalent of amine/aldehyde reacts with the other aldehyde/amine.

3.2.1 IR Studies of iminopyridyl ligands

The following IR spectrum (Fig 3.1) is a typical example of the spectra obtained for iminopyridyl ligands. The other IR spectra for the ligands are given in Appendix 1. A summary of the stretching frequencies of the main functional groups is given in Table 3.1

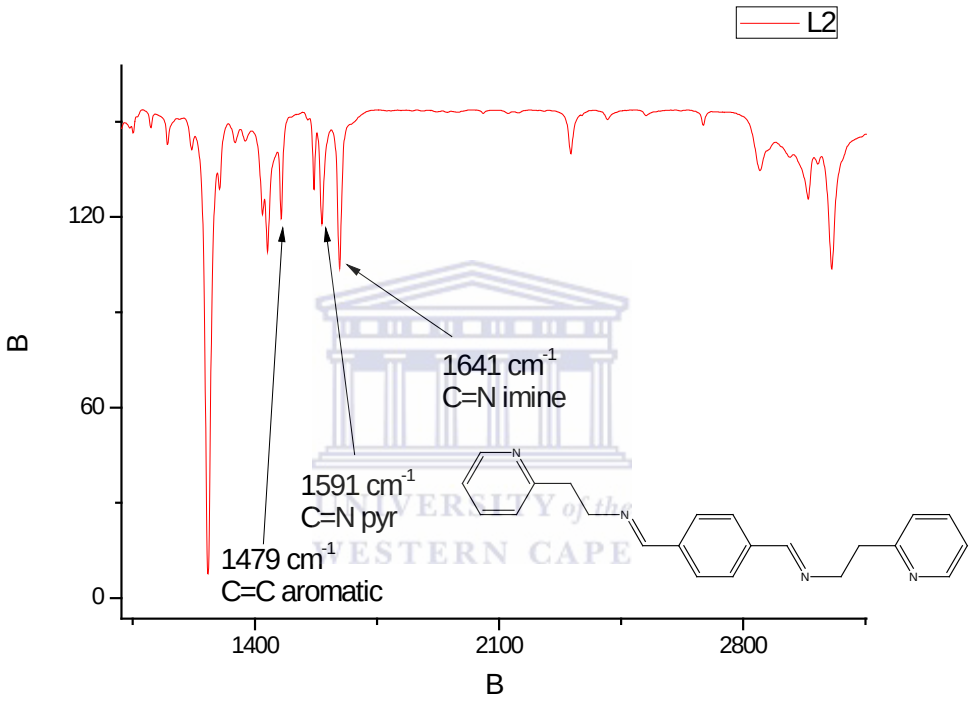

Figure 3.1: IR spectrum for Pyridin-2-ylmethyl-{4-[(pyridin-2-ylmethylimino)-methyl]-benzylidene}-amine **L2**

Infrared spectroscopy was used to identify the stretching frequencies of the functional groups in the ligands. The ligands showed the imino-group strong absorption bands between 1641-1655 cm^{-1} which was an indication that the terephthaldehyde (or 2-pyridinecarboxaldehyde with respect to **L3-L5**) was condensed with the amine groups to form the corresponding imine compounds. The absence of the C=O stretching frequencies at 1720 cm^{-1} and 1722 cm^{-1} [1] for terephthaldehyde [8] and 2-pyridinecarboxaldehyde [9] respectively in the IR spectra of

all the ligands further confirmed the formation of the imine group. In a report by Ben Hadda *et al.*, the imine C=N stretch for **L1** was observed at 1600 cm^{-1} [5]. This is significantly lower than the frequency observed in this work of 1641 cm^{-1}. This indicated that the imine carbon was not protonated, hence the lower frequency according to Ben Hadda *et al.* [5]. According to the report the frequency they observed was likely due to hydrogen bonding between the imine proton and the pyridyl nitrogen [5]. This formed a pseudo-six-membered ring which stabilized the ligand further [5]. This phenomenon was not observed in this work, therefore the imine carbon was protonated since the C=N stretching frequency falls within the standard frequency range of 1640-1690 cm^{-1} [5]. Other significant absorption bands observed were around 1594 and 1474 cm^{-1} which were assigned to the C=N of the pyridyl ring and the C=C of the benzene ring respectively. Since spectral data could not be found in the literature for **L2**, comparisons between **L1** and **L2** could only be made based on spectral data of compounds similar to them. Based on a report by Motswainyana *et al.*, there was very little difference in C=N stretching frequencies when the linker between imine and the pyridyl ring was only varied by one carbon with observed frequencies of 1648 cm^{-1} and 1650 cm^{-1} for the methylene and ethylene linkers respectively [10]. This phenomenon was also observed in **L1** and **L2** where the C=N stretching frequency was observed at 1641 cm^{-1} for both ligands. As far as the alkyl linked iminopyridyl ligands **L3-L5** are concerned **L5** was the only ligand that had a similar C=N stretching frequency compared to the literature. The experimental frequency of 1650 cm^{-1} is in agreement with the literature value found in a report by Sibanyoni *et al.* (1648 cm^{-1}) [7]. The experimental C=N stretching frequencies for **L3** and **L4** seem to contradict with the reported values by Rahaman *et al.* of 1590 cm^{-1} for both ligands [11]. This is also possibly due to the phenomenon explained by Ben Hadda *et al.* [5]. The main reason for the difference between the frequencies of the tetrahydrophenyl linked

iminopyridyl ligands (**L1-L2**) and the alkyl linked ligands (**L3-L5**) is the nucleophilicity of the phenyl compared to the alkyl [5, 7, 10-11].

The IR spectrum in Fig 3.1 is an example of the spectra obtained for the iminopyridyl ligands. The other IR spectra for the ligands are given in Appendix 1. A summary of the stretching frequencies of the main functional groups are given in Table 3.1 below.

Table 3.1: Summary of IR data and yields for ligands **L1-L5**

Ligand	**%Yield**	**(C=N) cm^{-1}** ***Imine***	**(C=N) cm^{-1}** ***pyridyl***	**(C=C) cm^{-1}** ***Pyridyl***
L1	69	1641	1594	1474
L2	87	1641	1591	1479
L3	27	1655	1585	1431
L4	26	1650	1552	1422
L5	50	1650	1589	1470

3.2.2 ^{1}H NMR studies of iminopyridyl ligands

3.2.2.1 Tetrahydrophenyl-linked iminopyridines

The proton NMR spectra were obtained from chloroform-d solution with reference as trimethysilane (TMS). All the ^{1}H NMR spectra of the ligands were equally consistent with reported literature results of iminopyridyl ligands [5, 10]. The ^{1}H NMR assignment for the ligands (Fig 3.2) was carried out by means of chemical shift of the relevant protons. The mode of the shift assigned of ^{1}H NMR of the iminopyridyl ligand **L1** is shown in Fig 3.3. An example of the proton spectrum is given in Fig 3.3 and other proton NMR spectra for the ligands can be found in Appendix 1. The chemical shift values of the protons are summarized in Table 3.2.

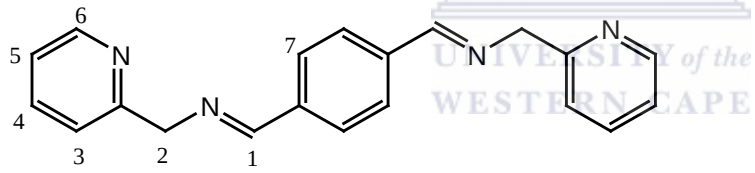

L1

Figure 3.2: Numbered structures for tetrahydrophenyl-linked iminopyridyl ligand **L1** for chemical shifts assignment

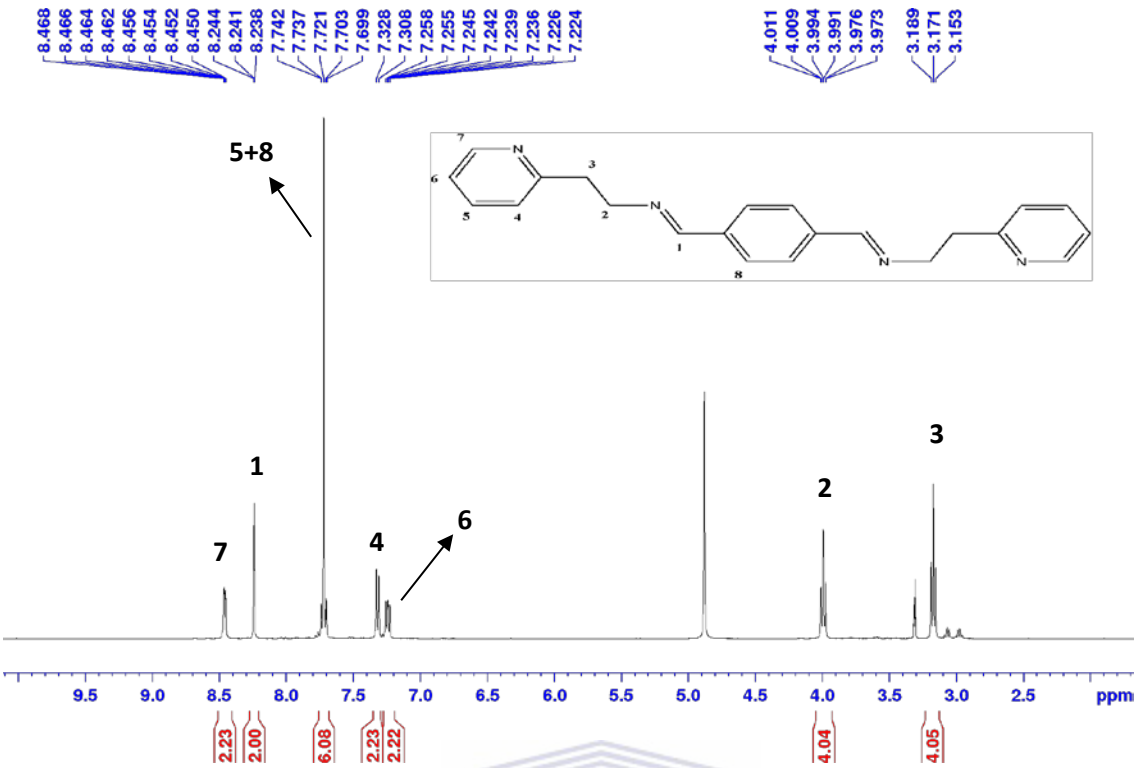

Figure 3.3: ^{1}H NMR Spectrum of (2-Pyridin-2-yl-ethyl)-{4-[(2-pyridin-2-yl-ethylimino)-methyl]-benzylidene}-amine **(L2)**

Table 3.2: Summary of ^{1}H NMR data for ligands **L1-L2**

Ligand (solvent)	**H-1**	**H-2**	**H-3**	**H-4**	**H-5**	**H-6**	**H-7**	**H-8**
1 ($CDCl_3$)	8.50 (s)	4.97 (s)	7.43 (d)	7.67 (dt)	7.17 (t)	8.57 (d)	7.86 (s)	-
2 (CD_3OD)	8.24 (s)	4.00 (t)	3.17 (t)	7.32 (d)	7.72 (m)	7.24 (dt)	8.46 (d)	7.72 (m)

There was strong evidence that a Schiff base condensation has taken place as observed by a proton signal at around 8.24 ppm (singlet) due to the imine hydrogen atom (**H**C=N) (Fig 3.3). The observed chemical shift values for the imine proton are 8.24 ppm and 8.50 ppm for **L2**

and **L1** respectively. This chemical shift for **L1** is in agreement with the reported value of 8.50 ppm by Ben Hadda *et al.* [5]. The singlet observed at 4.92 ppm in **L1** could be assigned to the methylene protons, and this value agrees with the observed singlet at 5.0 ppm reported by Ben Hadda *et al.* [5].

As mentioned earlier, spectral data could not be found in the literature for **L2**, so comparisons between **L1** and **L2** could only be made based on spectral data of compounds similar to them. In the report by Motswainyana *et al.* the signals for the imine proton was found at 8.48 ppm and 8.31 ppm when the methylene and ethylene were used respectively [10]. This is in agreement with the experimental value observed with **L2** of 8.24 ppm. The two triplets observed at 3.17 ppm and 4.00 ppm in **L2** could be assigned to the ethyl arm and these values agree with the observed triplets of 3.21 ppm and 3.91 respectively reported by Motswainyana *et al.* [10]. The doublet of triplets (dt) found in **H-4** and **H-6** for **L1** and **L2** respectively indicate that their neighbouring protons are in different electronic environments and couple differently, it also indicates the possibility of long-range coupling to **H-4** (for **L1**) and **H-6** (for **L2**). Furthermore, the disappearance of N**H**$_2$ signals at 1.91 ppm and 1.50 ppm for 2-picolylamine and 2-(2-pyridyl)ethylamine respectively [12] as well as the disappearance of the C**H**O signal of terephthaldehyde at 10.1 ppm confirmed the complete consumption of the starting material [7]. This along with the absence of other peaks other than the ^{1}H NMR solvent peaks confirms the purity of the compound.

3.2.2.2 Alkyl-linked iminopyridyl ligands

L3: n = 3
L4: n = 4
L5: n = 5

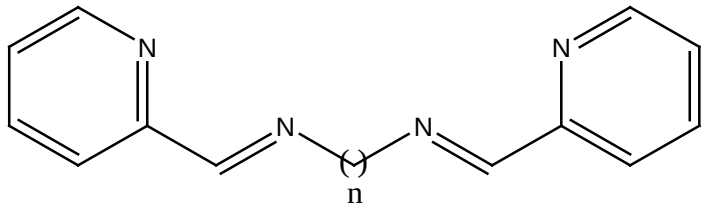

Figure 3.4: Alkyl-linked iminopyridyl ligands that will be discussed

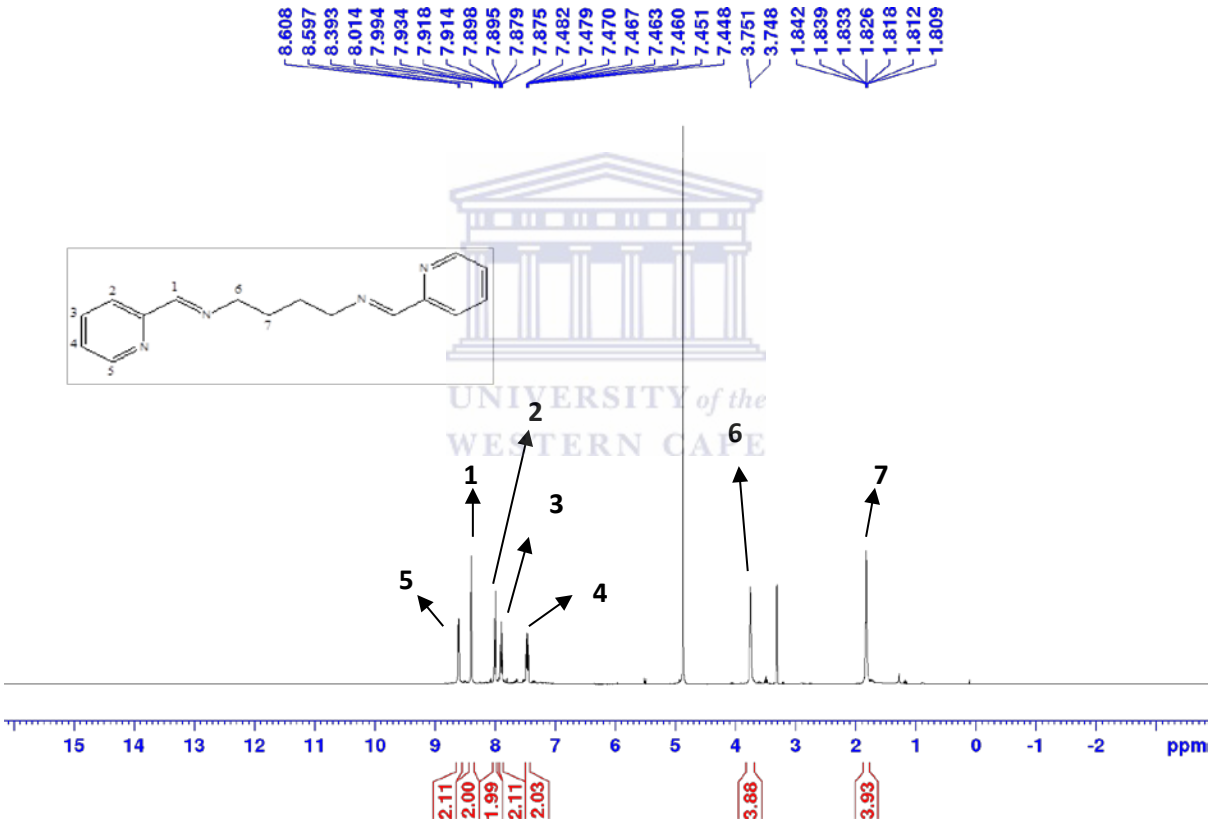

Figure 3.5: ^{1}H NMR of N,N'-bis-pyridin-2-ylmethylene-butane-1,4-diamine **(L4)**

Table 3.3: Summary of ^{1}H NMR data for ligand **L3-L5**

Ligand (solvent)	**H-1**	**H-2**	**H-3**	**H-4**	**H-5**	**H-6**	**H-7**	**H-8**
3 (CD_3OD)	8.41 (s)	8.02 (d)	7.89 (dt)	7.46 (m)	8.59 (d)	3.80 (dt)	2.15 (d)	-
4 (CD_3OD)	8.39 (s)	8.00 (d)	7.90 (m)	7.46 (m)	8.60 (d)	3.75 (d)	1.83 (m)	-
5 ($CDCl_3$)	8.36 (s)	7.96 (d)	7.72 (m)	7.29 (m)	8.63 (d)	3.68 (t)	1.78 quin	1.48 (m)

The signal at 8.36 ppm for **L5** is in good agreement with the value for the imine proton reported by Sibanyoni *et al.* of 8.37 ppm [7]. There was also a consistent upfield shift for these protons as the alkyl chain gets longer. This is consistent with reports by Motswainyana *et al.* where increasing the chain length from one to two decreased the chemical shift of the imine proton from 8.50 ppm to 8.31 ppm respectively [10].

This upfield shift pattern was also apparent when the alkyl protons were studied as seen for protons H-6 and H-7. This was also the case in a report by Motswainyana *et al.* which reported an upfield shift from 5.07 ppm to 3.91 ppm [10]. It can therefore be surmised that increasing the chain length weakens the nucleophilicity of the ligand and thus leads to progressively less deshielding from **L3** to **L5** [13]. The doublet of triplets (dt) found in **H-6** of **L3**, this indicates that these protons couple differently to its neighbouring protons.

Furthermore, proton signals at around 1.10 – 1.25 ppm due to the N**H**$_2$ group of the diamine (1.14 ppm for 1,3-diaminpropane, 1.11 ppm for 1,4-diaminobutane and 1.24 ppm for 1,5-diaminopentane) [14-15] and at 10.00 ppm due to the C**H**O group of 2-pyridinecarboxaldehyde disappeared in the ^{1}H NMR of all the ligands [9]. This confirmed the complete consumption of the starting material. This along with the absence of other peaks except the ^{1}H NMR solvent peaks confirms the purity of the compound.

3.2.3 ^{13}C NMR studies of iminopyridyl ligands

3.2.3.1 Tetrahydrophenyl-linked iminopyridyl ligands

The following spectrum (Fig 3.6) represents the ^{13}C NMR spectrum of the tetrahydrophenyl-linked iminopyridyl ligands prepared in this study. The other ^{13}C NMR spectra for the ligands are given in Appendix 1. A summary of the carbon signals of the main functional groups is given in Table 3.4

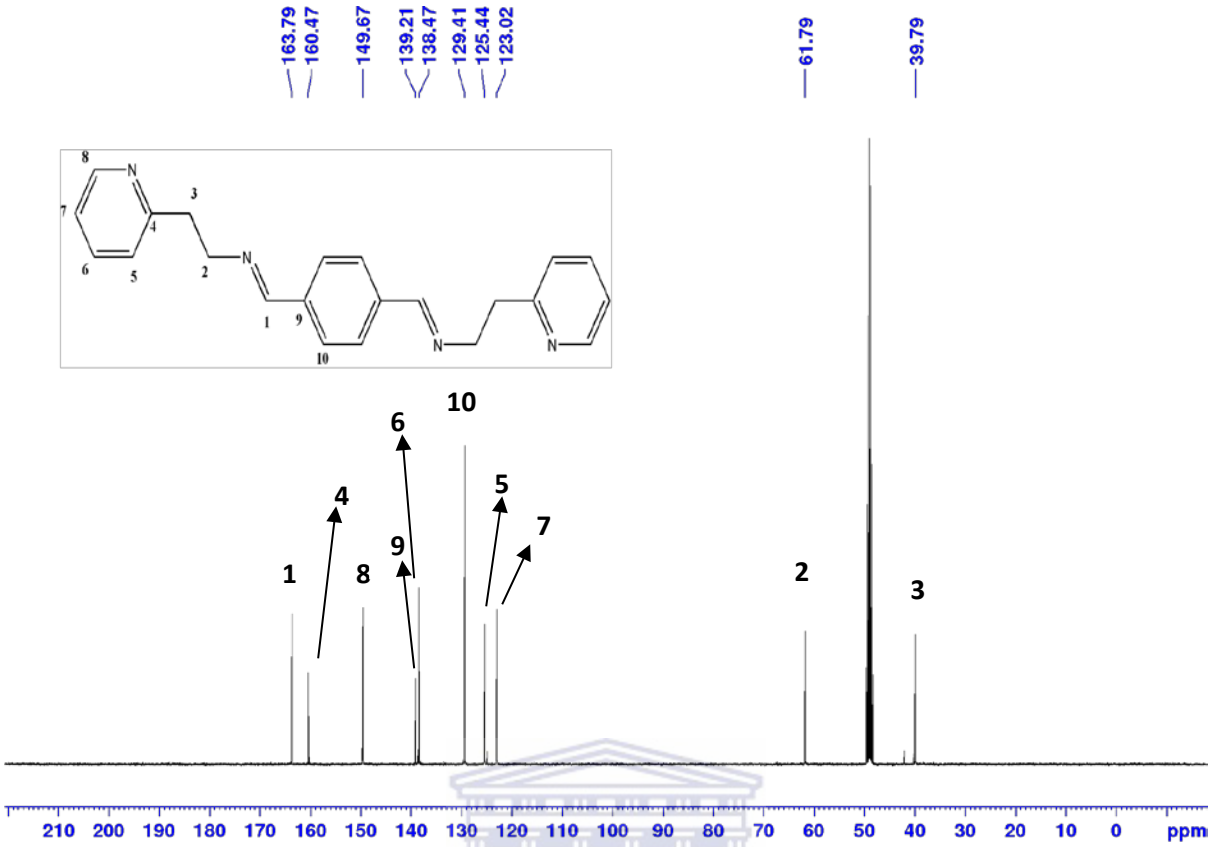

Figure 3.6: ^{13}C NMR of (2-pyridin-2-yl-ethyl)-{4-[(2-pyridin-2-yl-ethylimino)-methyl]-benzylidene}-amine **L2**

Table 3.4: Summary of ^{13}C NMR data for ligands **L1-L2**

Ligand (solvent)	**C-1**	**C-2**	**C-3**	**C-4**	**C-5**	**C-6**	**C-7**	**C-8**	**C-9**	**C-10**
L1 ($CDCl_3$)	162.5	67.0	159.1	122.4	136.6	122.2	149.4	138.3	128.7	-
L2 (CD_3OD)	163.8	61.8	39.8	160.5	125.4	138.5	123.0	149.7	139.2	129.4

In the ^{13}C NMR analysis (Fig 3.6), the characteristic signals for the imine carbons appeared at 165.4 ppm for **L1** and 163.9 ppm and **L2**. The chemical shift values for the imine carbons are within the range 160 – 165 which is in agreement with the value reported by Ben Hadda *et al.*

of 162.8 ppm [5]. The imine carbons revealed an upfield shift compared to the aldehyde carbons as expected, because the imine carbons experienced an increase in electron density as discussed in section 3.2.2. Due to the pyridine nitrogen acting as an electron sink the carbons in the 3- and 5- positions were less deshielded while the carbons in the 2- and 4-positions were more deshielded [13]. When the alkyl chain length increased, the nucleophilicity was lowered, hence the lower chemical shifts from **L1** to **L2** [13].

The carbon signal due to the methyl arm for **L1** at around 67.7 ppm, and the value is consistent with the value of 69.9 ppm reported in literature on related iminopyridyl ligands [7]. The carbon signals at 61.8 ppm and 39.8 ppm could be ascribed to the ethyl arm which is consistent with what was reported by Motswainyana *et al.* (30.6 ppm and 61.4 ppm) [10]. These signals revealed a downfield shift due to the decrease in electron density in the alkyl carbons, which has been discussed in 3.2.2.

3.2.3.2 Alkyl-linked iminopyridyl ligands

The following spectrum (Fig 3.7) represents the ^{13}C NMR spectrum of the alkyl-linked iminopyridyl ligands prepared in this study. The other ^{13}C NMR spectra for the ligands are given in Appendix 1. A summary of the carbon signals of the main functional groups is given in Table 3.5

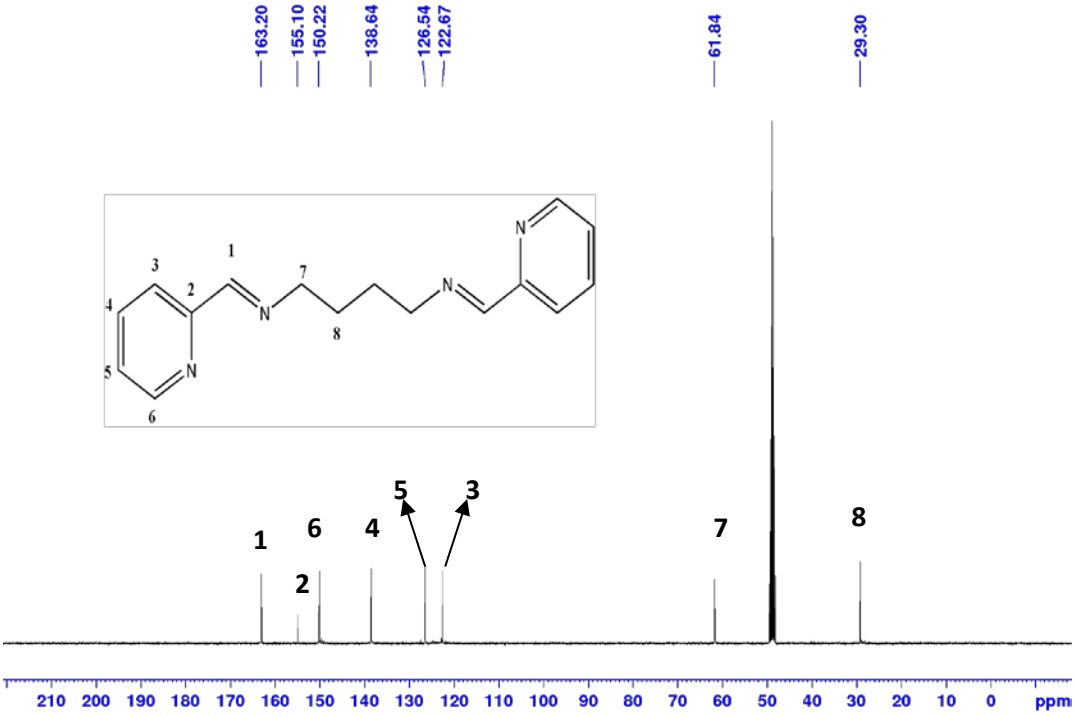

Figure 3.7: ^{13}C NMR of N,N'-bis-pyridin-2-ylmethylene-butane-1,4-diamine **L4**

Table 3.5: Summary of ^{13}C NMR data for ligands **L3-L5**

Ligand (solvent)	**C-1**	**C-2**	**C-3**	**C-4**	**C-5**	**C-6**	**C-7**	**C-8**	**C-9**
L3 ($CDCl_3$)	163.5	155.1	122.7	138.6	126.5	150.2	59.8	32.5	-
L4 (CD_3OD)	163.2	155.1	122.7	138.6	126.5	150.2	61.8	29.3	-
L5 ($CDCl_3$)	161.9	154.7	121.4	136.7	124.7	149.5	61.5	30.6	25.2

In the ^{13}C NMR analysis (Fig 3.7), the characteristic signals for the imine carbons appeared at 163.5 ppm for **L3**, 163.2 ppm for **L4** and 161.9 for **L5**. Once again a consistent upfield shift was observed when the length of the alkyl chain increased. The chemical shift values for the imine carbons are within the range 160 – 165 which are consistent with the values reported

by Motswainyana *et al.* [10]. The imine carbons revealed an upfield shift compared to the aldehyde carbons as expected, because the imine carbons experienced an increase in electron density as discussed in section 3.2.2.

The carbon signals due to the propyl arm for **L3** are around 59.8 ppm and 32.5 ppm. The carbon signals due to the butyl arm for **L4** are around 61.8 ppm and 29.3 ppm. The carbon signals due to the pentyl arm for **L5** are around 61.5 ppm, 30.6 ppm and 25.2 ppm. These are consistent with the reported values by Motswainyana *et al.* of 30.6 ppm and 61.4 ppm [10].

3.2.4 UV-Vis studies of iminopyridyl ligands

The following spectrum (Fig 3.8) represents the UV-Vis spectrum of the tetrahydrophenyl-linked iminopyridyl ligands prepared in this study. The rest of the UV-Vis spectra for the ligands are given in Appendix 1. A summary of the λ_{max} values of the ligands **L1** and **L2** are given in Table 3.6 below.

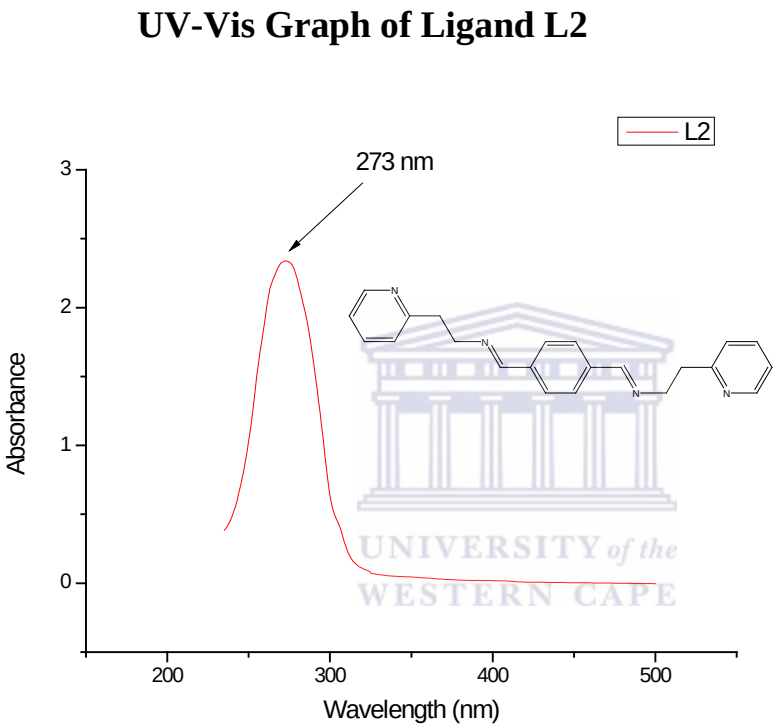

Figure 3.8: UV-Vis spectrum of (2-pyridin-2-yl-ethyl)-{4-[(2-pyridin-2-yl-ethylimino)-methyl]-benzylidene}-amine **L2**

Table 3.6: λ_{max} for ligands **L1** and **L2**

Ligand	**λ_{max}(nm)**
L1	272
L2	273

The λ_{max} values of 272 nm and 273 nm for **L1** and **L2** respectively are consistent with the transition of the C=N imine group. This is indicative of a π-π^* transition as described by

Kubota *et al.* which reported values of 269 nm [16]. The similarity of these λ_{max} values indicate that changing the length of the linker by only one carbon does not make a significant impact in UV-Vis spectroscopy of iminopyridyl ligands.

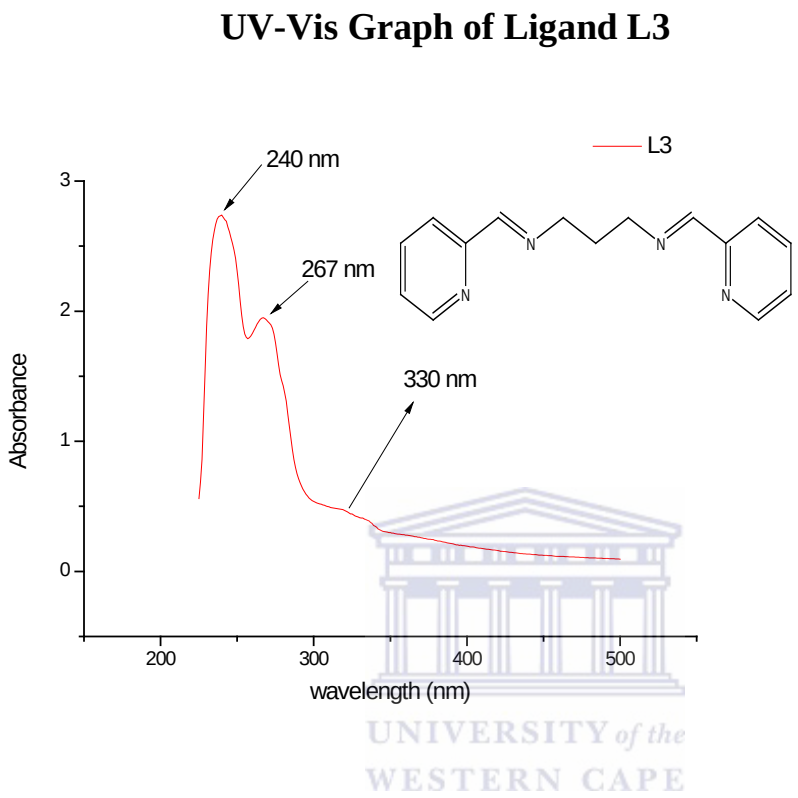

Figure 3.9: UV-Vis spectrum of N,N'-Bis-pyridin-2-ylmethylene-propane-1,3-diamine **(L3)**

Table 3.7: λ_{max} for ligands **L3-L5**

Complex	**λ_{max1}(nm)**	**λ_{max2}(nm)**
L3	240	267
L4	237	269
L5	239	269

The λ_{max} values between 237-240 nm, 267–269 nm as well as the shoulder around 330 nm for ligands **L3-L5** respectively are consistent with intraligand transitions such as n-π* and π-π* as described by Dehghanpour and Mahmoudi which report values of 245 nm for the n-π* transitions and 280 nm and 330 nm for the π-π* transitions [17]. A possible reason for the

significantly higher wavelength of 280 nm in the report is possibly due to the incorporation of an electron withdrawing fluoride (F^-) on one of the aromatic rings [17].

3.2.5 TGA studies of iminopyridyl ligands

The following spectra (Fig 3.10 and Fig 3.11) represent the TGA spectrum of the tetrahydrophenyl-linked iminopyridyl ligands prepared in this study.

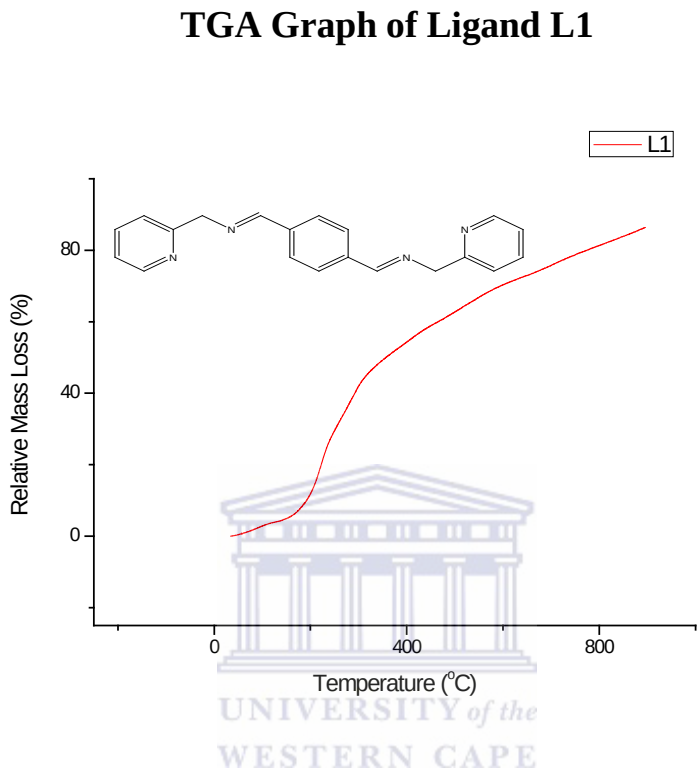

Figure 3.10: TGA spectrum of Pyridin-2-ylmethyl-{4-[(pyridin-2-ylmethylimino)-methyl]-benzylidene}-amine (**L1**)

Since there is no literature on the TGA of iminopyridyl ligands, the only reports cited will be those where the decomposition of similar compounds were be studied after they already underwent complexation. The decomposition points were found by looking at the inflection points on the curve. From the graph, it can be deduced that **L1** decomposes in two stages. It remains stable from 25 °C to 102 °C which is around the experimental melting point of **L1** (93 - 94 °C). The first decomposition stage is from 102 °C to 340 °C. There was a relative mass loss of 48.2%. This corresponds to the loss of both pyridyl groups (calculated loss 49.7%). The second stage starts from 340 °C and continues beyond the set temperature range of 900 °C most likely due to the loss of the imines, methylene groups and lastly the

quaternary carbons of the phenyl group. This method of interpreting the data of relatively similar compounds can be found in a report by Netalkar *et al.* [18]. In this report the compound was found to be stable from 25 °C to 200 °C [17]. The ligands decomposed from 250 °C – 425 °C with a reported loss values of 50-54% of the complex [18]. The ligand system in this work was shown to be quite stable since there was still approximately 20% of the compound remaining when it passed the set temperature range of 900 °C.

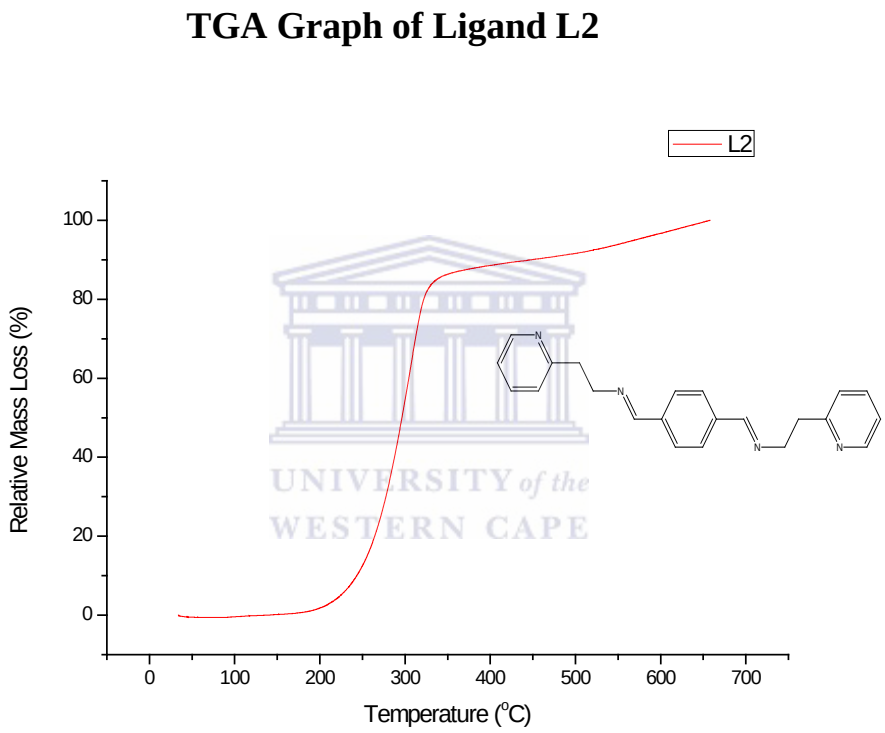

Figure 3.11: TGA spectrum of (2-pyridin-2-yl-ethyl)-{4-[(2-pyridin-2-yl-ethylimino)-methyl]-benzylidene}-amine (**L2**)

The decomposition of **L2** can be divided into three stages. It was stable from 25 °C to 186 °C. The first stage of decomposition occurred from 186 °C to 324 °C with a relative mass loss of 82.2%. This is most likely the loss of both iminopyridyl groups (calculated loss 77.2%). The third stage was from 324 °C to 474 °C with a further relative mass loss of 7.9%

which are likely the quaternary carbons of the tetrahydrophenyl ring (calculated loss 7.0%). The final stage is the loss of the remaining two ethylene groups from 474 °C to 657 °C [18]. When compared to the report by Netalkar *et al.*, **L2** was found to be more stable than the corresponding ligand but significantly less stable than **L1** since it fully decomposed at 654 °C [18].

3.2.6 Mass spectroscopic analysis of iminopyridyl ligands

The following spectrum (Fig 3.12) represents the ESI-MS spectrum of the tetrahydrophenyl-linked iminopyridyl ligands prepared in this study. The other ESI-MS spectra for the ligands are given in Appendix 1. A summary of the ESI-MS values of the ligands **L1** and **L2** can be found in Table 3.8

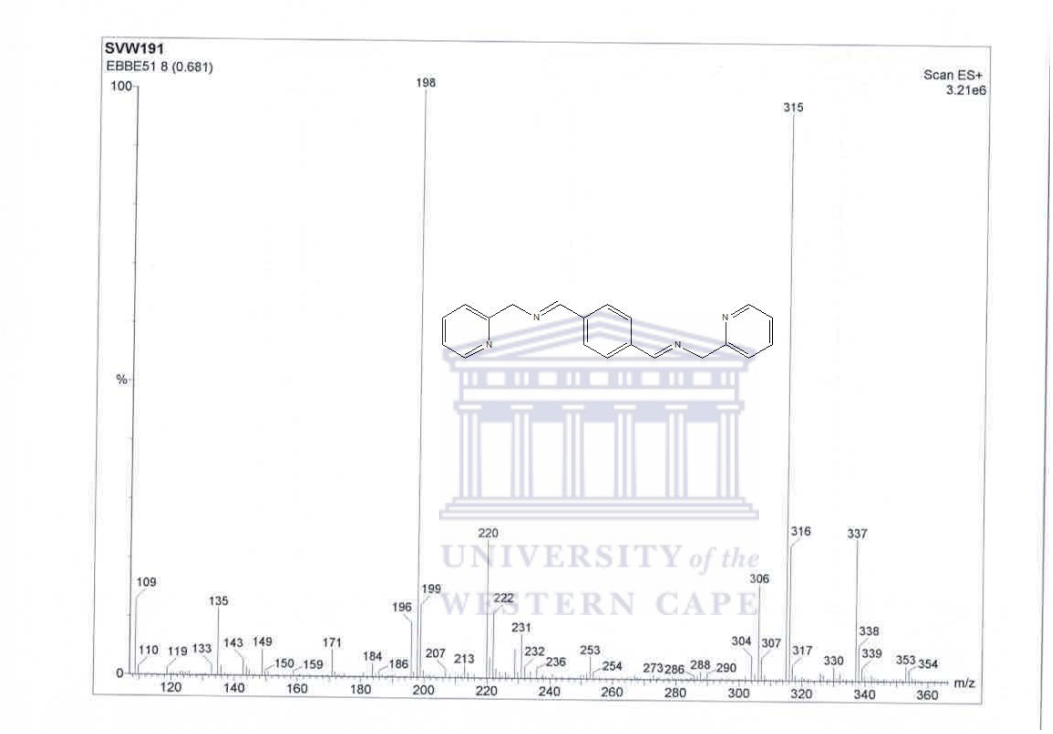

Figure 3.12: ESI-MS spectrum of Pyridin-2-ylmethyl-{4-[(pyridin-2-ylmethylimino)-methyl]-benzylidene}-amine (**L1**)

Table 3.8: Summary of the ESI-MS data of ligands **L1** and **L2**

Ligand	**ESI-MS** **$[M+H]^+$ (m/z)** **Calculated (found)**
L1	314 (315)
L2	342 (343)

The fragmented ion peaks show base peaks for ligand **L1** and **L2** at m/z = 315 and 343, which are similar to the calculated molecular weight of the compounds. This is attributed to monocharged parent ions. The spectrum for **L1** is in agreement with the value of the molecular ion found in the report by Ben Hadda *et al.* which is also at m/z = 315 [5].

3.3 Iminopyridyl complexes

3.3.1 Bimetallic Iminopyridyl Pd(II) complexes

The iminopyridyl complexes were synthesized by using mixed procedures of Pelletier *et al.* and Motswainyana *et al*. (Scheme 3.3) [2, 10]. The ligands were reacted in 2 equivalent moles of $PdCl_2(COD)$, which gave new Pd(II) complexes [7]. All of the complexes were isolated as stable yellow solids in high yields. Both complexes **C1** and **C2** were only soluble in DMSO and decomposed at 195 ˚C and 211 ˚C respectively. The new complexes were characterized by the standard analytical techniques: FTIR; elemental analysis; melting point apparatus; ^{1}H and ^{13}C NMR spectroscopy; TGA (where applicable); and lastly mass spectroscopy. These complexes have not been reported before to the best of our knowledge.

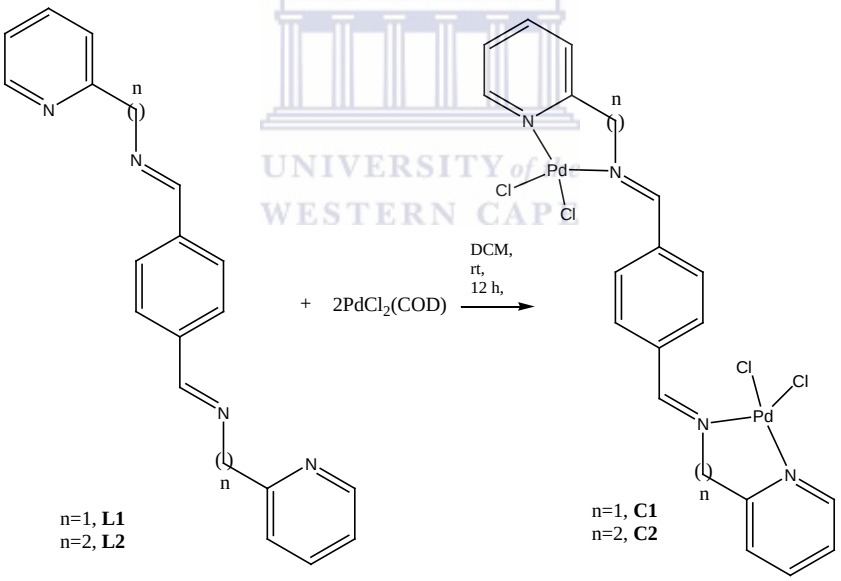

Scheme 3.3: Synthesis of tetrahydrophenyl-linked iminopyridyl palladium(II) complexes

3.3.1.1 FTIR studies of bimetallic iminopyridyl Pd(II) complexes

The following FTIR spectrum (Fig 3.13) is a typical example of the spectra obtained for iminopyridyl complexes. The other IR spectra for the ligands are given in Appendix 1. A summary of the stretching frequencies of the main functional groups is given in Table 3.9

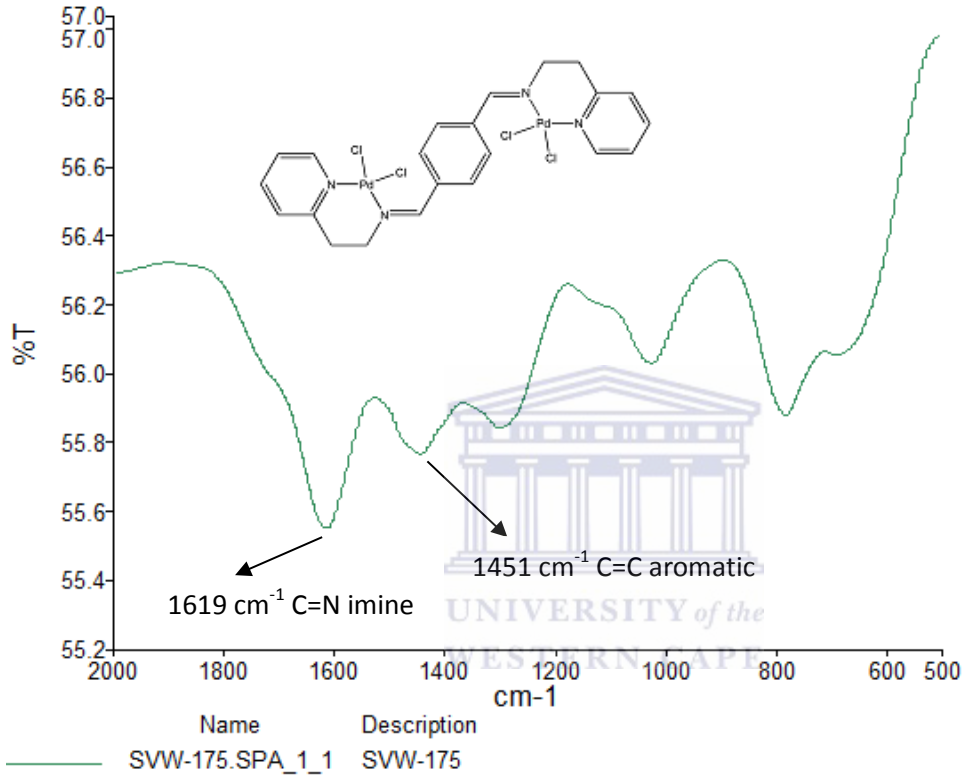

Figure 3.13: FTIR spectrum of complex **C2**

Table 3.9: FTIR Data of complexes of **C1** and **C2**

Complex	**%Yield**	**(C=N) cm^{-1}** ***Imine***
C1	69	1618
C2	58	1619

Infra-red spectra of all pyridyl-imine palladium complexes showed a red shift of the υ(C=N) band which occurred around 1645 cm^{-1} in the free ligand and upon coordination occurs around 1618 cm^{-1} for **C1** and 1619 cm^{-1} for **C2**. Literature reports indicated a red shift of the absorption band occurring about 20-30 cm^{-1} from the shift for the free ligand [10, 19]. Disappearance of the imino C=N absorption in the IR spectra might be ascribed to an inactive C=N vibration in the Pd (II) complexes as a result of coordination of the ligand to the metal centre as well as a reduction in electron density in the C=N bond arising from electron density flowing from the ligand to the metal centre [19].

3.3.1.2 ^{1}H and ^{13}C NMR studies of bimetallic Pd(II) complexes

The following spectra (Fig 3.14 and Fig 3.15) represent the ^{1}H and ^{13}C NMR spectra of the tetrahydrophenyl-linked iminopyridyl bimetallic Pd(II) complexes prepared in this study. The other ^{1}H and ^{13}C NMR spectra for the ligands are given in Appendix 1. A summary of the carbon signals of the main functional groups is given in Tables 3.10 and 3.11

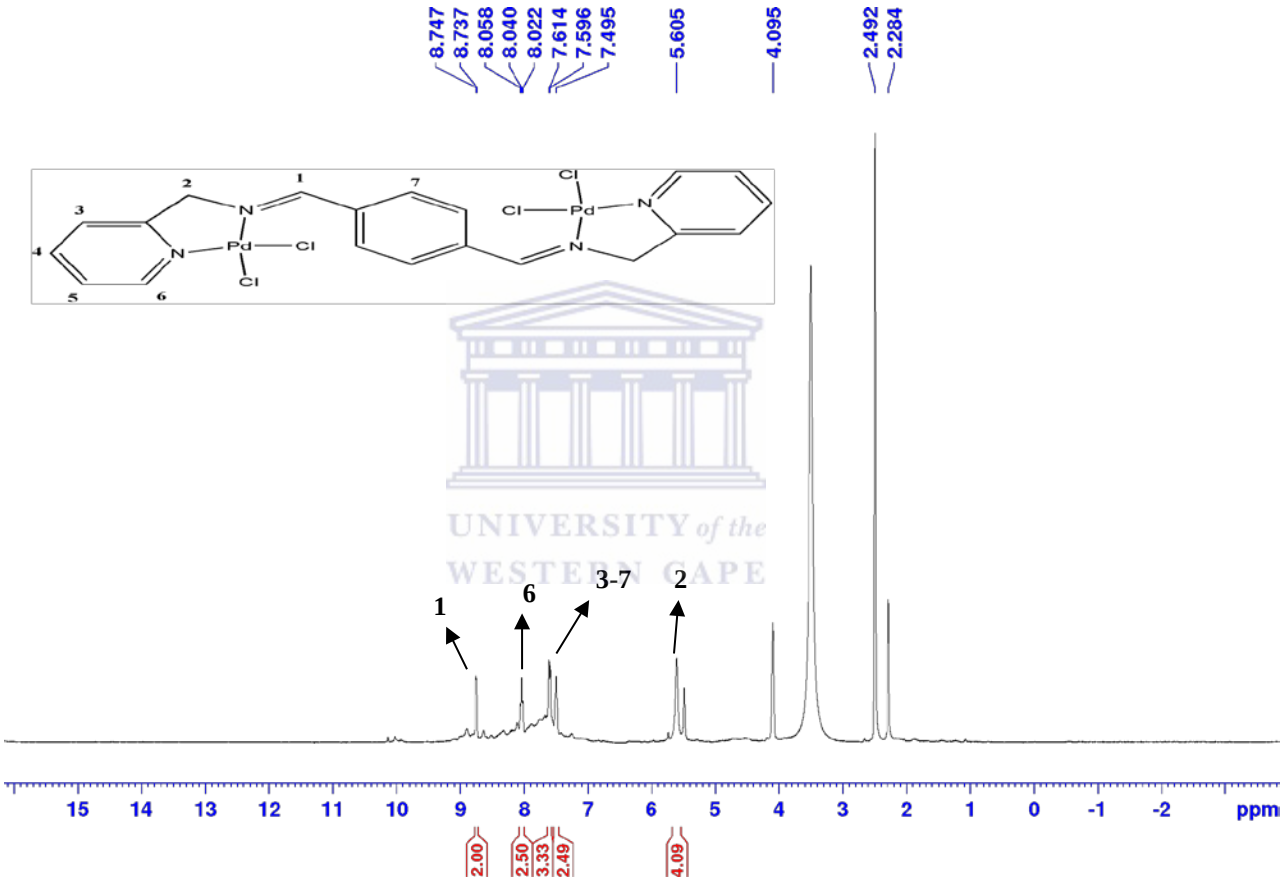

Figure 3.14: ^{1}H NMR spectrum of Tetrachloro-[pyridin-2-ylmethyl-{4-[(pyridin-2-ylmethylimino)-methyl]-benzylidene}-amine]dipalladium(II) (**C1**)

Table 3.10: ^{1}H NMR data of complexes **C1** and **C2**

Complex (solvent)	**H-1** **(ppm)**	**H-2** **(ppm)**	**H-3 (C2 only)** **(ppm)**
C1 (DMSO-d_6)	8.74 (s)	5.61	-
C2 (DMSO-d_6)	8.91 (s)	4.94	3.21

The iminopyridyl palladium (II) complexes showed proton singlets at 8.74 ppm and 8.91 ppm for complexes **C1** and **C2** respectively, which confirmed coordination of the nitrogen atoms to the metal centre. This showed a downfield shift from 8.50 ppm and 8.24 ppm for their ligands **L1** and **L2** respectively. The CH_2 proton signal of aliphatic methylene arm appeared as a singlet in the region 5.61 ppm for complex **C1** which is a downfield shift from the methylene protons of the free ligand which was at 4.92 ppm. The two signals due to an ethylene arm are assigned at 4.94 and 3.21 ppm for **C2** which indicate a downfield shift for both pairs of methylene protons from the ligand (4.00 ppm and 3.17 ppm respectively) with a more significant shift at H-2 from 4.00 to 4.94 [10]. One example in the literature where these shifts are typical for palladium-coordinated complexes can be found in a work by Radebe which reported a downfield shift from 8.41 ppm to 8.66 ppm for a complex similar to **C1** and a downfield shift was seen from 4.84 ppm to 5.30 ppm for the methylene arm [20]. In the same report a downfield shift was seen from 8.03 to 8.16 for the imine proton for a complex similar to **C2** as well as a downfield shift of the ethylene protons from 3.06 ppm and 3.86 ppm to 3.39 ppm and 4.09 ppm respectively [10].

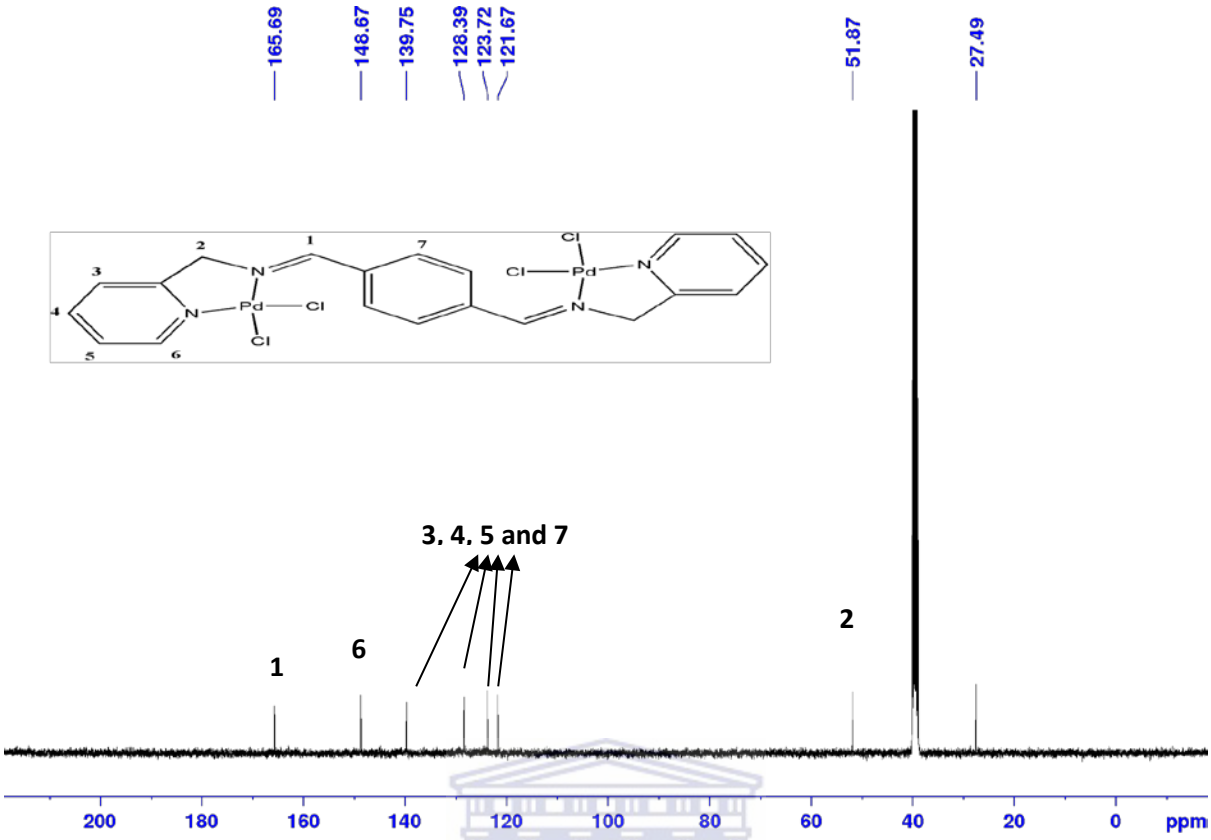

Figure 3.15: ^{13}C NMR spectrum of tetrachloro-[pyridin-2-ylmethyl-{4-[(pyridin-2-ylmethylimino)-methyl]-benzylidene}-amine]dipalladium(II) (**C1**)

Table 3.11: ^{13}C NMR data of key chemical shifts for complexes **C1** and **C2**

Complex (solvent)	**C-1 (ppm)**	**C-2 (ppm)**	**C-3 (C2 only) (ppm)**
C1 (DMSO-d_6)	165.7	51.9	-
C2 (DMSO-d_6)	158.4	37.3	36.4

In the ^{13}C NMR spectra, the imine carbons appeared in **C1** downfield in from its corresponding ligand **L1** with a shift from 162.5 ppm to 165.7 ppm. This shift is consistent with coordination of palladium to the iminopyridyl ligand and this can be confirmed by comparing it to a report by Radebe where the shift occurred from 159.3 ppm to 163.1 ppm for

a complex similar to **C1** [20]. The methylene carbon underwent an upfield shift from 67.0 ppm to 51.9 ppm. This is consistent with the report by Radebe where the methylene carbon underwent an upfield shift from 66.1 ppm to 64.6 ppm [20]. There was also an upfield shift for the imine carbon in **C2** from 163.8 ppm to 158.4 ppm. This is in contrast with the downfield shift reported for a complex similar to **C2** reported by Radebe which was from 159.5 ppm to 164.4 ppm [20]. This could possibly be due to the hemi-labile thiophene that was incorporated by Radebe while in this work there were no hemi-labile ligands used [20].

3.3.1.3 UV-Vis Studies of bimetallic Pd(II) complexes

The following spectrum (Fig 3.18) represents the UV-Vis spectrum of the bimetallic tetrahydrophenyl-linked iminopyridyl Pd(II) complexes prepared in this study. The other UV-Vis spectra for the ligands are given in Appendix 1. A summary of the λ_{max} values of the complexes **C1** and **C2** can be found in Table 3.12

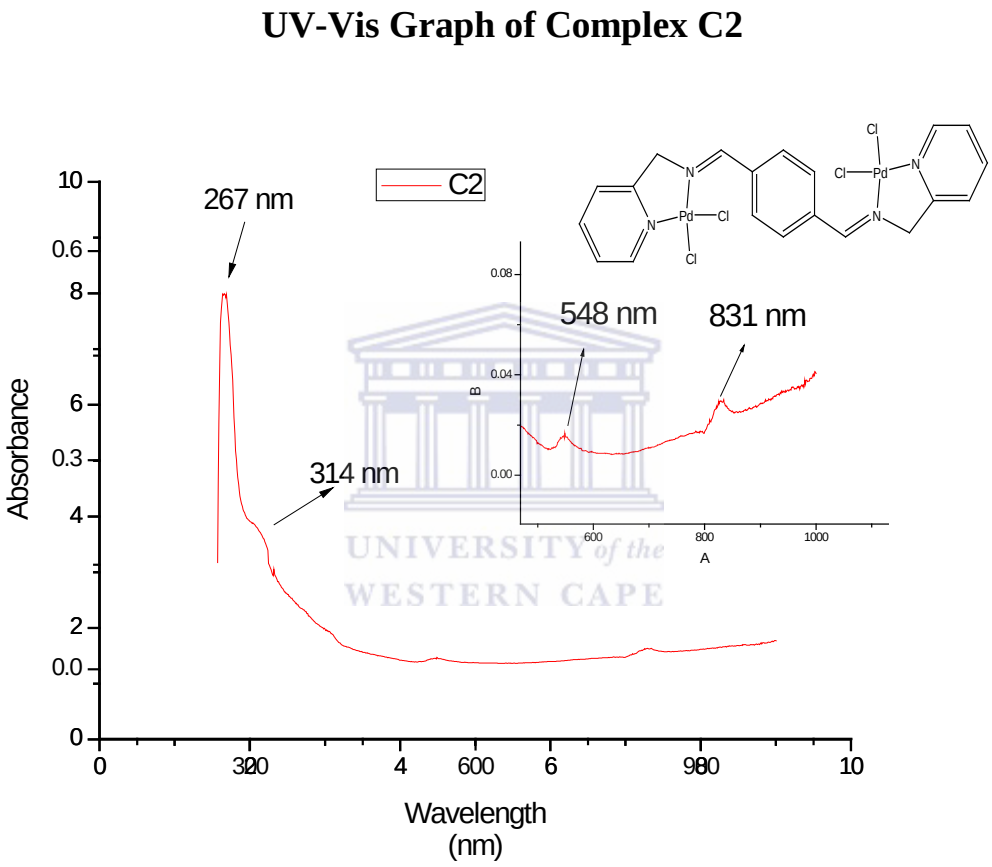

Figure 3.16: UV-Vis Spectrum of tetrachloro-[(2-Pyridin-2-yl-ethyl)-{4-[(2-pyridin-2-yl-ethylimino)-methyl]-benzylidene}-amine]dipalladium(II) (**C2**)

Table 3.12: Summary of UV-Vis data for ligands **C1** and **C2**

Complex	**λ_{max1}(nm)**	**λ_{max2}(nm)**
C1	264	549
C2	267	548

There were two significant peaks for both complexes **C1** and **C2**. Firstly there are peaks at 264 nm and 266 nm respectively. These represent the π to π^* transition of the aromatic rings. This is a blue-shift from the range of 272 nm - 273 nm for **L1** and **L2** which contrasts literature reports of red shifts from ligand to complex for similar compounds as is the case with Kubota *et al.* where the λ_{max} increased from 270 nm to 280 nm [16]. This is likely due to the nature of their respective ligands where Kubota *et al.* used a fluoride whereas with this work another iminopyridyl moiety was used [16]. In this work there was also a shoulder at 314 nm which was not observed in ligands **L1** and **L2** whereas in the report by Kubota *et al.* a shoulder was reported at 328 nm [16]. These both arise due to n to π^* transitions within the ligands, while the difference of 14 nm is most likely due to the different electronic natures of the ligands mentioned above [16].

There are also the peaks at 549 nm for both complexes, this is likely from metal-to-ligand ((Pd(dπ)-L(π*)) charge transfer transitions which in the report by Kubota *et al.* was 518 nm [16]. The differences are once again most likely due to the different electronic effects of the respective ligands on the metal centre [17].

3.3.1.4 TGA Studies of bimetallic Pd(II) complexes

The following spectrum (Fig 3.17) represents the TGA spectrum of the bimetallic tetrahydrophenyl-linked iminopyridyl complexes prepared in this study.

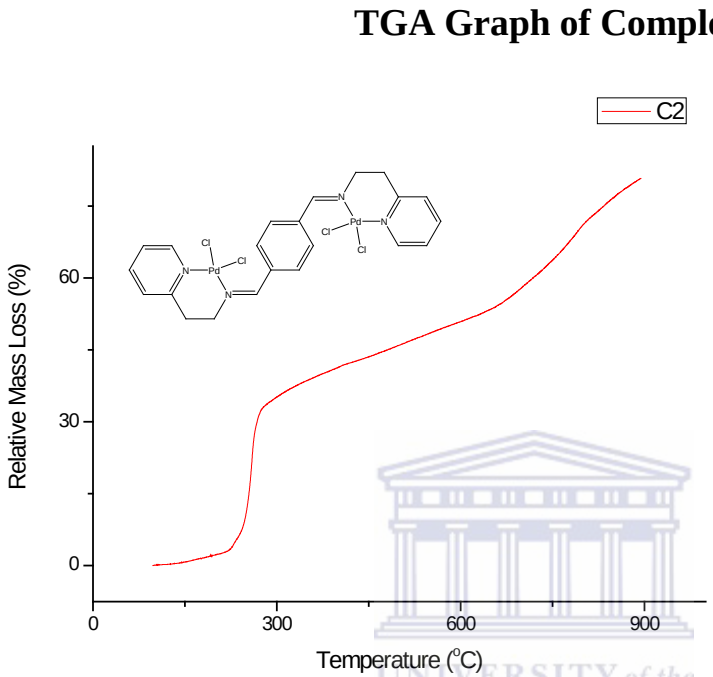

Figure 3.17: TGA Spectrum of tetrachloro-[(2-Pyridin-2-yl-ethyl)-{4-[(2-pyridin-2-yl-ethylimino)-methyl]-benzylidene}-amine]dipalladium(II) (**C2**)

The complex was initially stable from 25 °C to 220 °C. Afterwards it underwent at least three stages of decomposition. The first stage was from 220 °C to 274 °C with a relative mass loss of 32.3 %. This is most likely a loss of both iminopyridyl groups (calculated mass loss 37.9%). The second stage was from 274 °C to 654 °C and resulted in a further mass loss of 21.6% (a total loss of 53.9%). Based on the TGA spectrum of **L2** and the calculated loss value (a total of 49.0%), this is most likely the remaining ligand. The next stage was from 654 °C to 796 °C with a further relative mass loss of 16.7%, this most likely corresponds to the four chlorides (calculated loss 20.4%). The remaining two palladium fragments undergo

decomposition from 796 °C until beyond the set temperature range of 900 °C [14]. According to the report by Netalkar *et al.* the first stage of decomposition for a similar compound was from 225 °C – 250 °C where the chlorines were lost with reported values of 8.5 % [18]. For **C2** the initial loss was considered too high to come from the chlorides (with calculated mass loss of 16.7%), so it was deduced to come from the loss of the iminopyridyl groups. This was followed by the loss of the remaining ligand at 654 °C which is in agreement with the TGA of **L2** and the total mass loss percentage was similar to that of the literature compound(54%) [18].

3.3.1.5 Mass spectroscopic analysis of iminopyridyl palladium(II) complexes

Mass spectroscopy was used to characterize the bimetallic iminopyridyl palladium complexes **C1 – C2**. An example of the mass spectrum (Fig 3.18) and possible fragmentation pattern of **C2** (Scheme 3.4) are shown below. Due to insolubility problems with some of the compounds, it was necessary to carry out characterization such as mass spectrometry. The molecular weight ion peak is observed at m/z = 695. The scheme below showed a fragmentation pattern of a charged complex, with first fragmentation of a chloride ion coordinated to the palladium metal centre resulting to m/z = 659 ion peak, and then followed by the loss of another chloride peak showing an ion peak attributed at m/z = 623. Further fragmentation resulted in the first demetallation with an ion peak at m/z = 517. This followed a similar fragmentation pattern described in a work by Radebe where two chloride ions fragmented followed by the fragmentation of the metal (a loss of m/z = 106), which eventually resulted in the molecular ion of the original ligand [20]. This was followed by the loss of the remaining two chloride peaks with an ion peak at m/z = 447. Further fragmentation resulted in demetallation which leaves an ion peak at m/z = 343 which corresponds to the molecular ion peak of the ligand **L2**.

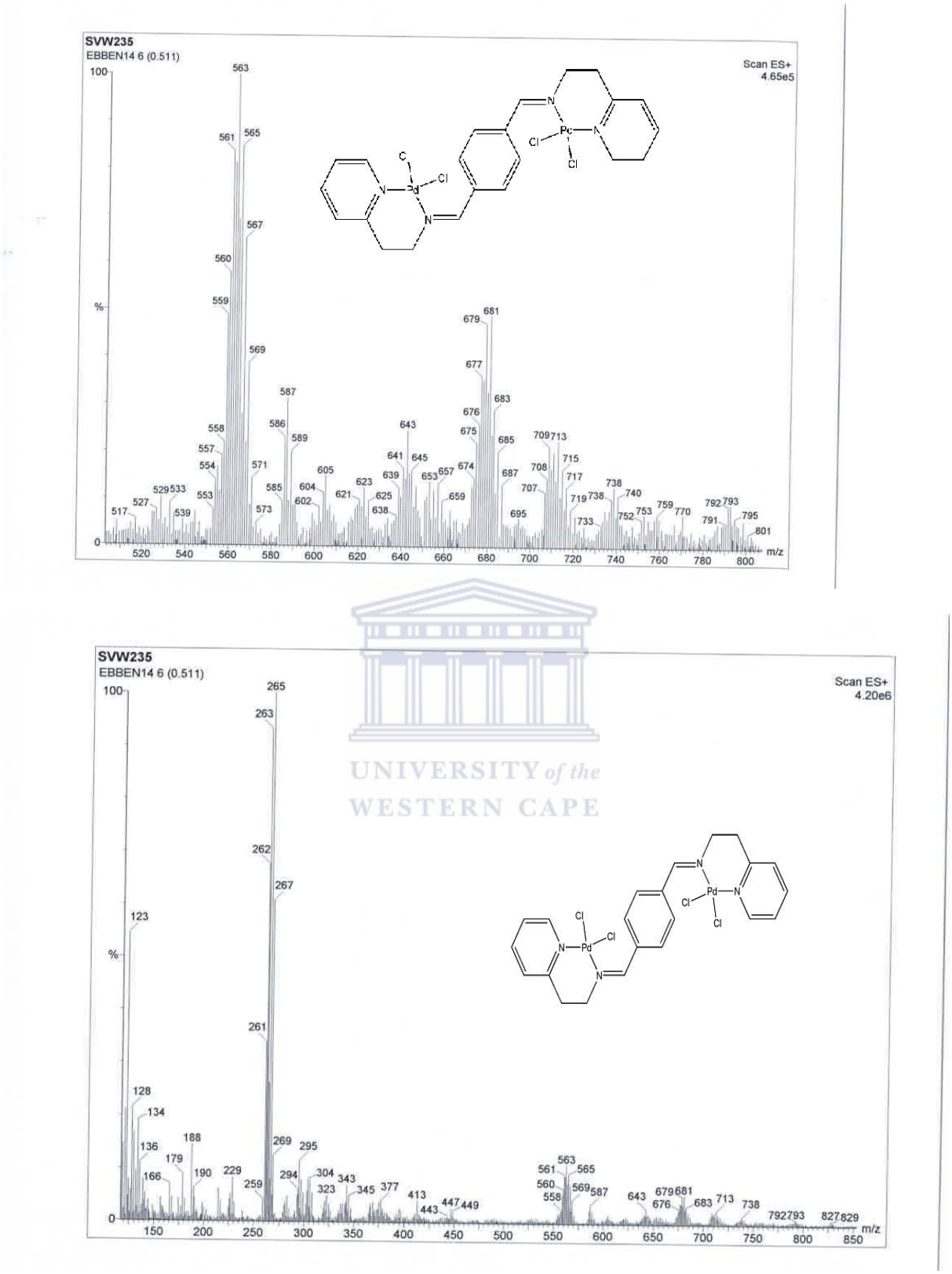

Figure 3.18: ESI-MS spectra of complex **C2**

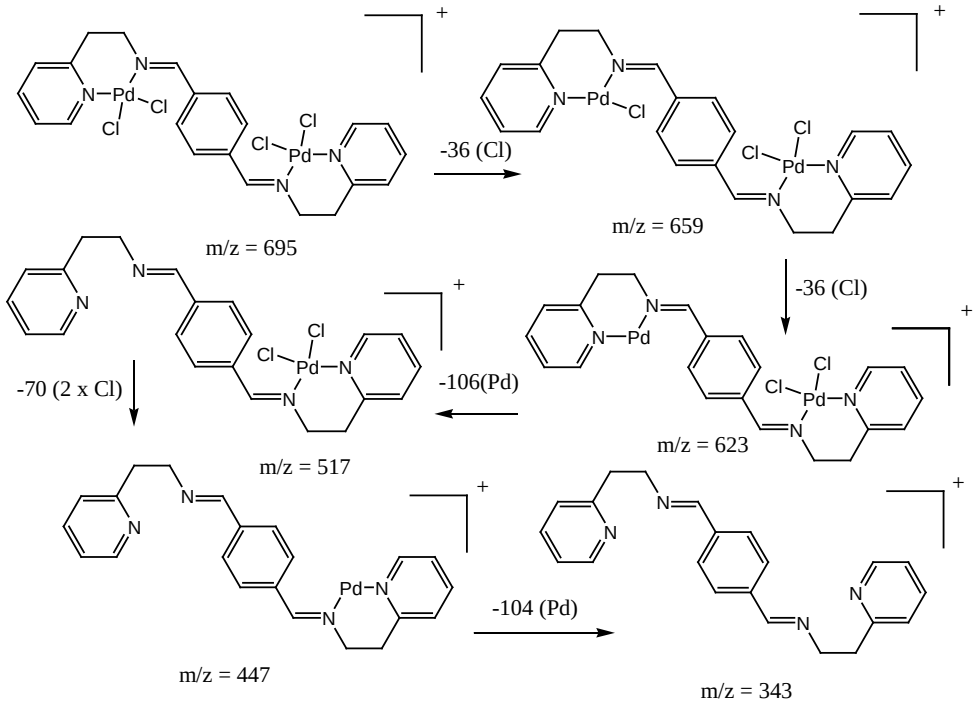

Scheme: 3.4: Possible fragmentation pattern for **C2**

3.3.2 Bimetallic Iminopyridyl Ni(II) complexes

The iminopyridyl nickel(II) complexes were synthesized by using mixed procedures of Pelletier *et al.* and Bahuleyan *et al*. (Scheme.5) [2, 21]. The ligands were reacted in 2 equivalent moles of either $NiCl_2$(DME) or $NiBr_2$(DME), which gave formation of new Ni(II) complexes [22]. All of the $NiCl_2$ complexes were isolated as blue or green solids. All the $NiBr_2$ complexes were isolated as brown or yellow solids. These complexes decompose in the temperature range of 105 ˚C – 225 ˚C. All of these complexes are only partially soluble in DMSO and insoluble in most organic solvents. The new complexes were characterized by: FTIR; elemental analysis; melting point and mass spectroscopy. Due to these complexes being paramagnetic, NMR could not be used as a characterization technique. Again these complexes have not been reported before to the best of our knowledge.

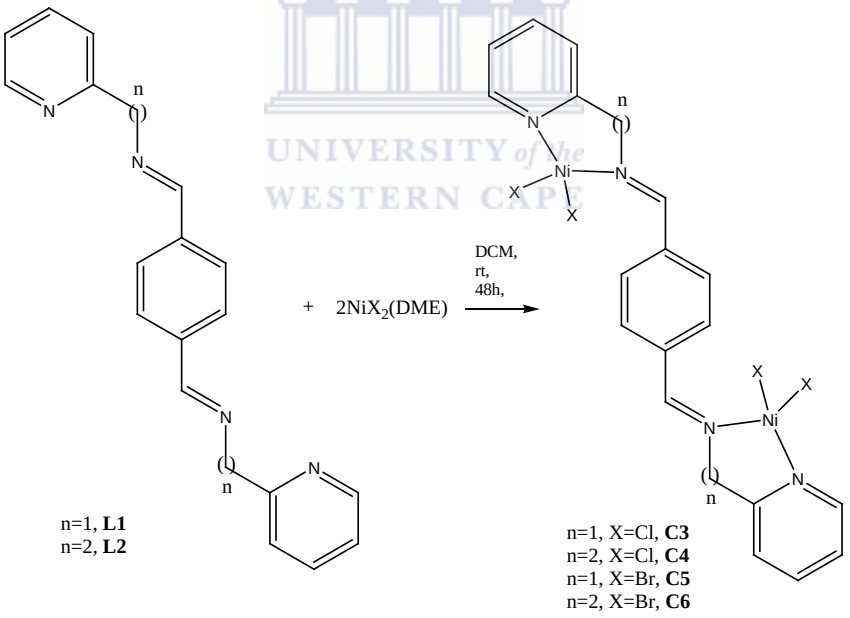

Scheme 3.5: Synthesis of tetrahydrophenyl-linked iminopyridyl nickel(II) complexes

3.3.2.1 FTIR studies of Bimetallic Iminopyridyl Ni(II) complexes

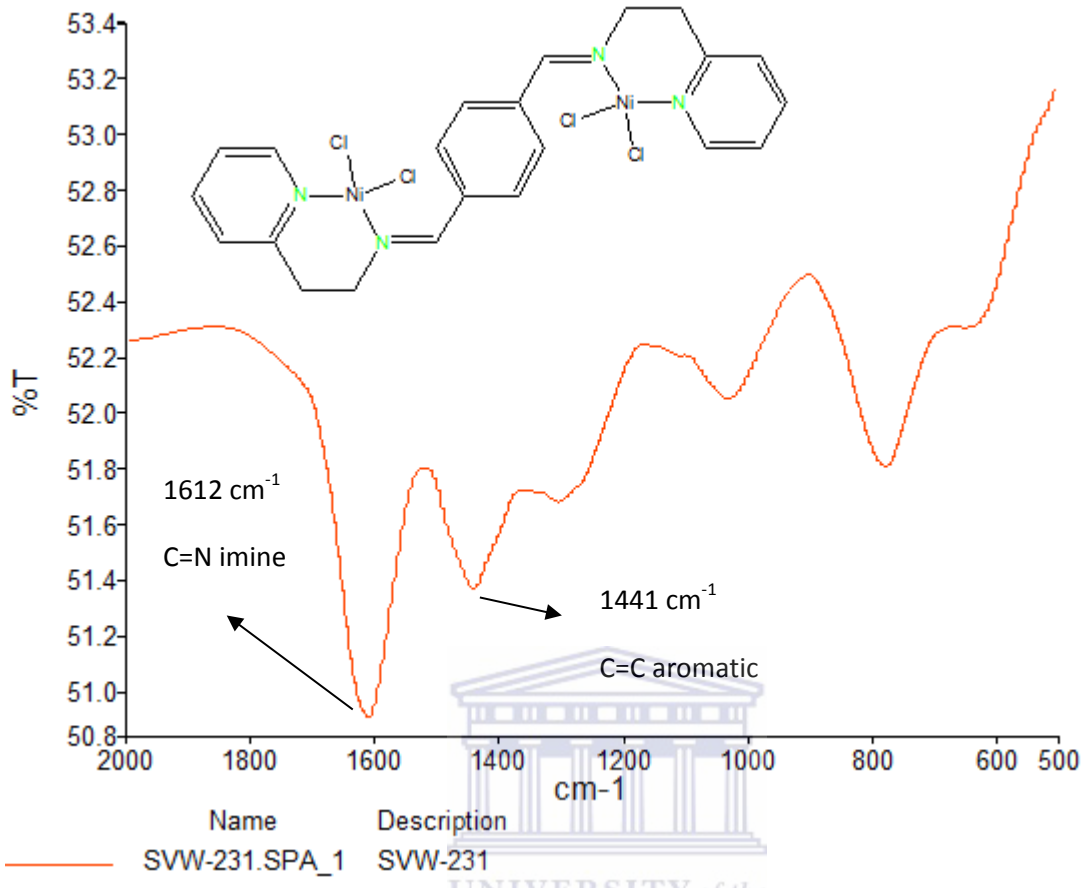

Figure 3.19: FTIR spectrum of complex **C4**

Table 3.13: Summary of FTIR data of complexes **C3-C6**

Complex	**%Yield**	**(C=N) cm^{-1}** ***Imine***
C3	94	1614
C4	73	1612
C5	66	1618
C6	61	1616

Infra-red spectra of all pyridyl-imine palladium complexes showed a red shift of the υ(C=N) band which occurs around 1640 - 1650 cm^{-1} in the free ligand and upon coordination occurs around 1614 cm^{-1} for **C3** and 1618 cm^{-1} for **C5** which is a shift of 27 cm^{-1} and 23 cm^{-1} respectively. This indicated that nickel(II) chloride coordinated more strongly to **L1** than nickel(II) bromide did. This was not as big a shift compared to the monometallic complexes synthesized by Motswainyana *et al.* where the wavenumber decreased from 1648 cm^{-1} to 1598 cm^{-1} from the ligand to the complex respectively [1]. This indicates that the coordination is not as strong in this work, which is likely due to the absence of a hemi-labile ligand whereas in the work by Motswainyana *et al.* a thiophene was incorporated as the hemi-labile ligand [1]. There was also a blue shift for complexes **C4** and **C6** from 1641 cm^{-1} for the free ligand to 1612 cm^{-1} and 1616 cm^{-1} respectively which once again indicated that nickel(II) chloride coordinated more strongly to **L2** than nickel(II) bromide did. Once again this was not as big a shift compared to the monometallic complexes synthesized by Motswainyana *et al.* where the wavenumber decreased from 1650 cm^{-1} to 1599 cm^{-1} from the ligand to the complex respectively [1]. A similar case could be made for the lack of a hemi-labile ligand [1]. Disappearance of the imino C=N absorption in the IR spectra might be ascribed to an inactive C=N vibration in the Ni (II) complexes as a result of coordination of the ligand to the metal centre as well as a reduction in electron density in the C=N bond arising from electron density flowing from the ligand to the metal centre. This can be corroborated using reports by Pelletier *et al.* and Bahuleyan *et al.* [2, 21].

3.3.2.2 UV-Vis Studies of bimetallic Ni(II) complexes

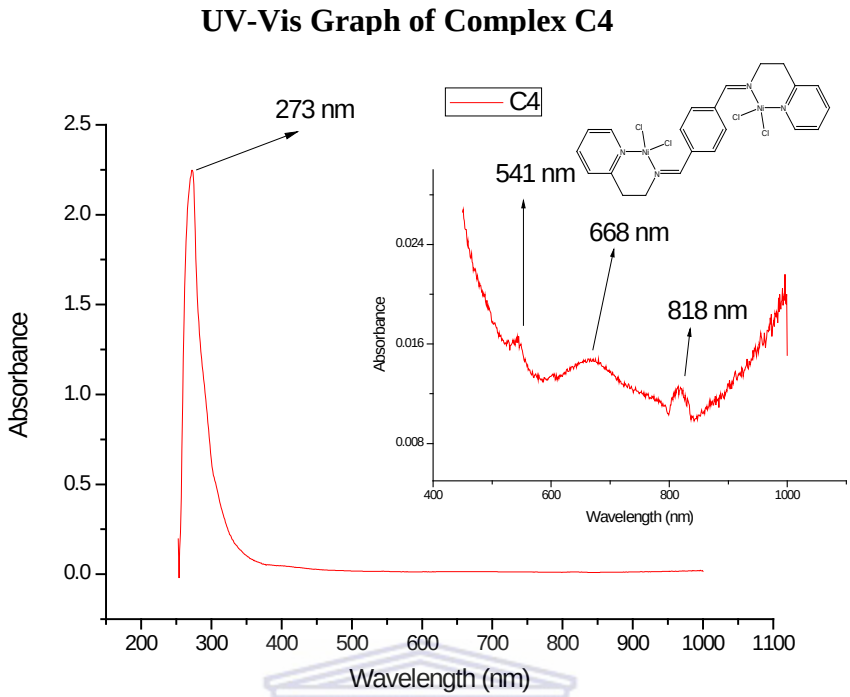

Figure 3.20: UV-Vis Spectrum of tetrachloro-[(2-Pyridin-2-yl-ethyl)-{4-[(2-pyridin-2-yl-ethylimino)-methyl]-benzylidene}-amine]dinickel(II) (**C4**)

Table 3.13: Summary of UV-Vis Data for **C3** and **C4**

Complex	**λ_{max1}(nm)**	**λ_{max2}(nm)**
C3	273	625
C4	273	668

The peaks at 273 nm are most likely from the π to π* transitions while the peaks around 668 nm are likely from metal-to-ligand ((Ni(dπ)-L(π*)) charge transfer transitions which in a report by Mandal *et al.* appears at around 652 nm [23]. This large difference shows how changing the linker between the two C=N by just one carbon can have a significant effect on coordination of nickel chlorides to iminopyridines.

3.3.2.4 Mass spectroscopic analysis of iminopyridyl nickel(II) complexes

Mass spectroscopy was used to characterize the bimetallic iminopyridyl nickel complexes **C3 – C6**. An example of the mass spectrum (Fig 3.23) and possible fragmentation pattern of **C6** (Scheme 3.6) are showed below. The molecular weight ion peak is observed at m/z = 782. The scheme below shows a fragmentation pattern of a charged complex, with first fragmentation of bromide ion coordinated to the nickel metal centre resulting to m/z = 702 ion peak, and then followed by the loss of another bromide as well as nickel showing an ion peak attributed at m/z = 561. This followed similar fragmentation pattern to a report by Radebe where first the two bromines are fragmented with two losses of m/z = 80 followed by the fragmentation of the metal with a loss of m/z = 80 eventually resulting in the molecular ion for the original ligand [20]. Further fragmentation resulted in a loss of another bromide with an ion peak at m/z = 481. This was followed by the loss of the remaining bromide peak with an ion peak at m/z = 401. Further fragmentation resulted in demetallation of the nickel centre attributed by an ion peak at 343 which corresponds to the molecular ion peak of the ligand **L2**.

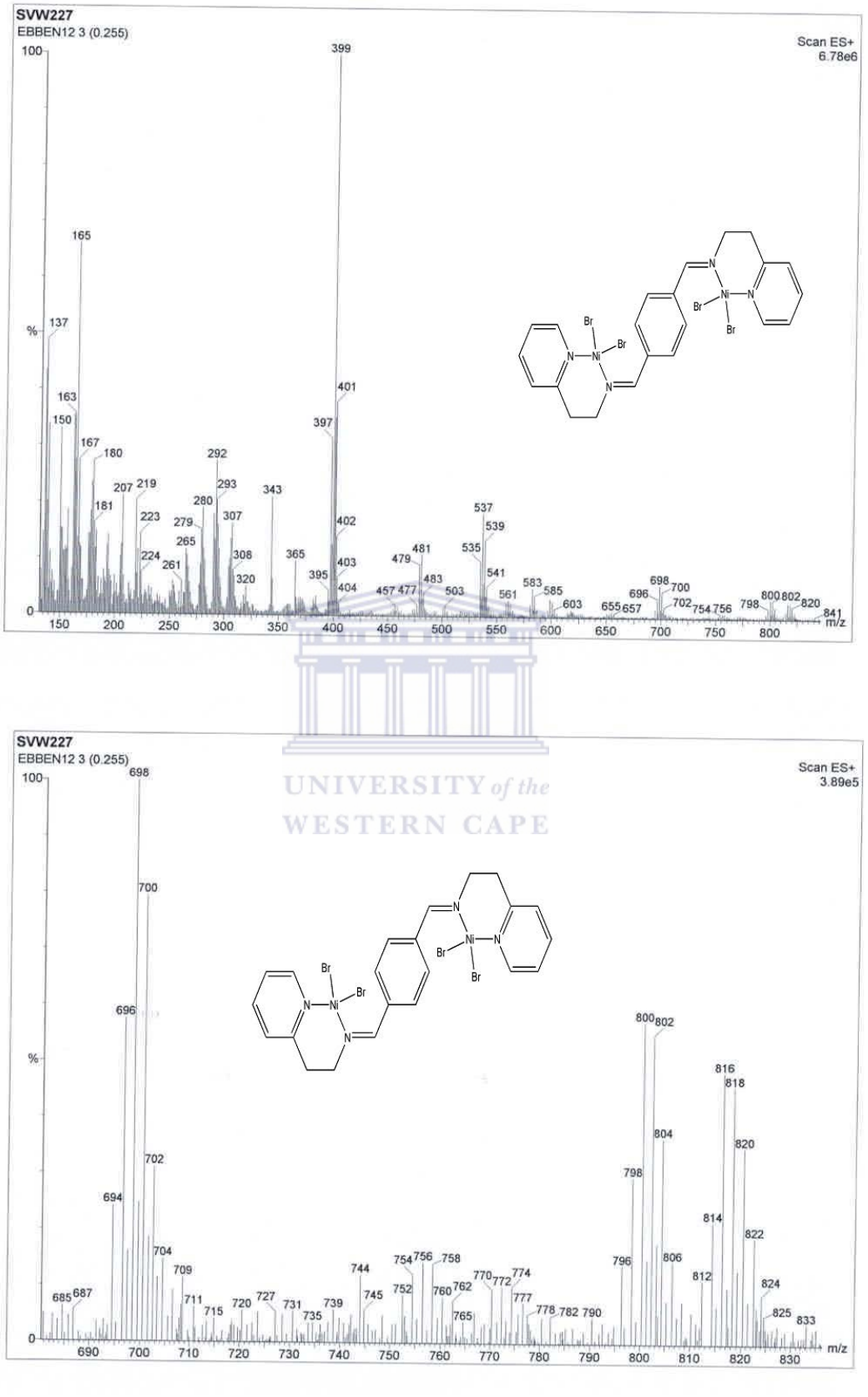

Figure 3.21: ESI-MS Spectra of **C6**

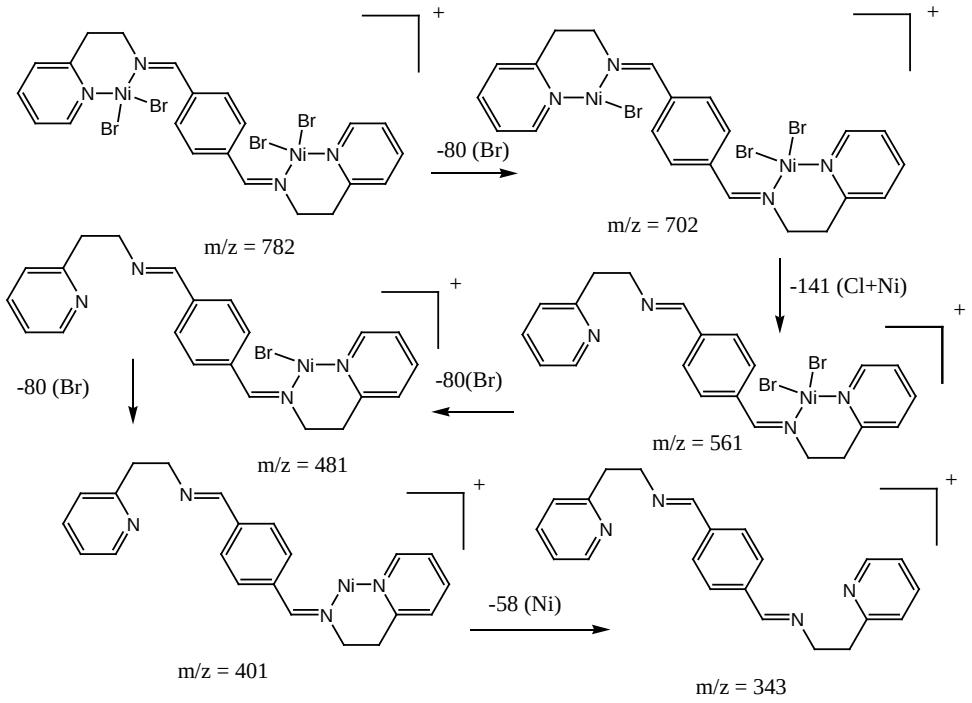

Scheme 3.6: Possible fragmentation pattern of **C6**

3.4 References

[1] Motswainyana, W.M., Onani, M.O., Ojwach, S.O., Omondi, B., *Inorg. Chim. Acta*, 2012, **397**, 93 - 97

[2] Pelletier, J.D.A., Fawcett, J., Singh, K., Solan, G.A., *J. Organomet. Chem.*, 2008, **693**, 2723 – 2731

[3] Ittel, S.D., Johnson, L.K., *Ittel*, M., *Chem. Rev.*, 2000, **100**, 1169 – 1204

[4] Gibson, V.C., Spitzmesser, S.K., *Chem. Rev.*, 2003, **103**, 283 – 316

[5] Ben Hadda, T., Daoudi, M., Aloui, S., Ben Larbi, N., Kerbal, A., Jalbout, A., *ARKIVOC*, 2007, **14**, 257 – 265

[6] Chiririwa, H., Moss, J.R., Su, H., Hendricks, D., Meijboom, R., *Acta Crystallogr. Sect. E: Struct. Rep. Online*, 2011, **67**, o921

[7] Sibanyoni, J.M., Bagihalli, G.B., Mapolie, S.F., *J. Organomet. Chem.*, 2012, **700**, 93-102

[8] Pelletier, G., Bechara, W.S., Charette, A.B., *J. Am. Chem. Soc.*, 2010, **132**, 12817 - 12819

[9] Velusamy, S., Ahamed, M., Punniyamurthy, T., *Org. Lett.*, 2004, **6**, 4821 - 4824

[10] Motswainyana, W.M., Ojwach, S.O., Onani, M.O., Iwuoha, E.I., Darkwa, J., *Polyhedron*, 2011, **30**, 2574 - 2580

[11] Rahaman, S.H., Fun, H.-K., Ghosh, B.K., *Polyhedron*, 2005, **24**, 3091 - 3097

[12] Lu, C., Xu, Z., Cui, J., Zhang, R., Qian, X., *Org. Lett.*, 2007, **72**, 3554 – 3557

[13] W. M. Motswainyana, MSc Thesis, University of the Western Cape, 2010

[14] Ma, G., McDonald, R., Ferguson, M., Cavell, R.G., Patrick, B.O., James, B.R., Hu, T.Q., *Organometallics*, 2007, **26**, 846 - 854

[15] Akhmetova, V.R., Vagapov, R.A., Nadyrgulova, G.R., Tyumkina, T.V., Starikova, Z.A.; Antipin, M.Y., Kunakova, R.V., Dzhemilev, U.M., *Tetrahedron*, 2007, **63**, 11702 – 11709

[16] Kubota, M., Covarrubias, D., Pye, C., Fronczek, F.R., Isovitsch, R., *J. Coord. Chem.*, 2013, **2013**, 1350 – 1362

[17] Dehghanpour, S., Mahmoudi, S., *Main Group Chem.*, 2007, **6**, 121 -130

[18] Netalkar, S.P., Navrekar, A.A., Revankar, V.R., *Catal. Lett.*, **144**, 1573-1583

[19] Wiedermann, J., Mereiter, K., Kirchner, K., *J. Mol. Cat. A: Chem.*, 2006, **257**, 67-71

[20] M. P. Radebe, MSc Thesis, University of the Western Cape, 2012

[21] Bahuleyan, B.K., Kim, J.H., Seo, H.S., Oh, J.M., Ahn, I.Y., Ha, C.-S., Park, D.-W., Kim, I., *Catal. Lett.*, 2008, **126**, 371 – 377

[22] Ward, L.G.L., *Inorg. Synth*, 1972, **13**, 154 -164

[23] Mandal, D., Abtab, S.M.T., Audhya, A., Tiekink, E.R.T., Endo, A., Clérac, R., Chaudhury, M., *Polyhedron*, 2013, **52**, 355 – 363

Chapter 4

4. Catalytic Application of the Iminopyridyl Complexes

4.1 Ethylene Oligomerization Reactions

4.1.1 Background

Catalysis can be described as an acceleration of a chemical reaction by lowering the activation energy of the process in the presence of a catalyst [1]. Catalysis has in the past few decades played a pivotal role in the industrial production of liquid fuels and fine chemicals. Homogeneous and heterogeneous catalytic processes have been used to form desired petrochemicals and fine chemicals products [1]. Homogeneous catalysis has become increasingly popular recently, this is true especially in certain C-C coupling reactions such as Heck coupling, Suzuki coupling and ethylene oligomerization/polymerization [2-4]. This section will focus on ethylene oligomerization/polymerization reactions. The catalytic reaction for the prepared Ni(II) and Pd(II) iminopyridyl complexes can be best represented by the following scheme (Scheme 1). The end products are known as oligoethylenes (C_4-C_{20}) and polyethylenes ($C_{>20}$). Polyethylene is the most common plastic known. Many kinds of polyethylene are documented, with most having the chemical formula $(C_2H_4)_n$. The annual global production is 80 million tons [5]. Polyethylene was first synthesized by the German chemist Hans von Pechmann who prepared it by accident in 1898 while investigating diazomethane [6-7].

They are mainly used in packaging. Polyethylenes are placed into many categories based mostly on density and branching but the most important ones are high density polyethylenes (HDPEs) [8a], low density polyethylenes(LDPEs) [8b] and linear low density polyethylenes(LLDPEs) [8c]. Their various uses are illustrated below (Fig 4.1 and Table 4.1).

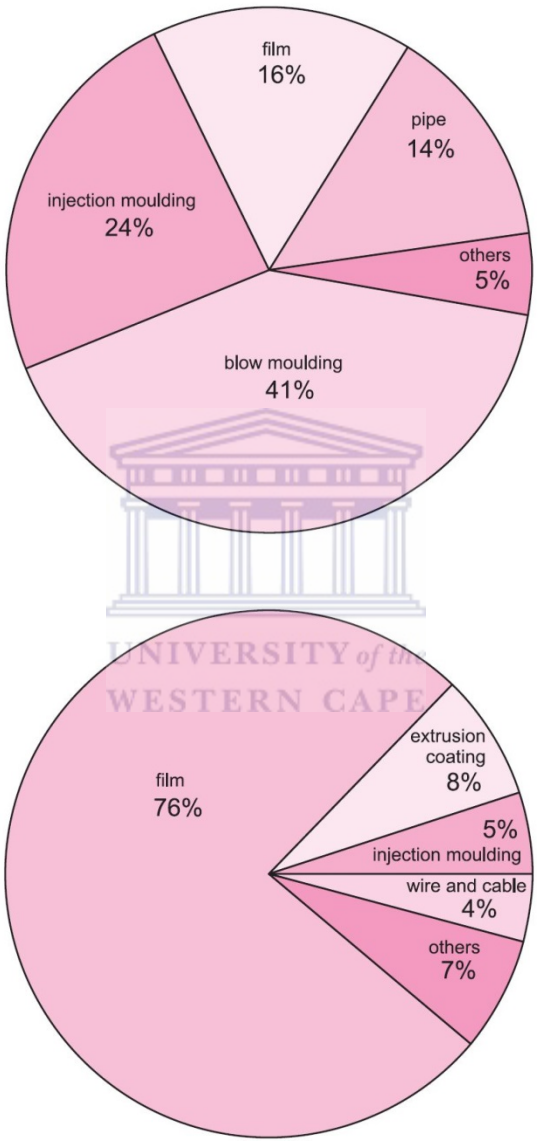

Figure 4.1: % distribution of processes of polyethylene for HDPE and LLDPE/LDPE [9]

Table 4.1: Main uses of polyethylene by type [9]

Process	HDPE	LDPE	LLDPE
Making film	Food packaging Shopping bags	Cling film Milk carton lining	Stretch film
Injection moulding	Dustbins Crates	Buckets Bowls	Food boxes
Blow moulding	Detergent bottles Drums	Squeezable bottles	
Extrusion	Water pipes	Flexible water pipes Cable jacketing	Cable coating

According to the first pie chart (Fig 4.1), HDPEs are mainly used in blow moulding, which according to Table 4.1 shows that it is mainly manufactured as detergent bottles and drums. As for LDPEs and LLDPEs, they are mainly used in making film, which leads to products such as cling film/milk carton lining and stretch film respectively.

Linear α-olefins (C_4-C_{20}) have been useful in industry as comonomers in production of LLDPEs. This is particularly true for C_4-C_8 oligomers. C_4-C_8 oligomers are also used to synthesize aldehydes for hydroformylation. The remaining oligomers were found to be useful in lubricants, surfactants and additives in synthesizing in plastic material using HDPE [10].

4.1.2 Mechanism of ethylene oligomerization/polymerization reaction

The first step of this mechanism is where the inactive form of the precatalyst undergoes migratory insertion of the alkyl ethylene. The next stage is either where trapping of the initially formed alkyl species by ethylene insertion resulting in chain growth or branching, alternatively before trapping and insertion, a series of β-hydride eliminations and re-additions could take place, leading to the metal migrating or walking along the polymer chain (in Scheme 1.7) [11]. The following section discusses our complexes which were successfully tested as ethylene oligomerization reactions.

4.2 Palladium(II) and Nickel(II) Iminopyridyl Complexes Catalyzed Ethylene Oligomerization reactions

Four bimetallic complexes were tested for catalytic activity of ethylene oligomerization, involving a palladium complex **C1** and three nickel complexes **C3**, **C5** and **C6** (As seen in Fig 4.2). The reaction scheme is illustrated in Scheme 4.3. The experimental data has been summarized in Table 4.2.

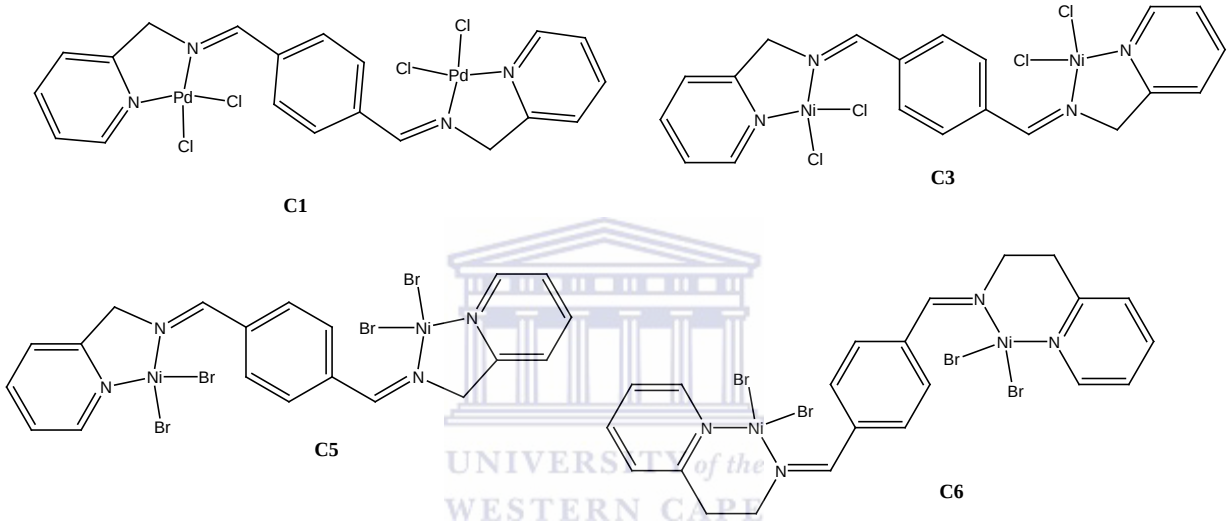

Figure 4.2: Bimetallic tetrahydrophenyl linked iminopyridyl Pd(II) and Ni(II) complexes.

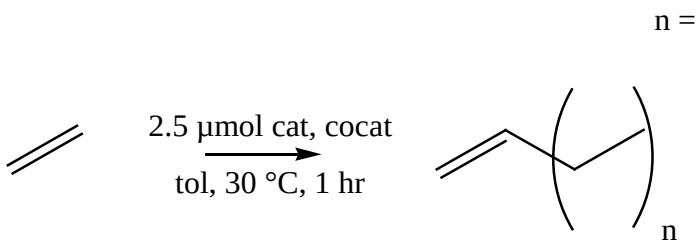

Scheme 4.1: Scheme for ethylene oligomerization reaction using nickel and palladium bimetallic precatalysts

Table 4.2: Ethylene oligomerization data for complexes **1, 3, 5** and **6**[a]

Entry	Catalyst	Al:M (M=Ni or Pd)	Pressure (bar)	Yield (g)	Activity[b]	%Oligomer distribution[c]		
						$C_4(\alpha\text{-}C_4)$	$C_6(\alpha\text{-}C_6)$	C_8
1	**1**	200	20	2.7	540	74(89)	26(92)	-
2	**3**	200	20	6.2	1 240	78(71)	19(23)	3
3	**5**	200	20	6.5	1 300	75(75)	20(26)	5
4	**6**	200	20	4.9	980	71(80)	26(21)	3
5	**3**	100	20	2.1	420	80(89)	16(26)	4
6	**3**	250	20	6.8	1360	77(72)	19(20)	4
7	**3**	200	10	3.6	720	70(76)	26(26)	4
8	**3**	200	30	14.3	2 860	81(73)	17(23)	2
9[d]	**1**	1 000	20	2.1	420	81(95)	19(87)	-
10[d]	**5**	1 000	20	4.0	800	72(69)	18(27)	10

[a] Reaction conditions: 5 µmol M; solvent, toluene, 80 mL; time, 1 h; temperature, 30 °C. [b] In kg-oligomer $mol.M^{-1}.h^{-1}$. [c] Determined by GC. [d] MAO as cocatalyst

The ethylene oligomerization reactions involve the reaction of the substrate ethene gas, Pd(II) or Ni(II) as the catalyst, MAO or EADC as the cocatalyst and toluene as the solvent.

Before ideal reaction conditions could be found, some trial reactions were carried out to find the best cocatalyst between ethyl aluminium dichloride (EADC) or methylaluminoxane (MAO). The activities of two complexes namely the palladium complex **C1** and **C5** were first checked (**Fig 4.3**), followed by their oligomer selectivity (**Fig 4.4**). It was found that using

EADC resulted in higher activity than MAO. As a result all four precatalysts were tested for catalytic activity of ethylene oligomerization using EADC as the cocatalyst, this is represented in **Fig 4.5**.

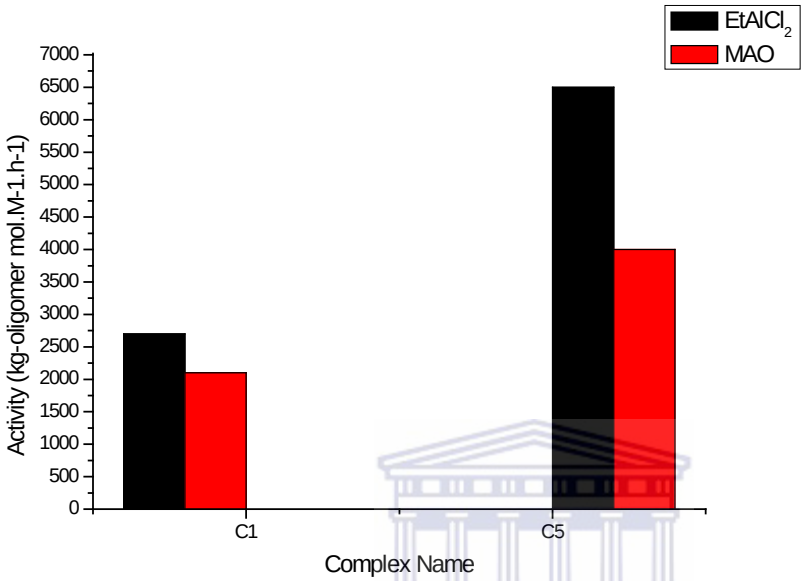

Figure 4.3: Activities of trial reactions involving **C1** and **C5** where EADC and MAO were used as cocatalysts

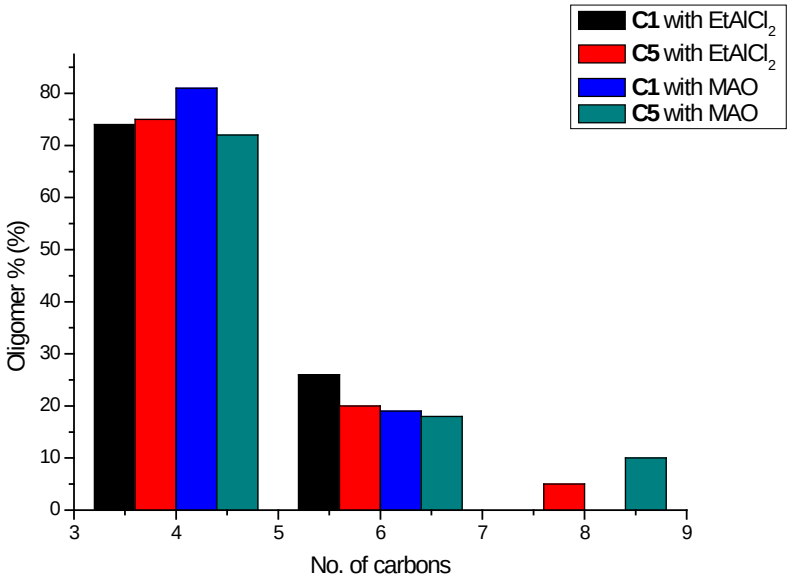

Figure 4.4: Oligomer selectivities of trial reactions involving **C1** and **C5** where EADC and MAO were used as cocatalysts

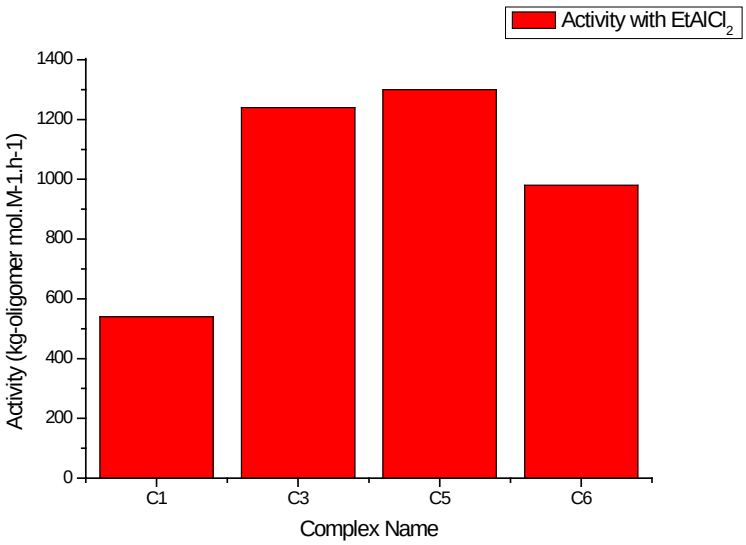

Figure 4.5: Bar graph of oligomerization activity when EADC is used as the cocatalyst

All four complexes were highly active as precatalysts for ethylene oligomerization reactions. The most active of them was **C5** while the least active was **C1**. One of the trends noticed was that the palladium precatalyst **C1** was less active than its nickel analogue **C3**. This is likely attributed to the energy barrier for ethylene insertion being lower for nickel complexes than for their palladium counterparts. Due to ethylene insertion being the turnover limiting step, the activity would thus be lower for palladium precatalysts than for nickel precatalysts. This theory can be corroborated using reports by Ittel *et al.* and Ivanchev [3, 11-14]. In a report involving similar compounds by Irrgang *et al.* the activities for the palladium(II) chlorides were found to range from 12-20 $kgmol_{cat}^{-1}h^{-1}bar^{-1}$ while their nickel(II) chloride analogues had activities that ranged from 140-156 $kgmol_{cat}^{-1}h^{-1}bar^{-1}$ [15]. With the nickel dibromide catalyst **C5** only having a slightly higher activity than its nickel chloride counterpart **C3**, this was unexpected since there were many literature reports in which a higher activity was achieved with the nickel chloride analogue [16-17]. An example of this can be found in a report by Nyamato *et al.* where the nickel(II) chloride precatalyst had an activity of 1072 kg-

oligomer mol.M^{-1}.h^{-1} while the nickel(II) bromide analogue achieved an activity of 871 kg-oligomer mol.M^{-1}.h^{-1} [16]. A possible explanation for the higher activity of the nickel(II) bromide can be found in a report by Mungwe [17]. It was pointed out that although chloride is a better leaving group than bromide and thus resulting in faster formation of vacant sites and active complexes, bromine is less electrophilic, which in turn makes it easier to remove leading to more active catalysts in theory [17]. One other trend that was noticed was that **C6** had a much lower activity than **C5** which indicates that the length of the spacer between the imine nitrogen and pyridyl nitrogen does have a significant effect on catalytic activity. When an ethylene spacer was used the activity was lower as opposed to a methylene spacer. This is likely due to the imines of the ligand in **C6** causing the metal centre to be less electrophilic due to itself being less nucleophilic. This notion of lower nucleophilicity is further corroborated using the ^{1}H NMR spectra for ligands **L1** and **L2** found in the **Appendix** and in the **Chapter 2** respectively. As a result it will not be able to donate electron density to the metal as well as **C5**. In turn the metal in **C6** will not be as strong a back donor to the π-acceptor ethylene group as **C5** [18]. In a report by Bluhm *et al.*, when the chain length was increased by one carbon the activity decreased from a turnover frequency of 9526 h^{-1} to 43 h^{-1} [19]. This trend is also observed in this work but the difference in altering the chain length was not nearly as vast. Due to this phenomenon migratory insertion is inhibited and activity is lowered.

The catalytic activity of these precatalysts in ethylene oligomerization reactions can be summarized in the order of increasing magnitude when EADC is used as the cocatalyst:

C5 > **C3** > **C6** > **C1**

The oligomer selectivity was then determined using GC-MS (**Fig 4.6**). All precatalysts produced oligomers not longer than C_8 with stronger selectivity for C_4 oligomers. This is likely due to there being no bulky groups *ortho* to the imine nitrogens. This aided chain

termination and thus the lower molecular weight. There was generally a high degree of branching for the C_4 oligomers, but for C_6 oligomers there was a low degree of branching. This was also likely due to the lack of steric bulk *ortho* to the imine nitrogens. The data is summarized in **Table 4.3** and **Fig 4.7**.

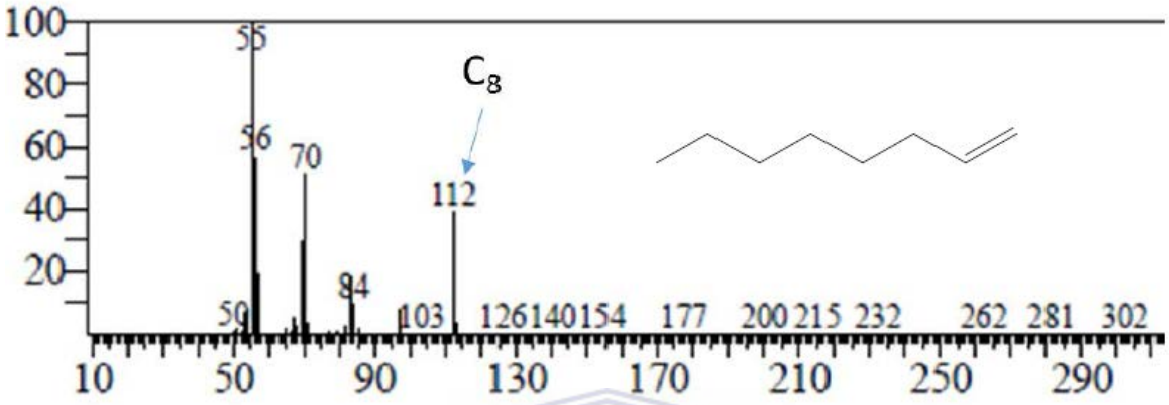

Figure 4.6: GC-MS spectrum of the product formed using catalyst **5** at 30 °C and 20 bar for 1 h confirming the formation of octene.

Table 4.3: Ethylene oligomerization selectivity data for complexes **C1, C3, C5** and **C6**[a]

Entry	Catalyst	Al:M	Pressure (bar)	MW[b] (g.mol^{-1})	%Oligomer distribution[c]		
					C_4(α-C_4)	C_6(α-C_6)	C_8
1	**1**	200	20	63.4	74(89)	26(92)	-
2	**3**	200	20	63.1	78(71)	19(23)	3
3	**5**	200	20	64.5	75(75)	20(26)	5
4	**6**	200	20	65.1	71(80)	26(21)	3

[a] Reaction conditions: 5 µmol M; solvent, toluene, 80 mL; time, 1 h; temperature, 30 °C. [b] Weighted average.
[c] Determined by GC.

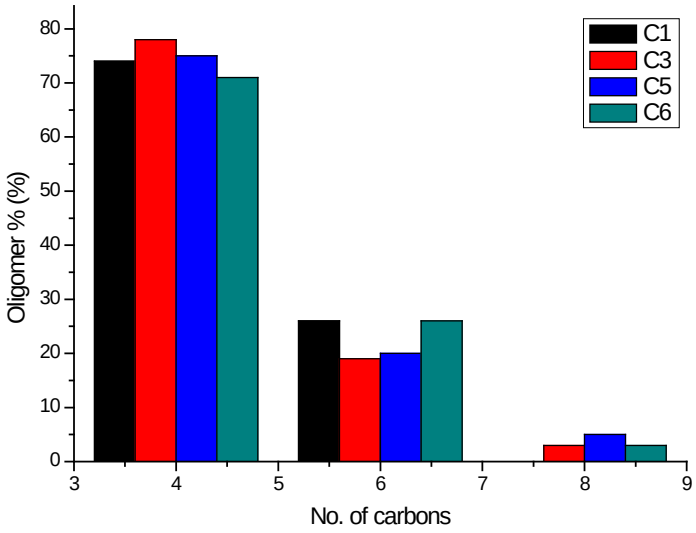

Figure 4.7: Graph of oligomer selectivity for **C1**, **C3**, **C5** and **C6** when EADC is used

When comparing the effects of the metal it was found that **C1** and **C3** have similar molecular weights but **C3** has a higher selectivity for C_8 oligomers than **C1**. In fact **C1** does not produce any C_8 oligomers. There was also a higher degree of branching that resulted from **C1** than **C3**. This was particularly the case for C_6 oligomers. This phenomenon is likely due to the agostic metal alkyl species undergoing numerous β-hydrogen eliminations and additions. This phenomenon is referred to as metal migrating or "chain walking". This was expected to be the case as can found in reports by Ittel *et al.* and Ivanchev [3, 11-14]. This is in agreement with a report by Johnson *et al.* where the branching decreased from 116 branches per 1000 carbons to 6 branches per 1000 carbons for the palladium and nickel catalysts respectively [13]. There were no significant differences when the halides were used, only a slight increase in molecular weight and selectivity for C_8 oligomers, as well as slightly more branching when the bromide **C5** was used compared to the chloride **C3**. In precatalysts **C5** and **C6**, it was found that **C6** produced higher molecular weight polymers while **C5** resulted in higher selectivity for C_8 oligomers. The former phenomenon was possibly due to the larger ethylene

spacer in **C6** found *ortho* to the pyridyl nitrogen donor compared to the methyl spacer found in **C5**. This would have led to inhibition of chain termination, hence the lower molecular weight. The latter phenomenon is likely due to the six-membered ring about the metal centre in **C6** being less stable than the five-membered ring found in **C5** due to the chelate effect of five-membered rings containing metals. This could have led to **C6** destabilizing more often before the third oligomerization cycle is reached.

To summarize the average molecular weights of the oligomers produced by these precatalysts are in the following order when EADC is used as the cocatalyst:

C6 > **C5** > **C3** > **C1**

Due to **C3** and **C5** being most active precatalysts as well as having similar activities, it was decided to carry out the optimization on **C3** only. The following effects were explored namely: pressure effects and Al:M ratio

Pressure effects

The catalytic activities and oligomer selectivities of **C3** were studied by varying the pressure to 10, 20 and 30 bar using EADC as the cocatalyst. The data is summarized in **Table 4.4**

Table 4.4: Activity and oligomer selectivities for at various pressures[a]

Entry	Catalyst	Al:M	Pressure (bar)	Yield (g)	Activity[b]	%Oligomer distribution[c]		
						$C_4(\alpha\text{-}C_4)$	$C_6(\alpha\text{-}C_6)$	C_8
1	**3**	200	10	3.6	720	70(76)	26(26)	4
2	**3**	200	20	6.2	1 240	78(71)	19(23)	3
3	**3**	200	30	14.3	2 860	81(72)	17(23)	2

[a] Reaction conditions: 5 µmol M; solvent, toluene, 80 mL; time, 1 h; temperature, 30 °C. [b] kg-oligomer mol.M^{-1}.h^{-1}. [c] Determined by GC.

The pressure effects on catalytic activity are represented in **Fig 4.8**

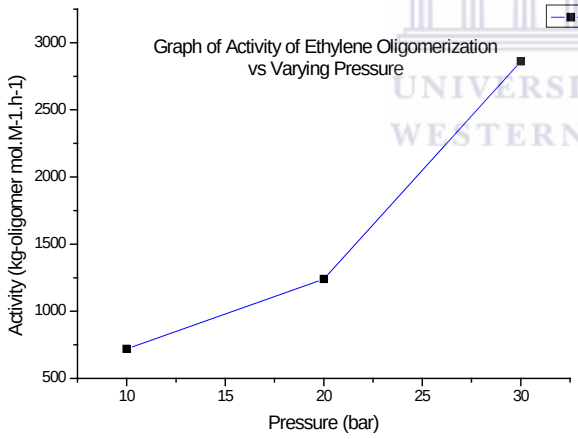

Figure 4.8 Catalytic activity of **C3** at various pressures

It was found that the activity increased as the pressure increased, especially when the pressure was increased from 20 to 30 bar where the activity more than doubled. This is likely due to the higher pressure aiding ethylene trapping. This in turn aids chain propagation [12]. This is in agreement with experiments carried by Nyamato *et al.* where the activities were 473 kg-oligomer mol.M^{-1}.h^{-1}, 1072 kg-oligomer mol.M^{-1}.h^{-1}, 1743 kg-oligomer mol.M^{-1}.h^{-1}

and 2462 kg-oligomer mol.M^{-1}.h^{-1} when the pressures were 5 bar, 10 bar, 20 bar and 30 bar respectively [16]. From 5-20 bar the activities from Nyamato *et al.* were higher than the values achieved in this work but at 30 bar the activities in this work were higher [16].

The effects on the activity on **C3** can be summarized in the following way:

30 bar > 20 bar > 10 bar

The pressure effects on oligomer selectivity are represented in **Fig 4.9**

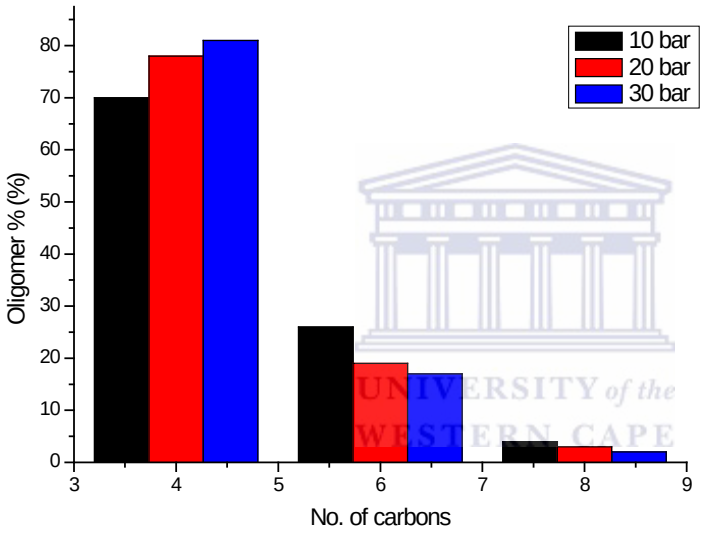

Figure 4.9: Oligomer selectivities resulting from **C3** at various pressures

It was found that the highest molecular weight and selectivity for C_8 oligomers was achieved at 10 bar (65.65 g.mol^{-1} and 4% respectively). The selectivity towards C_4 increased as pressure increased. In fact as the pressure increased, the molecular weight, C_8 oligomer selectivity and branching decreased. This is likely due to the increased pressure aiding trapping of ethylene while overcoming chain transfer. The results and this notion are in agreement with a report by Johnson *et al.* where the branching when α-diimine nickel

complexes decreased from 24 branches per 1000 carbons to 5 branches per 1000 carbons when the pressure was increased from 1 atm to 4 atm [13].

To summarize the average molecular weights of the oligomers produced by **C3** are in the following order:

10 bar > 20 bar > 30 bar

Effects of Al:Ni ratio

Table 4.5: Activity and oligomer selectivities for **C3** at various Al:Ni ratios[a]

Entry	Catalyst	Al:Ni	Pressure (bar)	Yield (g)	Activity[b]	%Oligomer distribution[c]		
						$C_4(\alpha\text{-}C_4)$	$C_6(\alpha\text{-}C_6)$	C_8
1	**3**	100	20	2.1	420	80(89)	16(26)	4
2	**3**	200	20	6.2	1 240	78(71)	19(23)	3
3	**3**	250	20	6.8	1 360	77(72)	19(20)	4

[a] Reaction conditions: 5 µmol M; solvent, toluene, 80 mL; time, 1 h; temperature, 30 °C. [b] kg-oligomer $mol.M^{-1}.h^{-1}$. [c] Determined by GC.

The effects on catalytic activity are represented by **Fig 4.10**

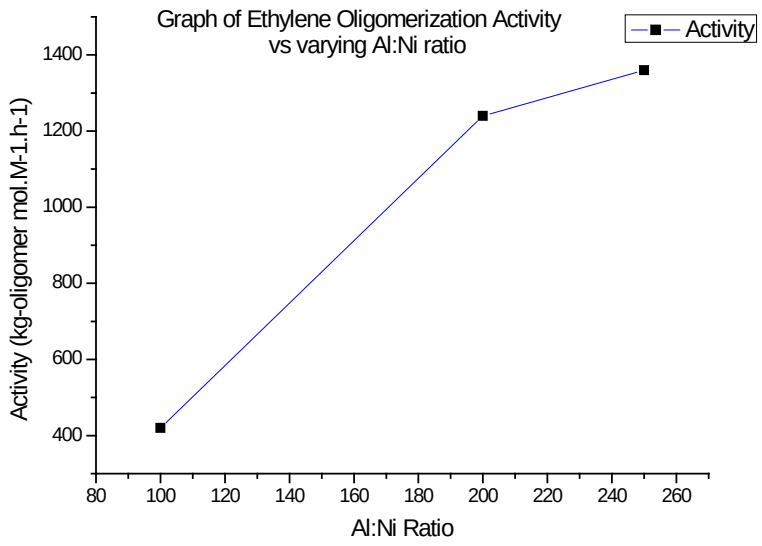

Figure 4.10: Catalytic activity of **C3** at various Al:Ni ratios

When the Al:Ni was increased from 100 to 200 the activity nearly tripled from 420 kg-oligomer mol.$M^{-1}.h^{-1}$ to 1240 kg-oligomer mol.$M^{-1}.h^{-1}$ while it plateaued from 1240 kg-oligomer mol.$M^{-1}.h^{-1}$ to 1360 kg-oligomer mol.$M^{-1}.h^{-1}$. From this it can be determined that 250 is the ideal Al:Ni ratio for ethylene oligomerization.

The activity effects on **C3** can summarized in the following way in terms of Al:Ni ratios:

$$100 << 200 < 250$$

The effects on oligomer selectivity are represented by **Fig 4.11**

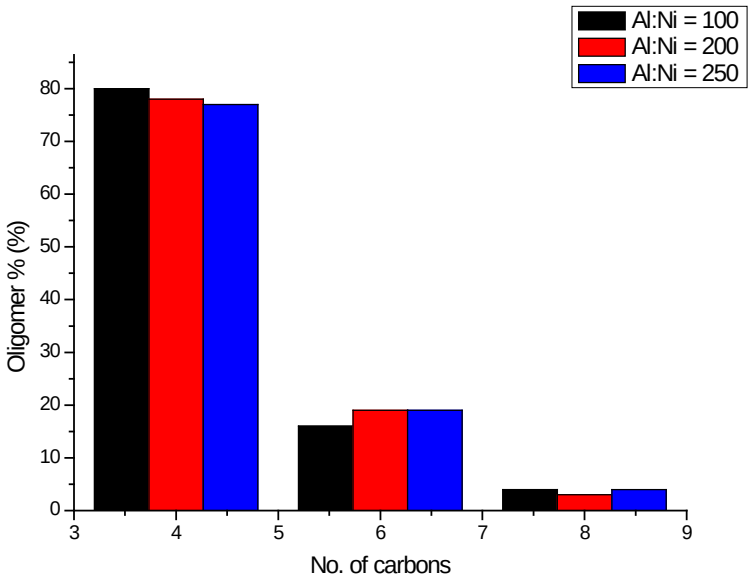

Figure 4.11: Oligomer selectivities resulting from **C3** at various Al:Ni ratios

While studying these effects there was no significant change in the molecular weight when the Al:Ni ratio was varied. Selectivity for C_8 oligomers as well as branching decreased as the Al:Ni ratio increased. The only significant change was that there was less branching as the Al:Ni ratio was increased. This indicates that increasing the Al:Ni ratio somehow inhibited chain transfer [20]. When comparing this to a report by Wang *et al.* where the Al:Ni ratios were 200, 400, 600, 800 and 1000 the selectivity towards C_4 increased (79.1%, 84.4%, 87.0, 88.4% and 89.0%) while in this work selectivity for C_4 decreased when the Al:Ni increased from 100 to 250 [20]. This decrease was possibly due to an excessive amount of cocatalyst interfering with formation of the active metal species and/or caused their over-reduction which caused the lower selectivity [20].

4.3 References

[1] van Leeuwen, P.W.N.M., *Homogeneous Catalysis, Understand the Art*., **2005**, Kluwer Academic Publishers, p 1-28.

[2] Motswainyana, W.M., Onani, M.O., Ojwach, S.O., Omondi, B., *Inorg. Chim. Acta*, 2012, **397**, 93 - 97

[3] Domin, D., Benito-Garagorri, D., Mereiter, K., Frohlich, J., Kirchner, K., *Organometallics*, 2005, **24**, 3957 – 3965

[4] Bahuleyan, B.K., Lee, U., Ha, C.-S., Kim, I., *Appl. Catal., A: Gen.*, 2008, **351**, 36 - 44

[5] Piringer, O.G., Baner, A.L., *Plastic Packaging: Interactions with Food and Pharmaceuticals*, **2008**, Wiley-VCH, Weinheim, 2nd edn., p 32

[6] von Pechmann, H., *Chem. Ber*., 1898, **31**, 2640 - 2646

[7] Bamberger, E., Tschirner, F., *Chem. Ber*., 1900, **33**, 955 – 959

[8] (a) *Market Study: Polyethylene – HDPE*, Ceresana, Constance, Germany, 2015, pp. 1

(b) *Market Study: Polyethylene – LLDPE*, Ceresana, Constance, Germany, 2014, pp. 1

(c) *Market Study: Polyethylene – LDPE*, Ceresana, Constance, Germany, 2014, pp. 1

[9] The Essential Chemical Industry Online, http://www.essentialchemicalindustry.org/polymers/polyethene.html, (Accessed September 2015)

[10] D. Vogt, *Oligomerization of Ethylene to Higher Linear α-Olefins. In Applied Homogeneous Catalysts with Organometallic compounds*, VCH, New York, 1996.

[11] Ittel, S.D., Johnson, L.K., *Ittel*, M., *Chem. Rev.*, 2000, **100**, 1169 – 1204

[12] Ivanchev, S.S., *Russ. Chem. Rev.*, 2007, **76**, 617 – 637

[13] Johnson, L.K., Killian, C.M., *Ittel*, M., *J. Am. Chem. Soc.*, 1995, **117**, 6414 – 6415

[14] Tempel, D.J., *Ittel*, M., *Organometallics*, 1998, **17**, 2290 – 2296

[15] Irrgang, T., Keller, S., Maisel, H., Kretschmer, W., Kempe, R., *Eur. J. Inorg. Chem.*, 2007, **2007**, 4221 – 4228

[16] Nyamato, G.S., Ojwach, S.O., Akerman, M.P., *J. Coord. Chem.*, 2014, **394**, 274 - 282

[17] N.W. Mungwe, MSc thesis, University of the Western Cape, 2007

[18] W. M. Motswainyana, MSc Thesis, University of the Western Cape, 2010

[19] Bluhm, M.E., Folli, C., Walter, O., Döring, M., *J. Mol. Catal. A: Chem.*, 2005, **229**, 177 – 181

[20] Wang, T, Dong, B., Mao, G.-L., Jiang, T., *J. Organomet. Chem.*, 2015, in press, 1 - 5

Chapter 5

5. Conclusion and recommendations

5.1 Conclusion

The study involved synthesis of new iminopyridyl palladium (II) and nickel (II) complexes which could act as catalysts for Heck coupling reactions. Tetrahydrophenyl-linked iminopyridyl ligands **L1 – L2** were successfully synthesized and obtained as a white and yellow solid respectively in good yields from 69-87%. They were observed to be air and moisture stable, but light sensitive. Alkyl-linked iminopyridyl ligands **L3 – L5** were successfully synthesized with two of them obtained as red oils and one of them as an orange solid in low to moderate yields from 25-50%. These compounds were fully characterized by FTIR, ^{1}H NMR spectroscopy, ^{13}C NMR spectroscopy, mass spectroscopy, and elemental analysis.

The formation of the ligands **L1 – L5** was confirmed by the presence of an imine absorption band around 1641 - 1655 cm^{-1} in the IR spectra. ^{1}H NMR further confirmed the formation of the imine moiety (**H**C=N) by observing proton signals at around 8.20 to 8.55 ppm (singlet) and around 8.40 to 8.63 ppm (doublet) attributed to pyridyl ring imine proton. The ^{13}C NMR spectra showed imine carbons downfield chemical shifts around 160.00 – 165.00 ppm and mass spectra of the synthesized compounds were in good agreement with the calculated molecular weight m/z values.

The ligands were reacted with two molar equivalents of $PdCl_2$(COD), $NiCl_2$(DME), and $NiBr_2$(DME) to give palladium (II) and nickel complexes **C1 – C6** in moderate to high yields of 58-93%. All the complexes were observed to be stable both as solid and in liquid. The iminopyridyl complexes were characterized by FTIR, ^{1}H NMR spectroscopy, ^{13}C NMR

spectroscopy, thermogravimetric analysis, mass spectroscopy and elemental analysis. Coordination of the ligands to the metal centre was confirmed by red shift of the imine absorption band to around 1612 – 1619 cm^{-1} respectively. The proton NMR analysis of complex **C1 – C2** showed a proton signal in the region of 8.74 – 8.91 ppm as a singlet peak which provided evidence of coordination of ligand to the metal.

Iminopyridyl nickel (II) complex **C3 – C6** could not be analyzed using NMR spectroscopy suggesting that they were paramagnetic. Mass spectroscopic analyses were in good agreement with the calculated molecular weight of all analyzed the iminopyridyl complexes.

All four complexes were highly active as catalysts for ethylene oligomerization. They were most active when EADC was used as the cocatalyst compared to MAO. **C5** was the most active (1300 kg-oligomer mol.M^{-1}.h^{-1}), followed by **C3** (1240 kg-oligomer mol.M^{-1}.h^{-1}), **C6** (980 kg-oligomer mol.M^{-1}.h^{-1}) and lastly the palladium complex **C1** (540 kg-oligomer mol.M^{-1}.h^{-1}). All four complexes had good selectivity for C_4 oligomers with all the nickel precatalysts producing a small amount of C_8 oligomers while the palladium precatalyst only produced C_4 and C_8 oligomers. The palladium precatalyst **C1** produced highly branched oligomers while the nickel precatalysts, **C1**, **C3** and **C5** produced oligomers with significantly less branching. The pressure and Al:Ni optimization studies were carried out using **C3** as the precatalyst. When the pressure was increased the activity increased (maximum 2860 kg-oligomer mol.M^{-1}.h^{-1}) and branching decreased with the optimum pressure being 30 bar. When the Al:Ni was varied it was found that increasing the ratio to 250 led to the highest activity (1360 kg-oligomer mol.M^{-1}.h^{-1}) with slightly decreased branching.

5.2 Recommendations

Palladium (II) and nickel (II) iminopyridyl complexes were synthesized and characterized by various analytical and spectroscopic techniques. Some of the complexes were tested for ethylene oligomerization reactions, and showed high activity to become ethylene oligomerization reaction catalysts. However, we recommend the following future work on this project:

1. Test the remaining two bimetallic iminopyridyl complexes as well as the monometallic analogues of **C1-C6** for ethylene oligomerization to study the cooperative effect

2. Synthesize bimetallic nickel and palladium complexes from alkyl linked iminopyridyl ligands **L3-L5**

3. Single X-ray diffraction studies should be done on the nickel and palladium complexes to confirm the coordination mode of the ligands to the metal to support the spectroscopic analysis results

4. Investigate the catalytic activity of heterobimetallic nickel(II) and palladium(II) complexes for ethylene oligomerization/polymerization

5. The complexes should also be investigated for Heck coupling

Appendix

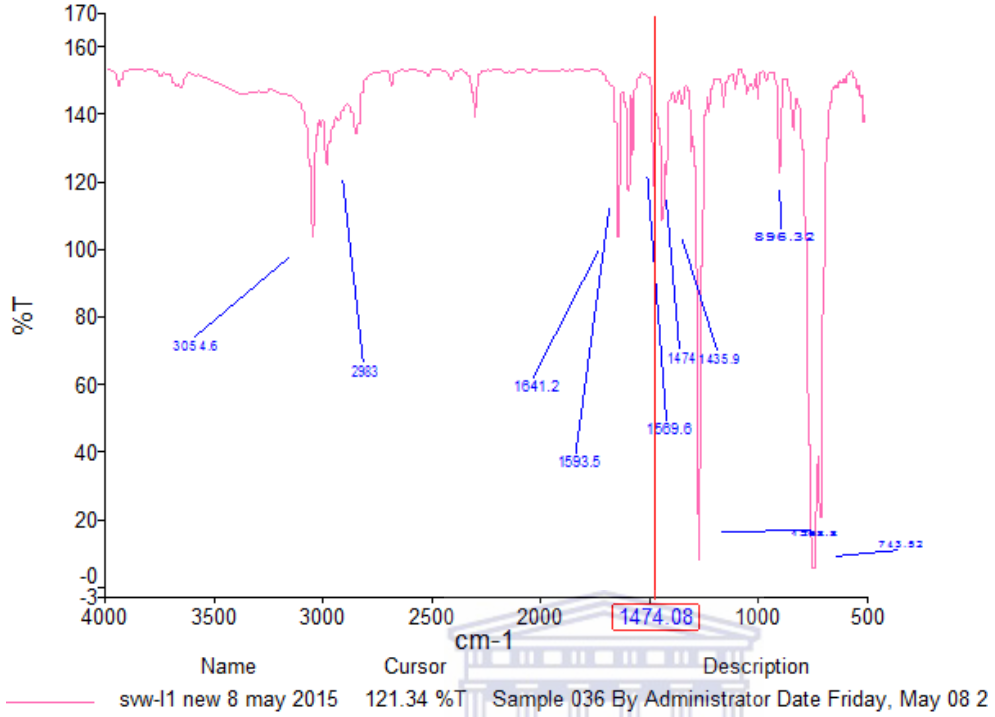

FTIR for **L1**

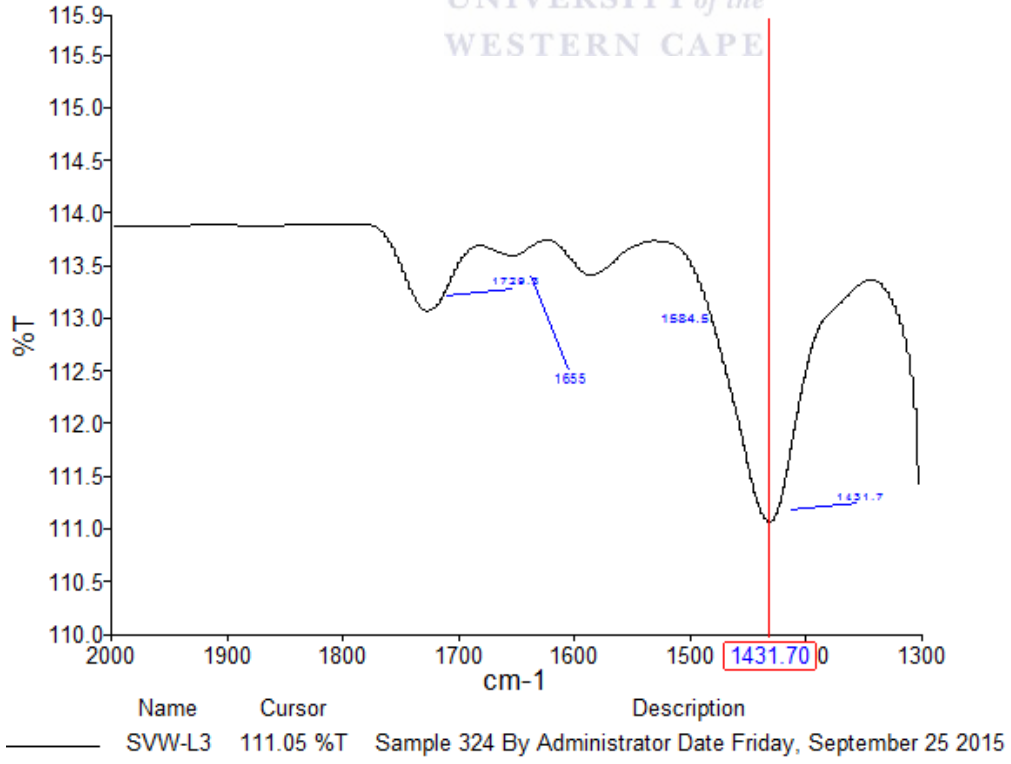

FTIR for **L3**

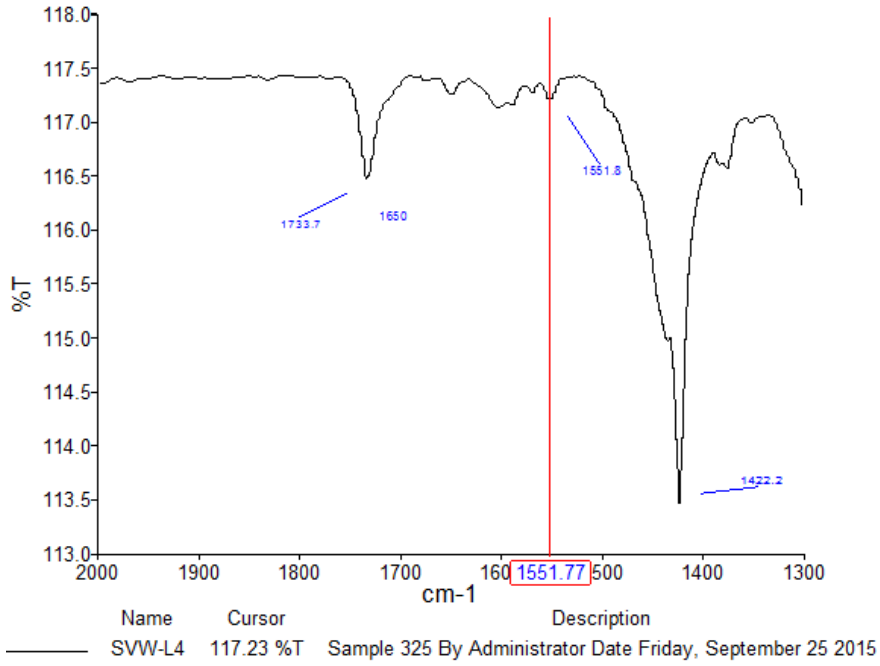

FTIR for **L4**

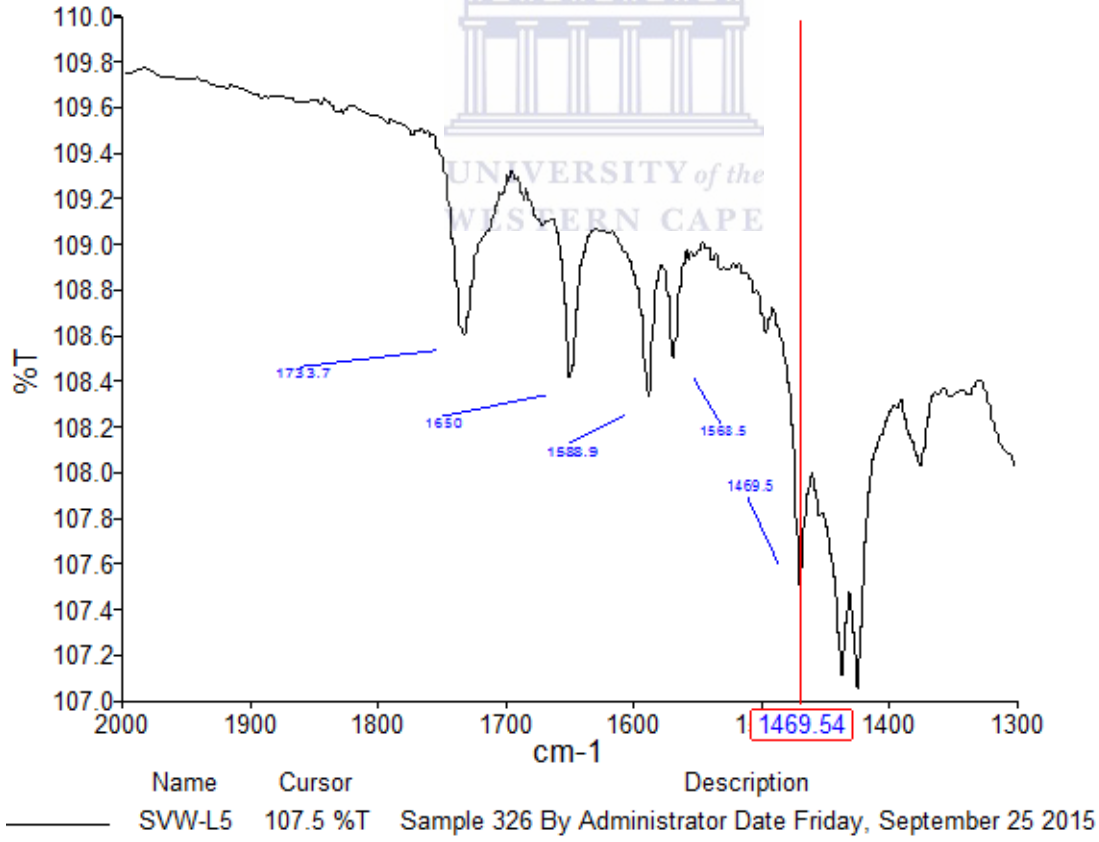

FTIR for **L5**

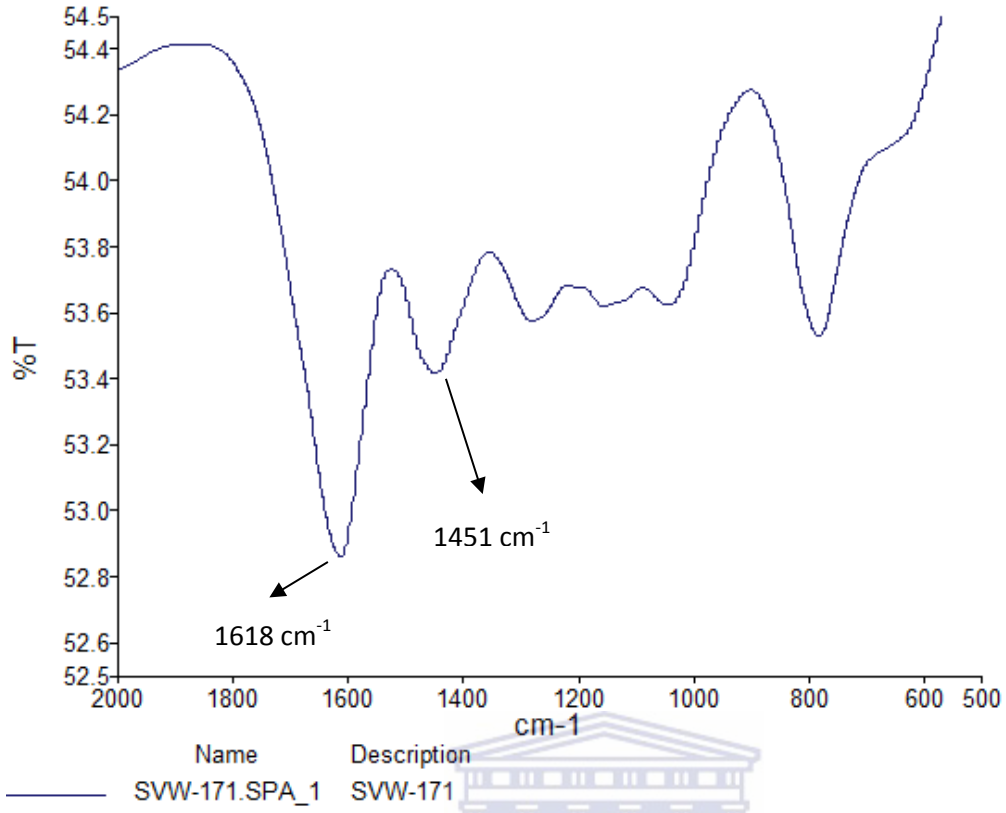

FTIR for **C1**

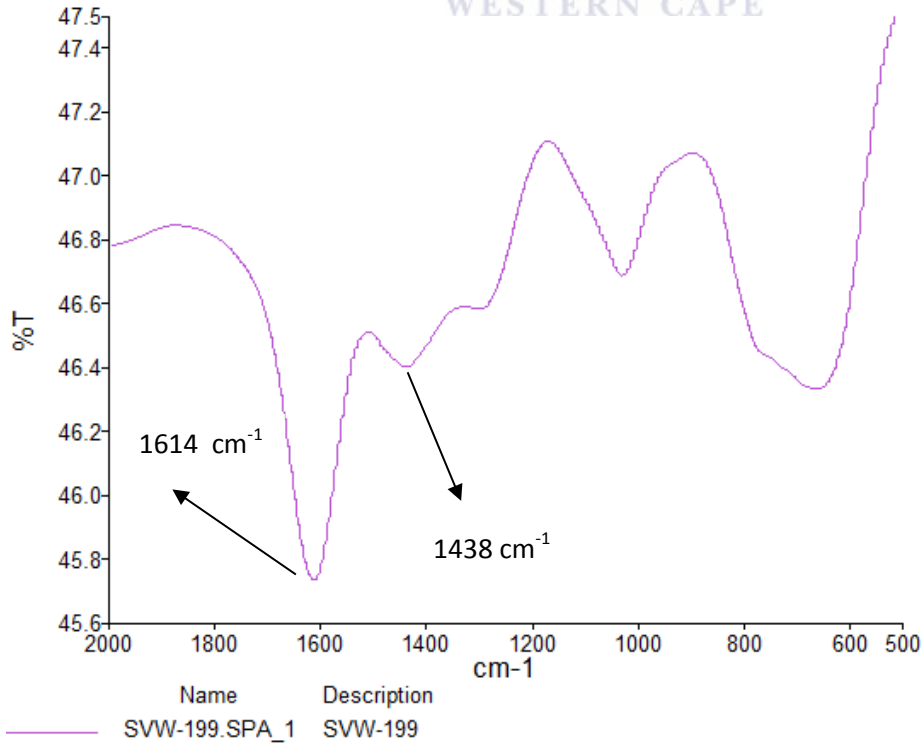

FTIR for **C3**

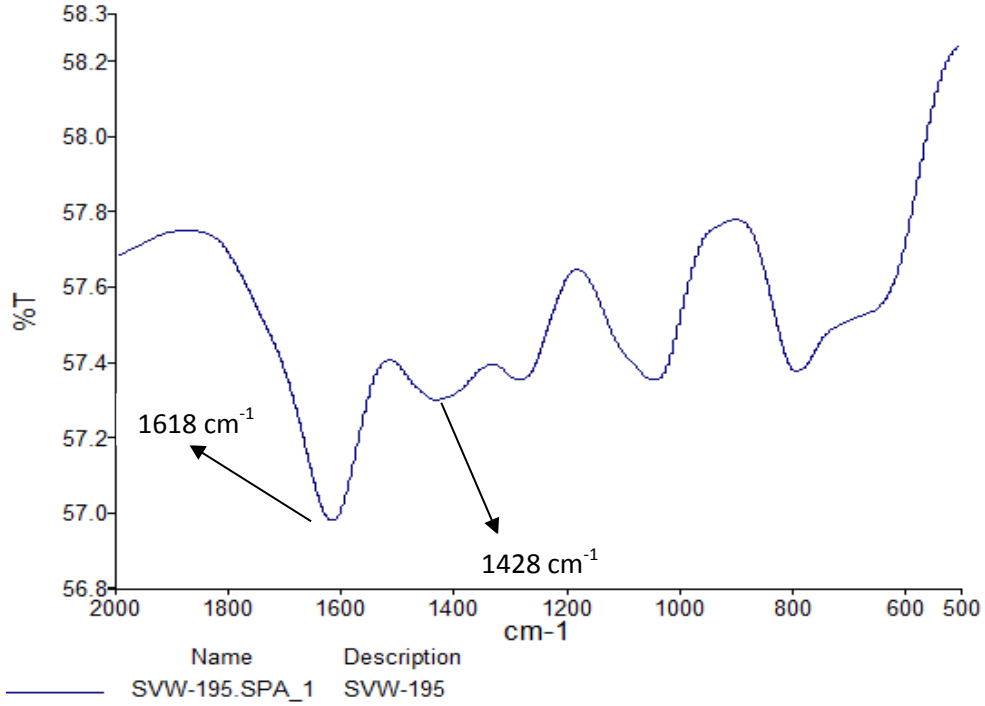

FTIR for **C5**

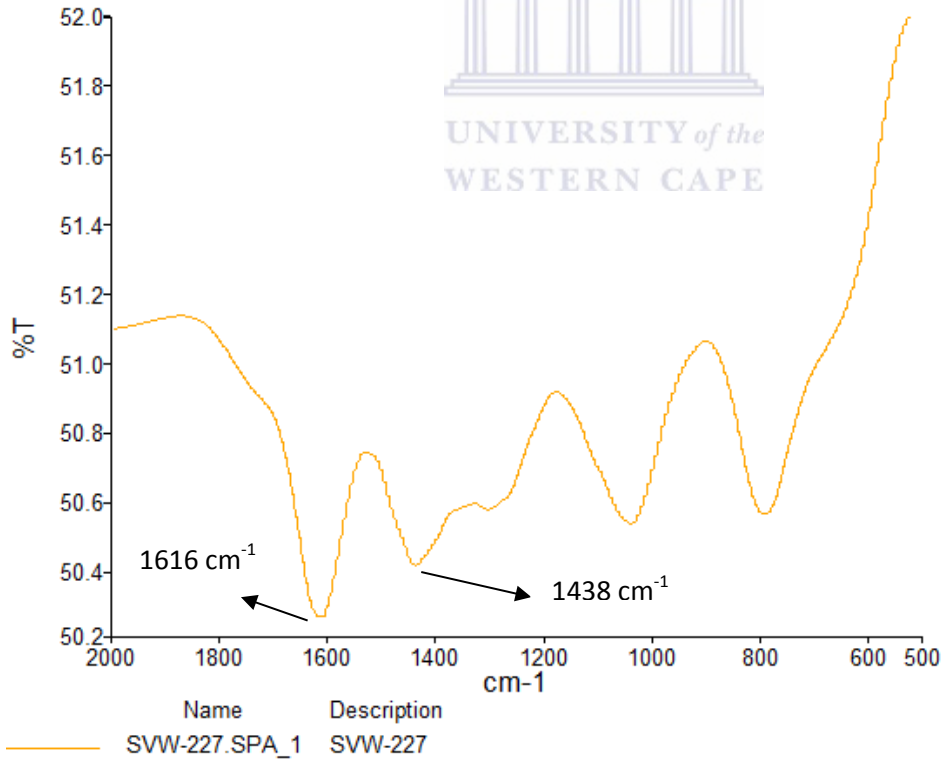

FTIR for **C6**

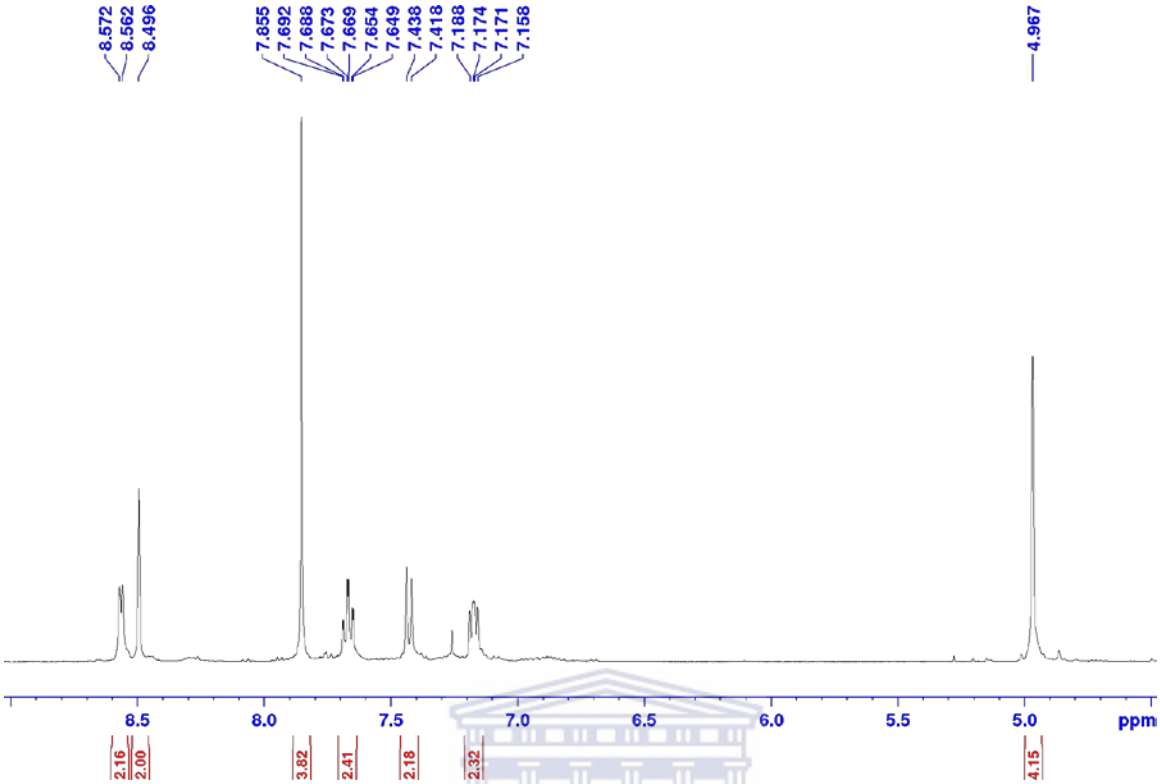

^{1}H NMR for **L1**

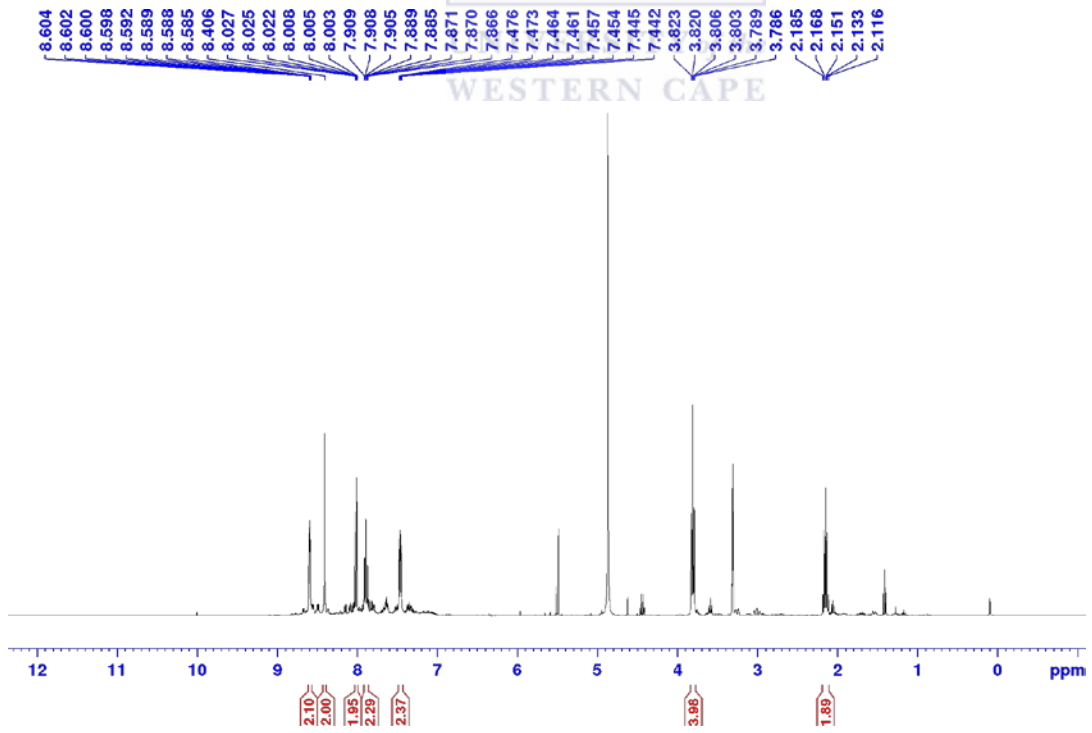

^{1}H NMR for **L3**

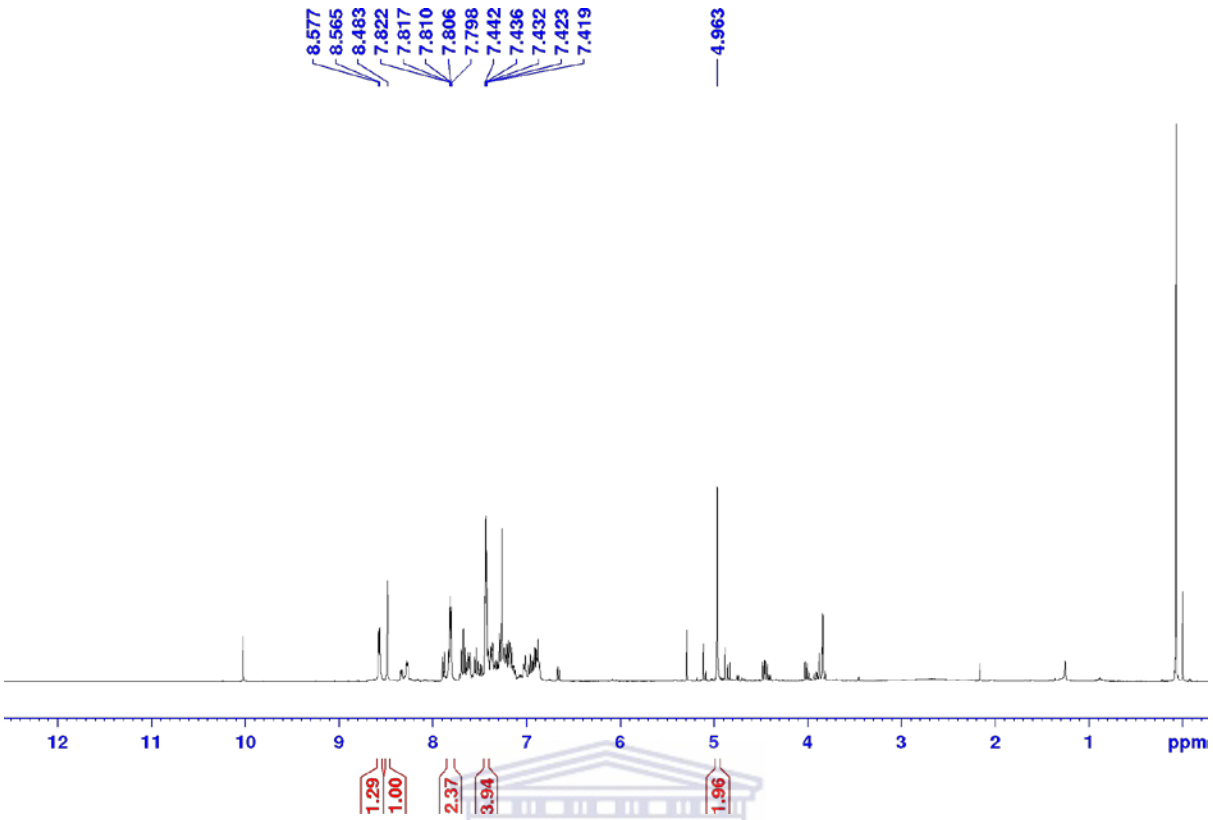

^{1}H NMR for **L5**

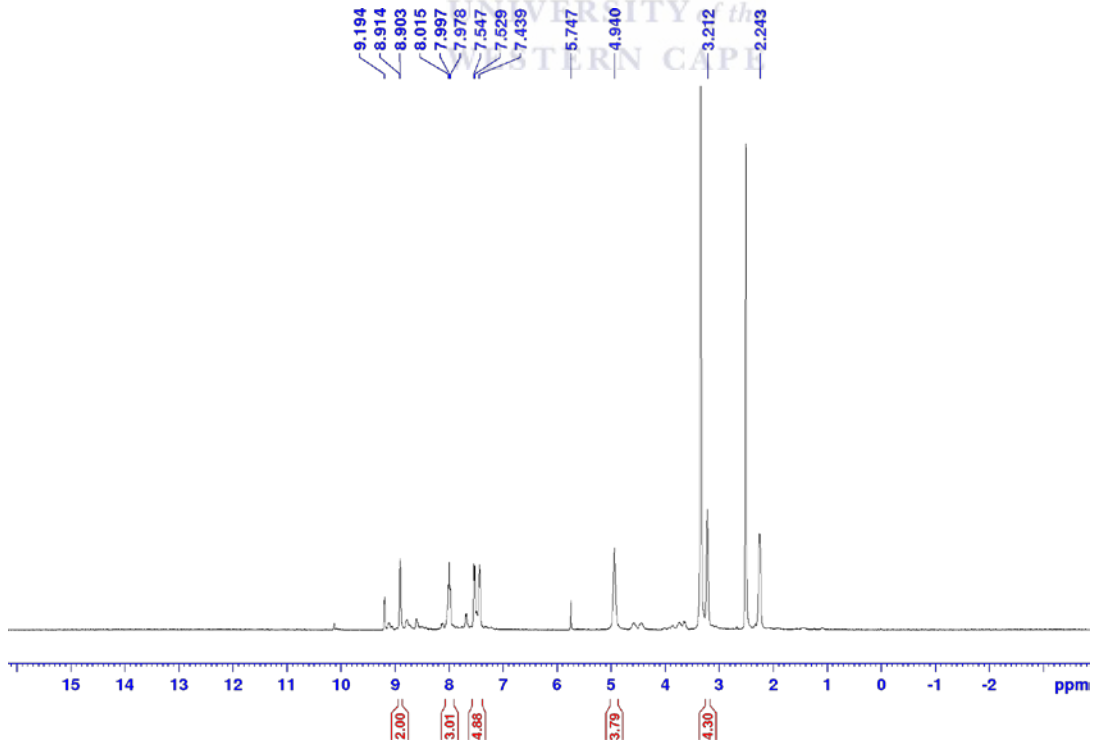

^{1}H NMR for **C2**

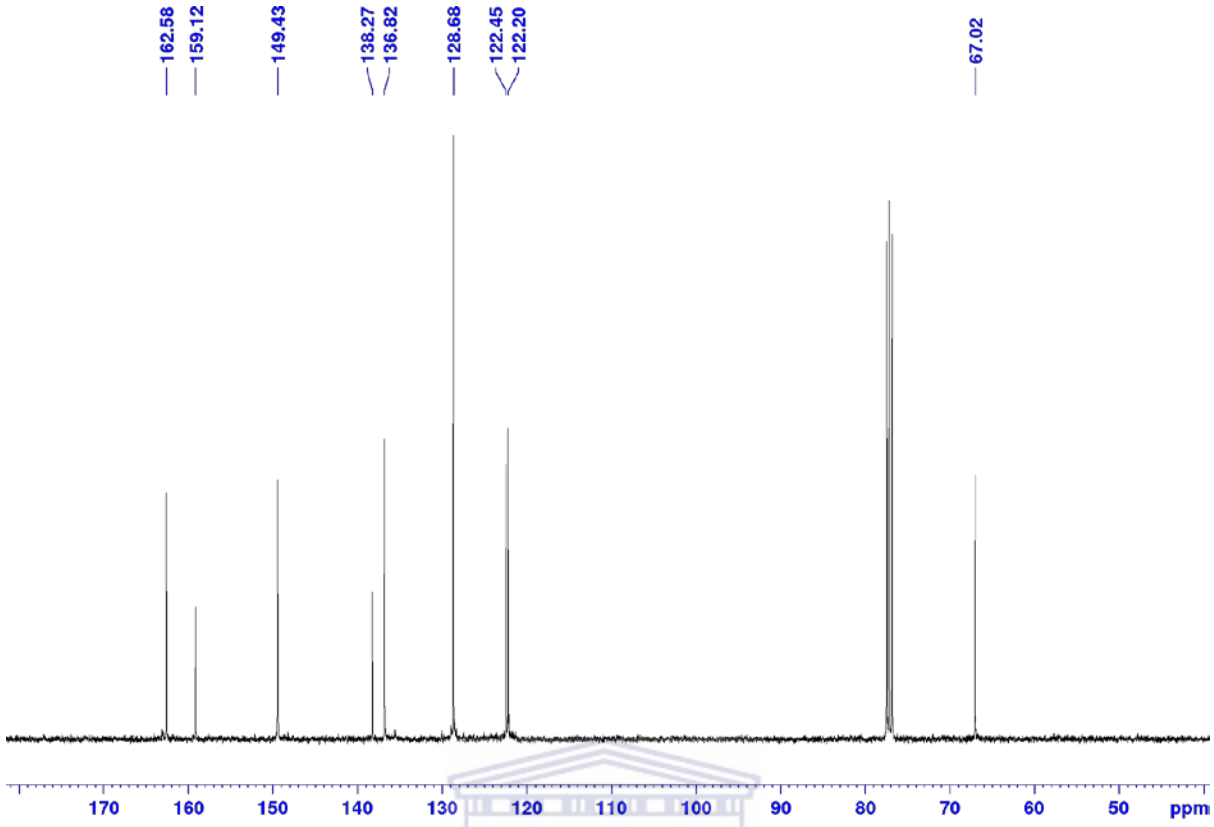

^{13}C NMR for **L1**

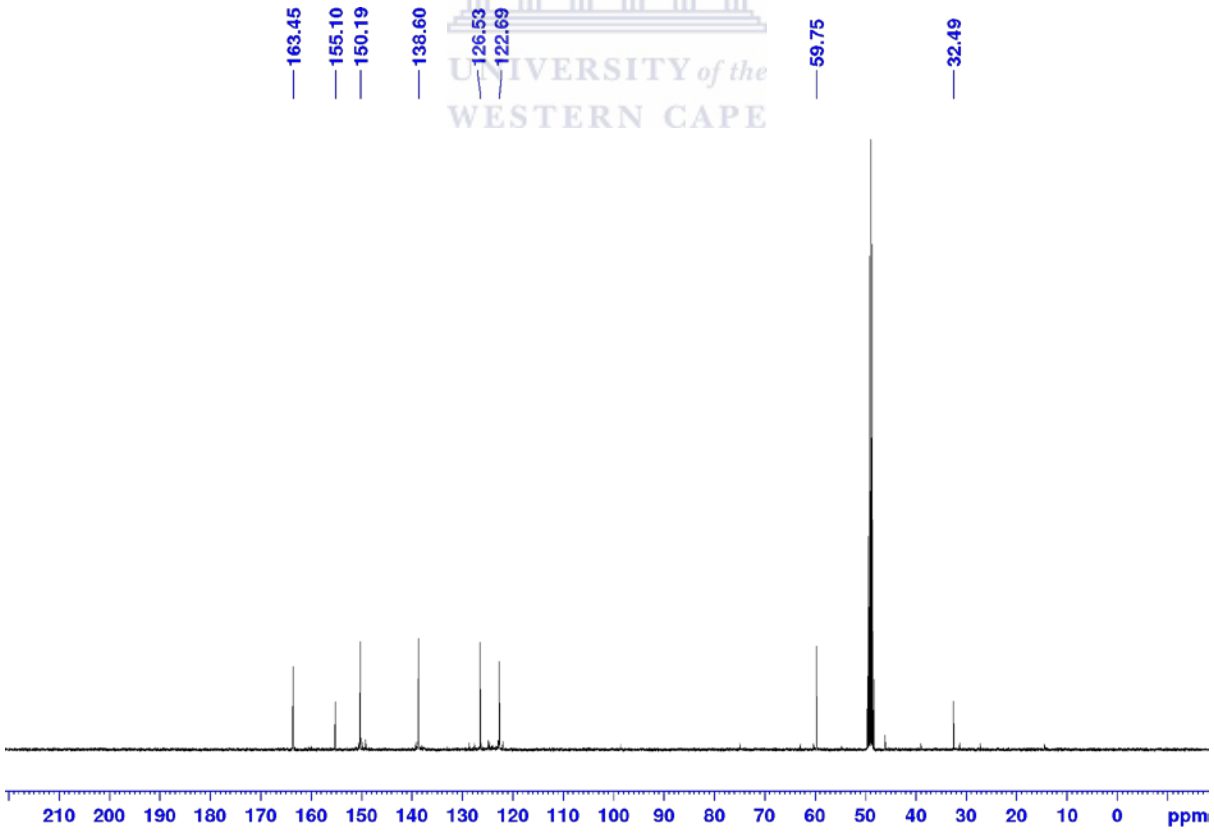

^{13}C NMR for **L3**

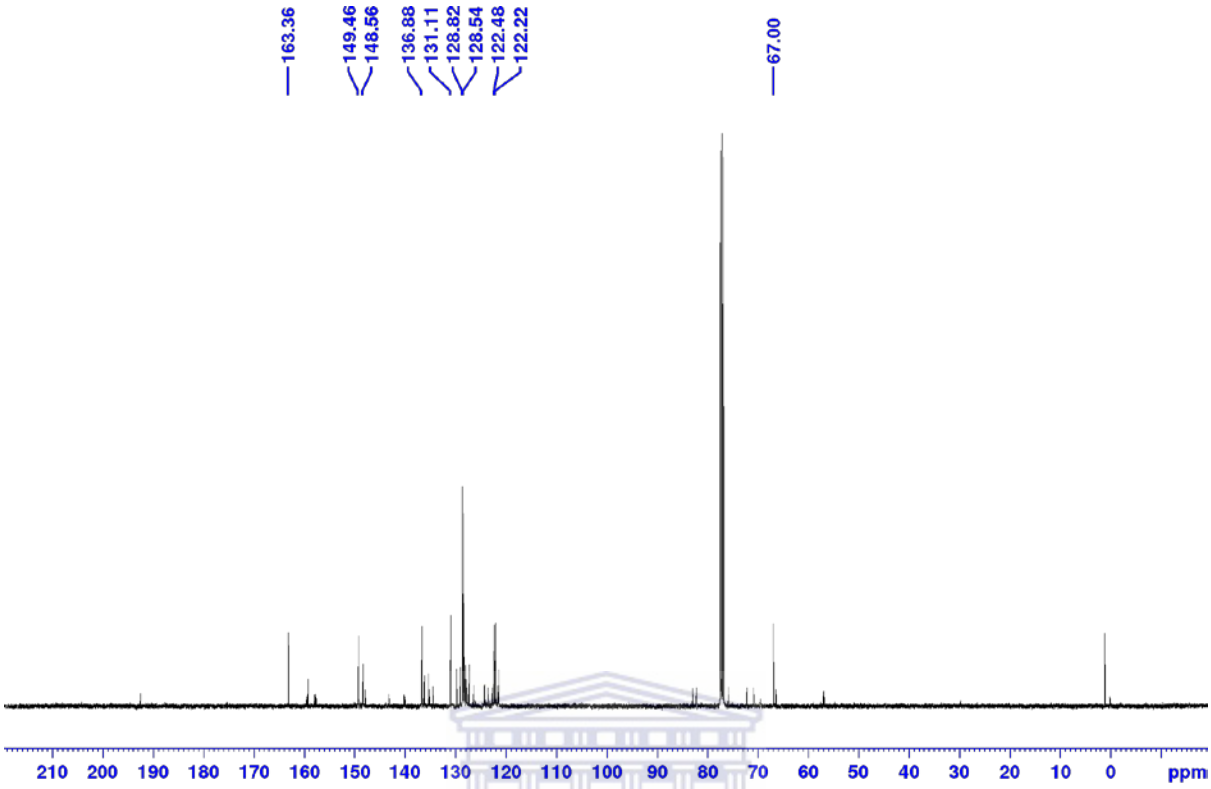

^{13}C NMR for **L5**

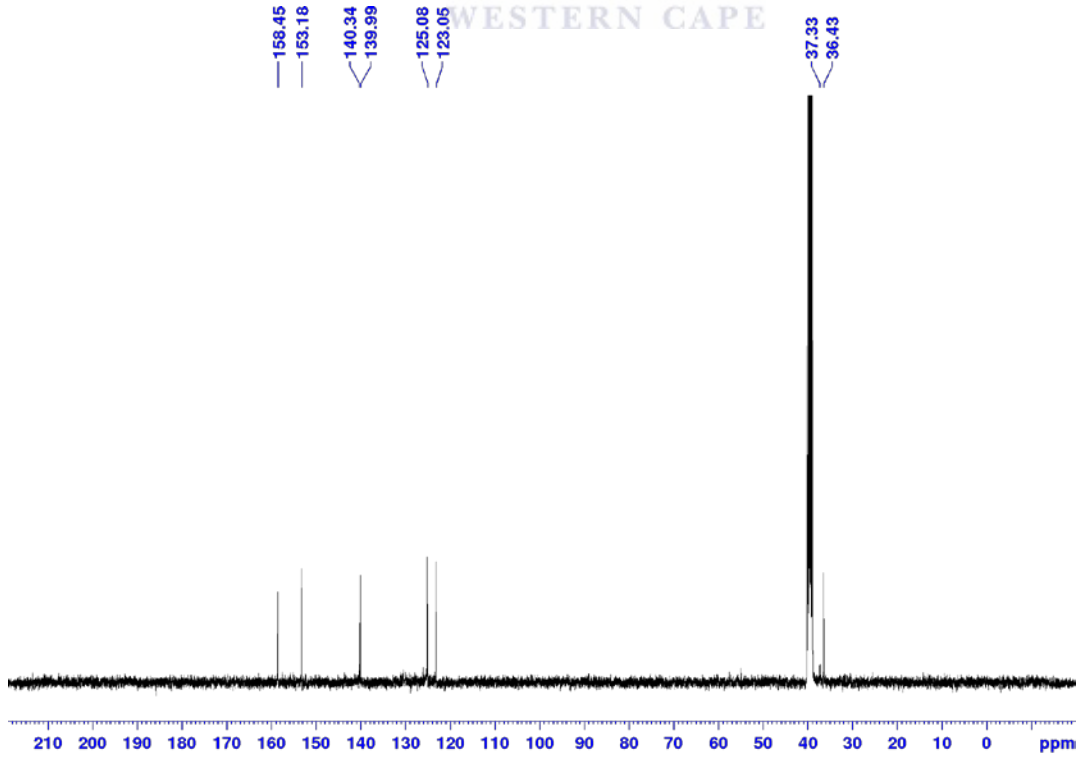

^{13}C NMR for **C2**

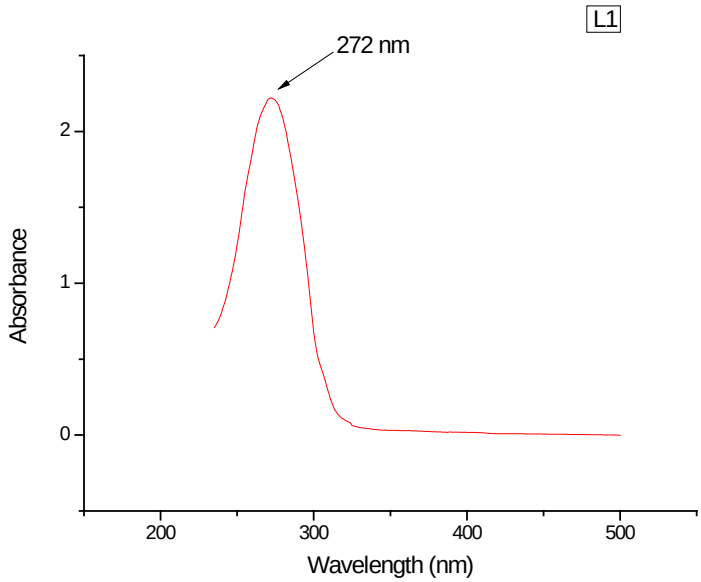

UV-Vis for **L1**

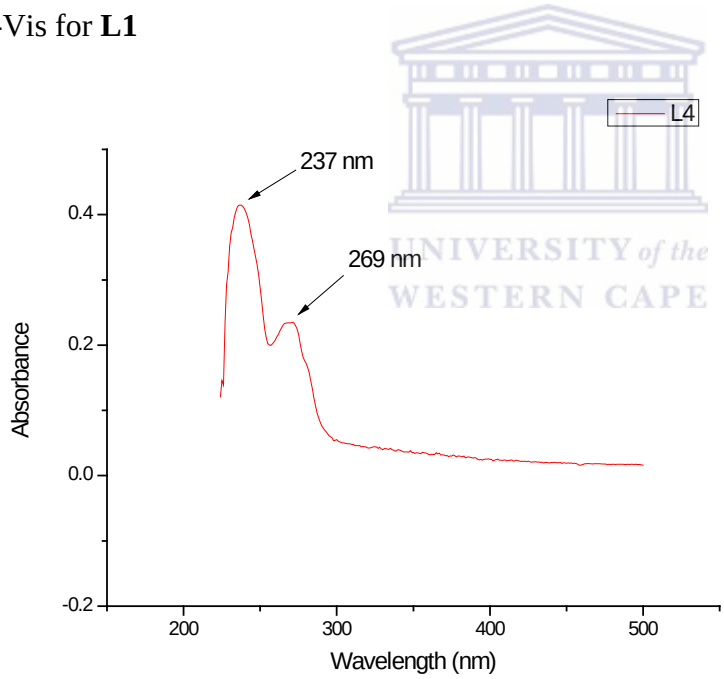

UV-Vis for **L4**

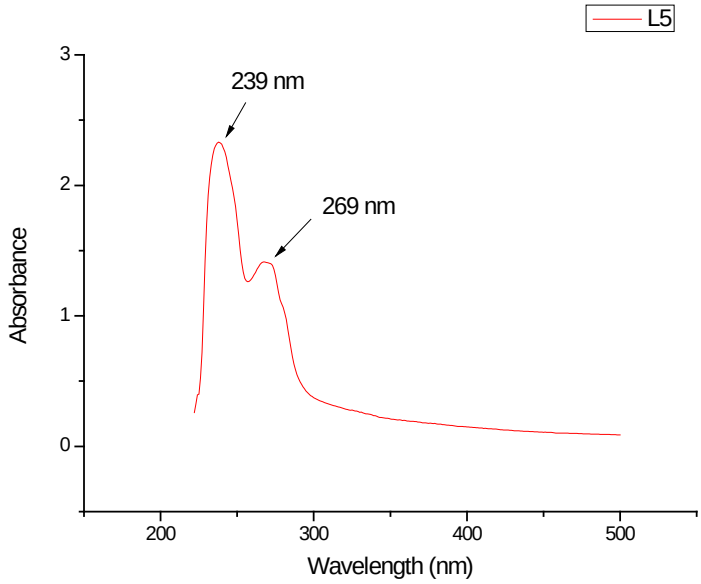

UV-Vis for **L5**

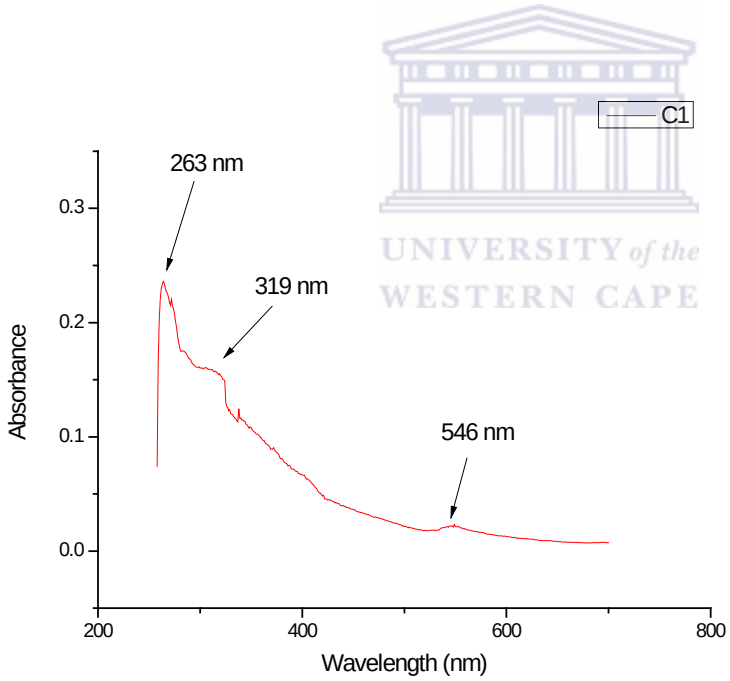

UV-Vis for **C1**

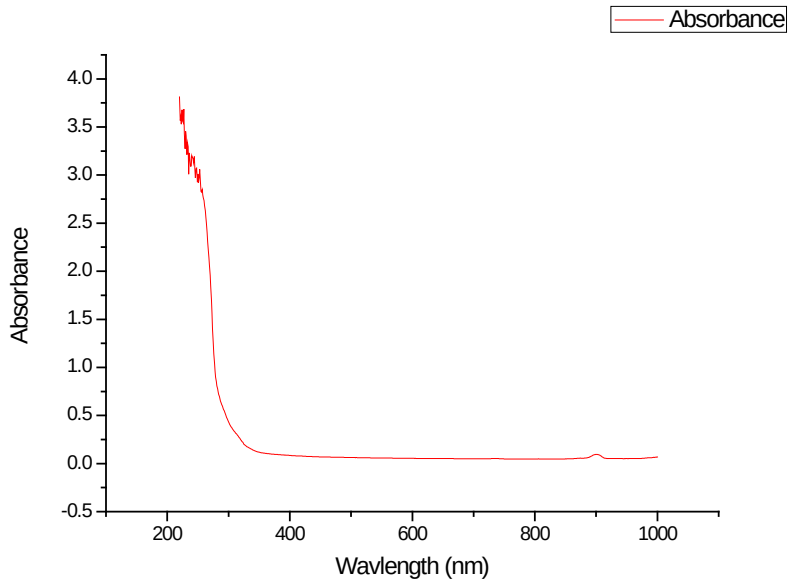

UV-Vis for **C3**

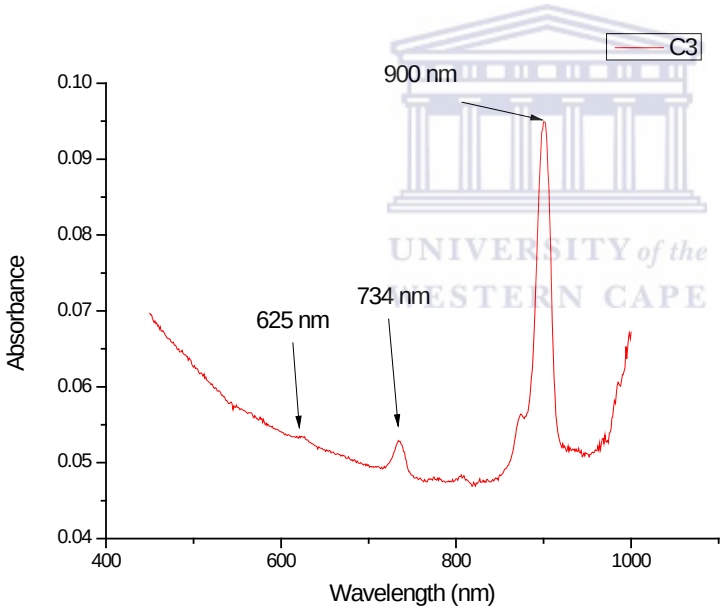

UV-Vis for **C3** enlarged

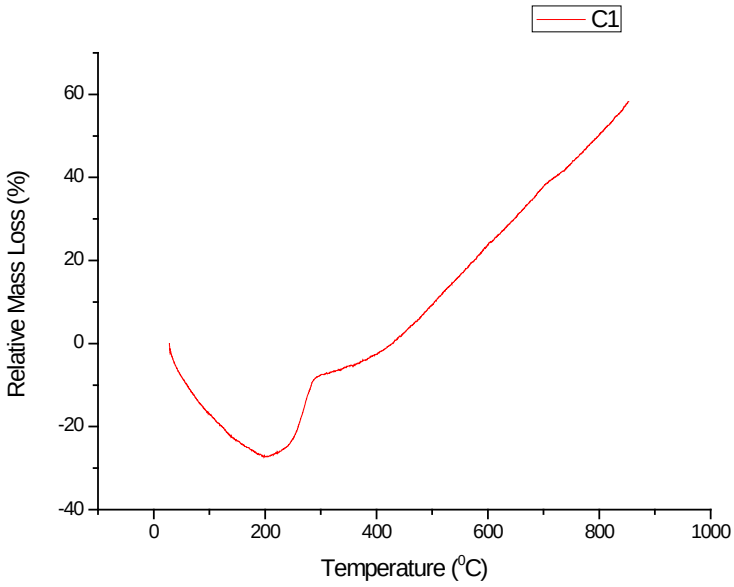

TGA for **C1**

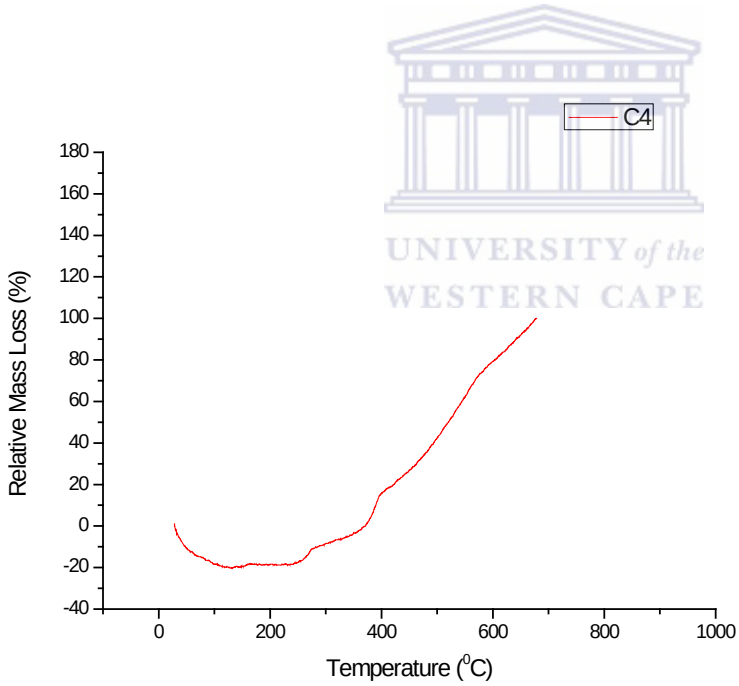

TGA for **C4**

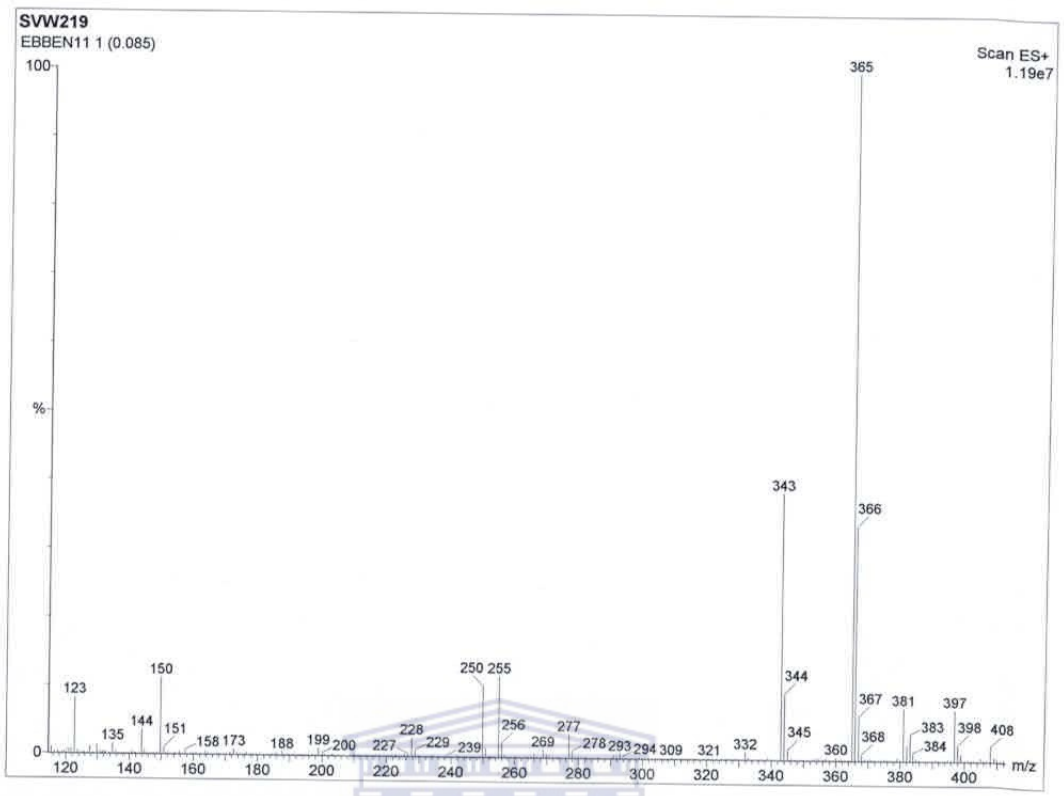

ESI-MS for **L2**

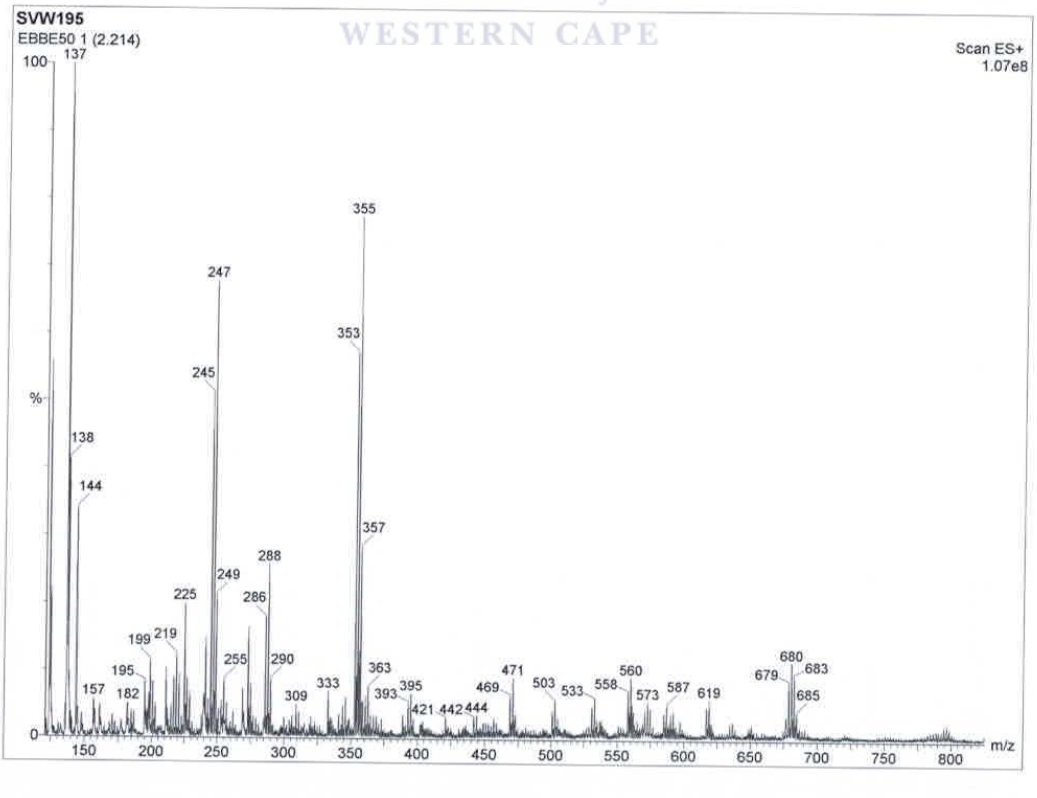

ESI-MS for **C5**

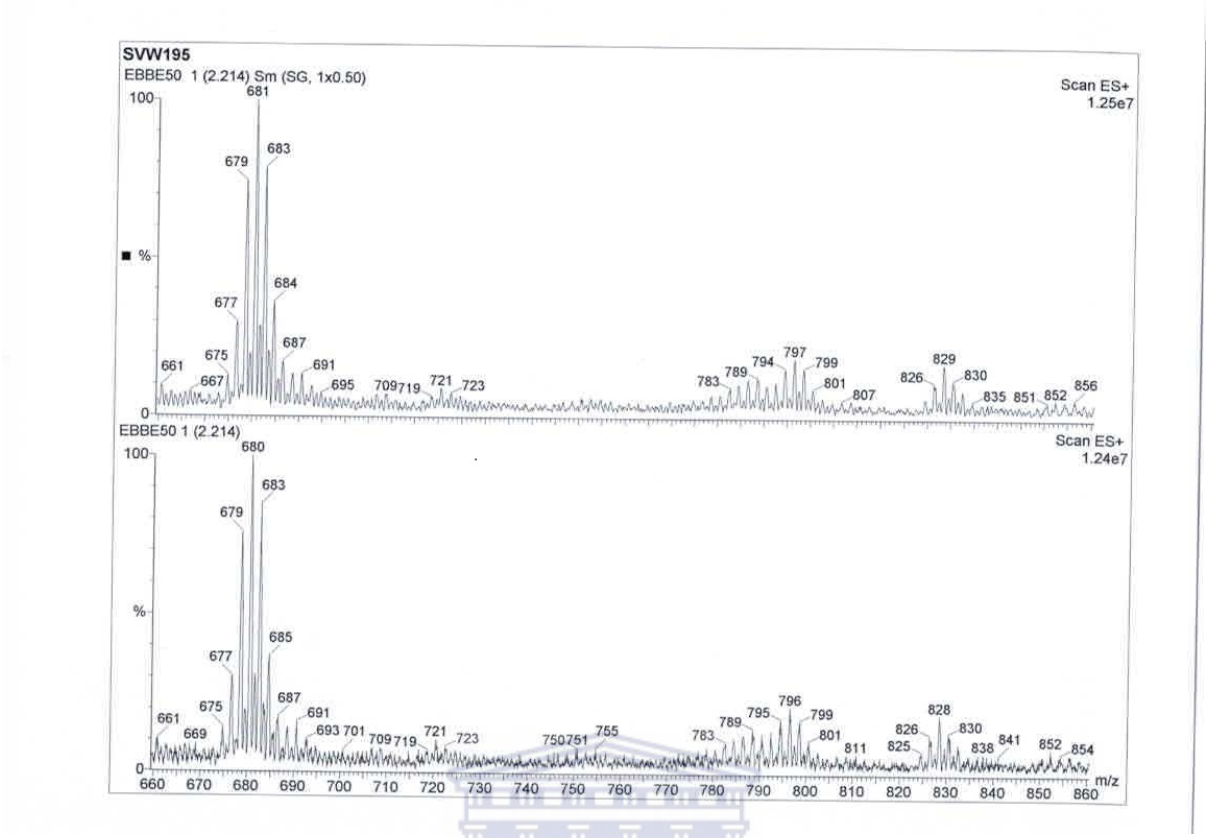

ESI-MS for **C5** enlarged

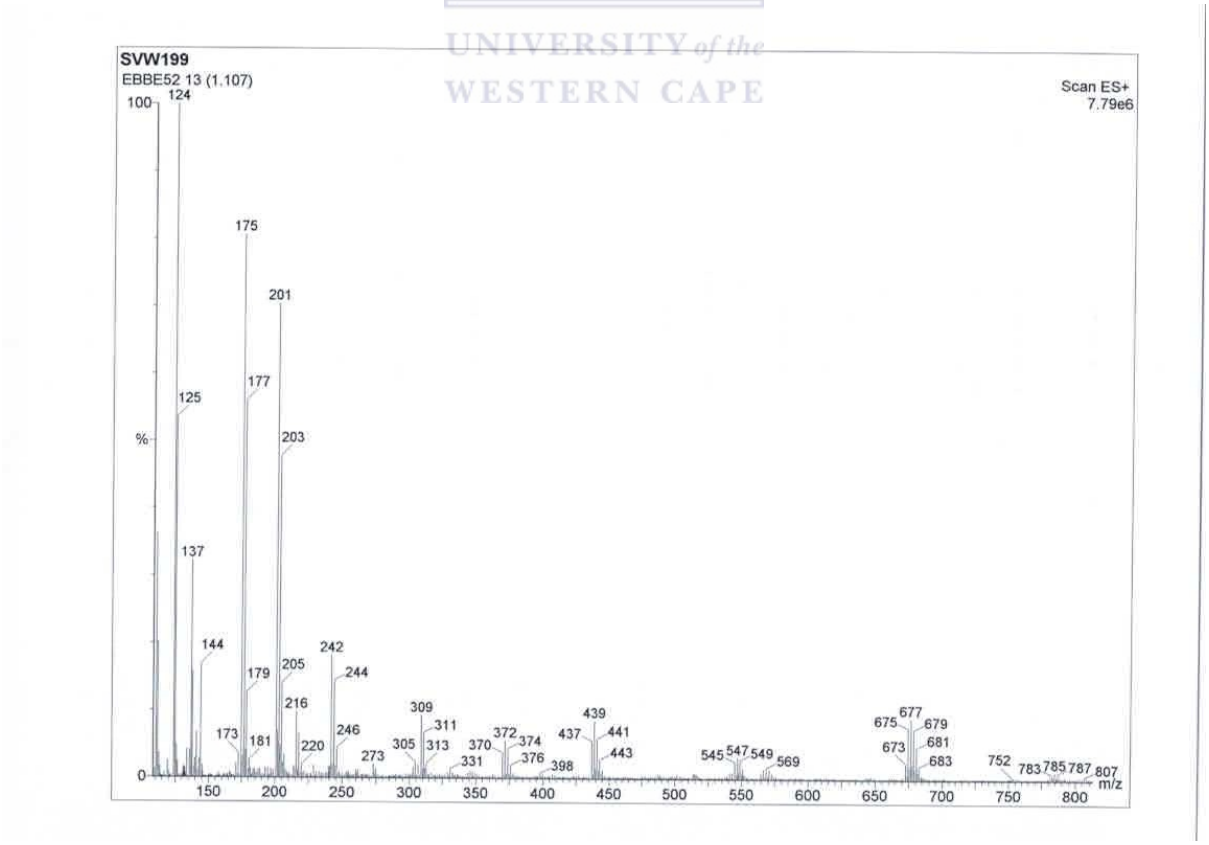

ESI-MS for **C3**

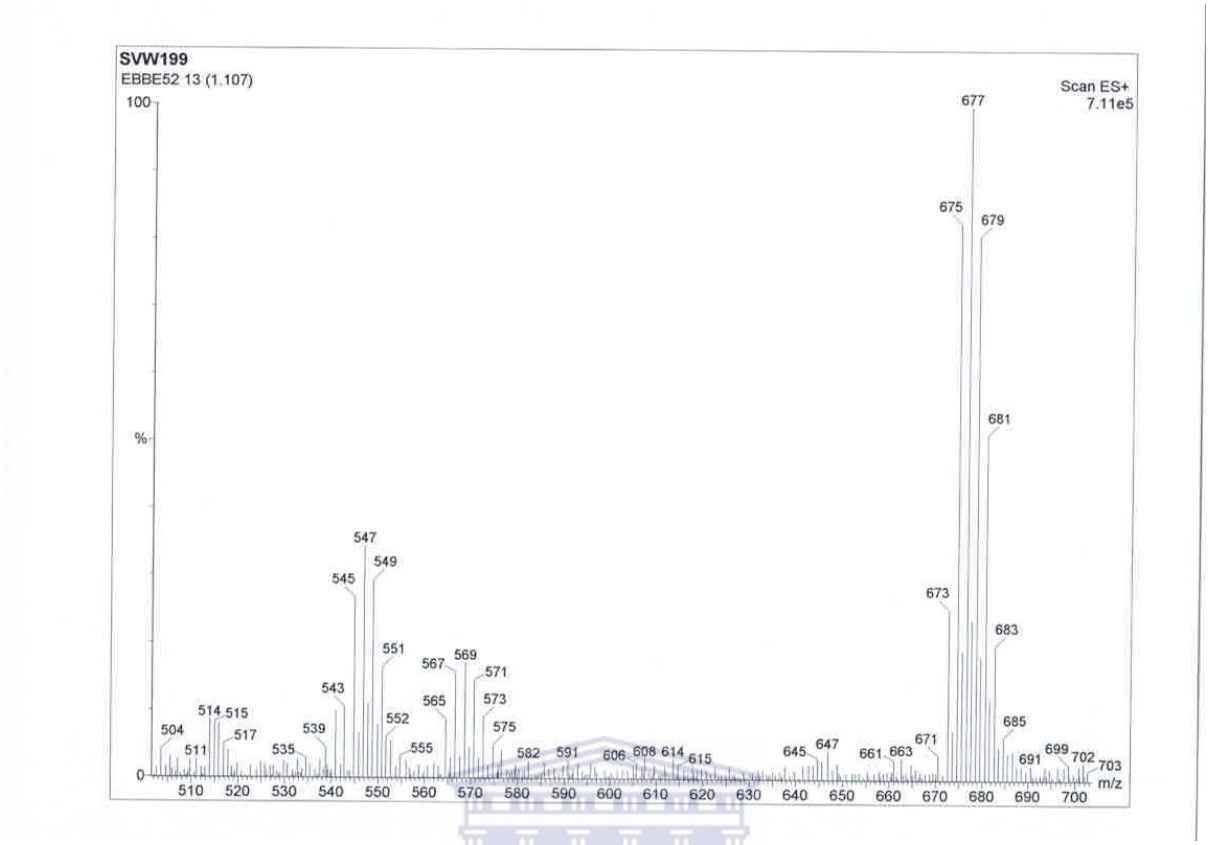

ESI-MS for **C3** enlarged

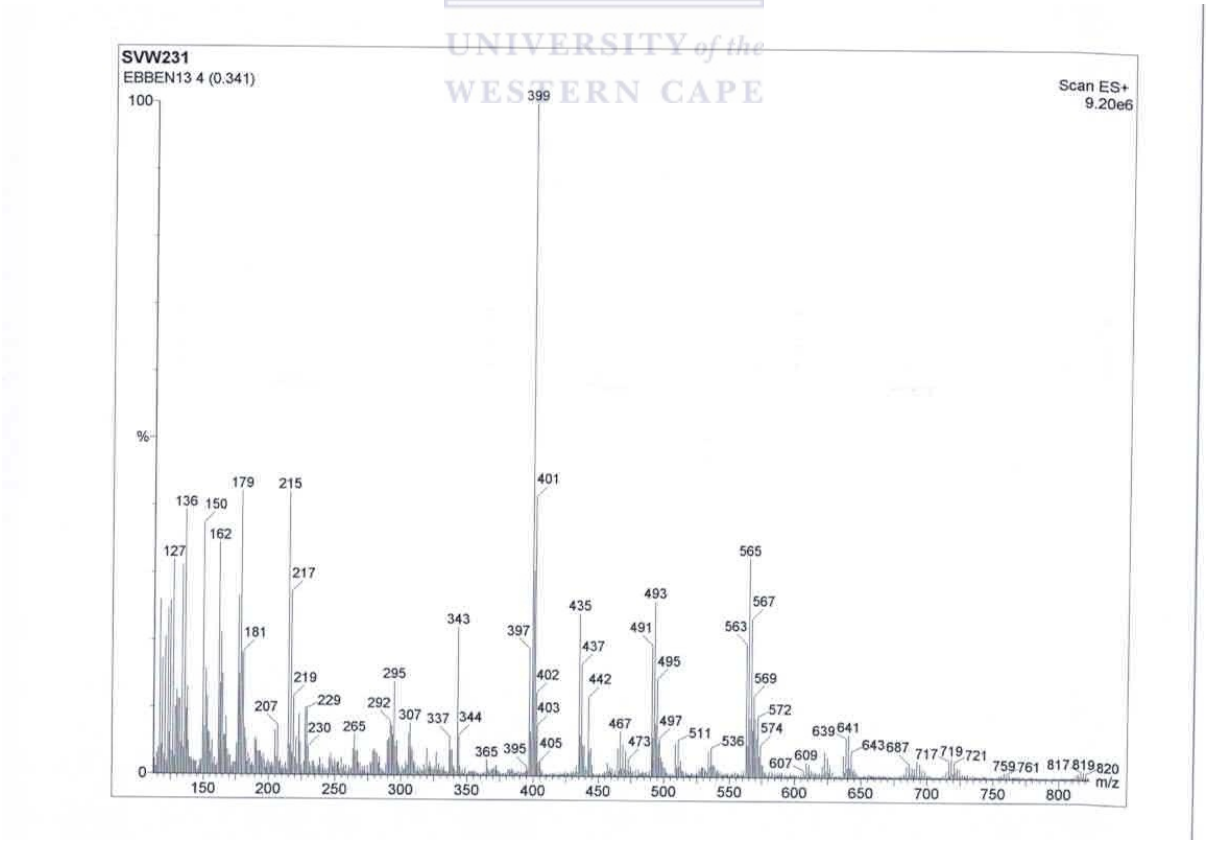

ESI-MS for **C4**

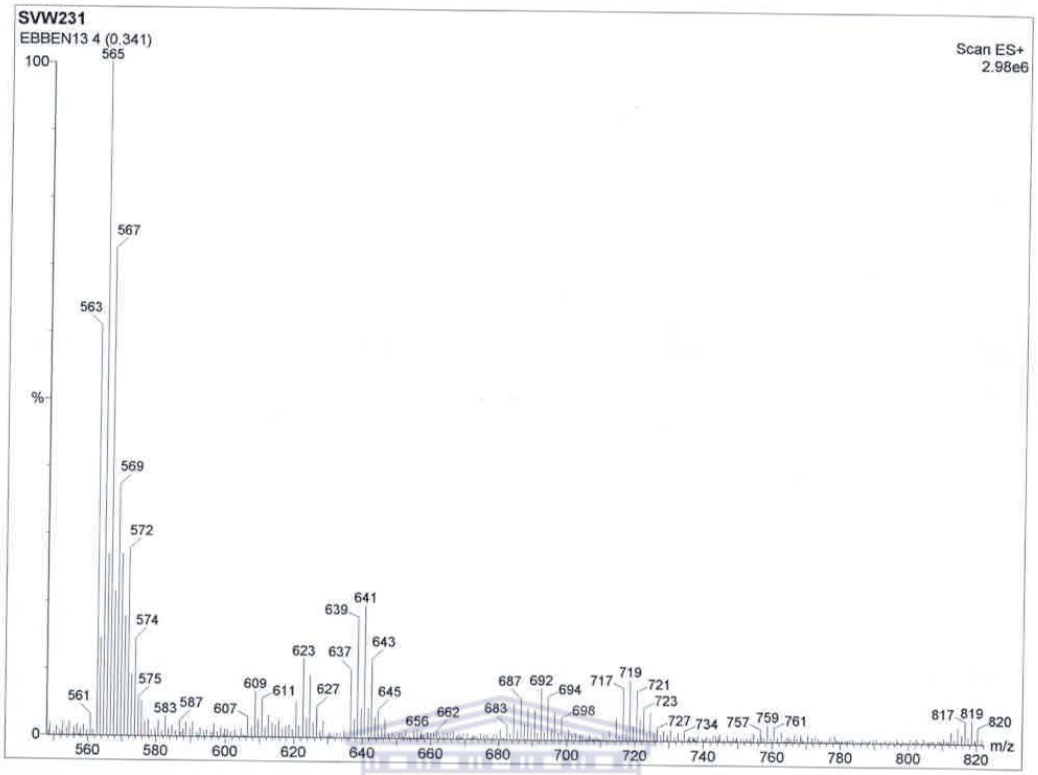

ESI-MS for **C4** enlarged

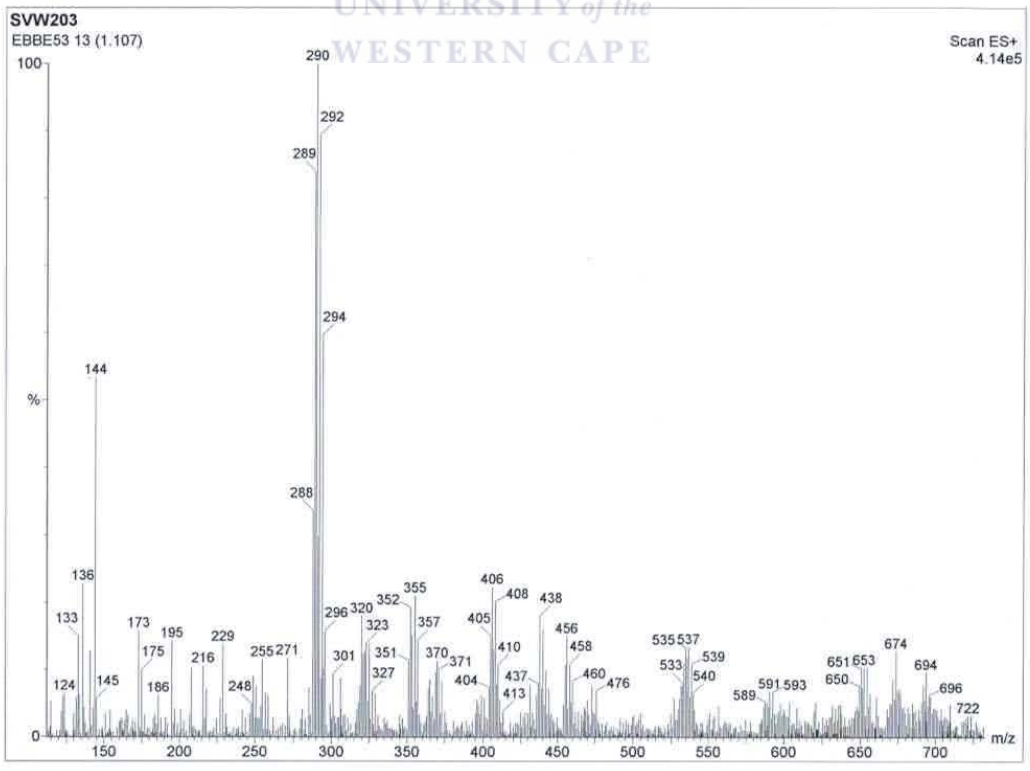

ESI-MS for **C1**

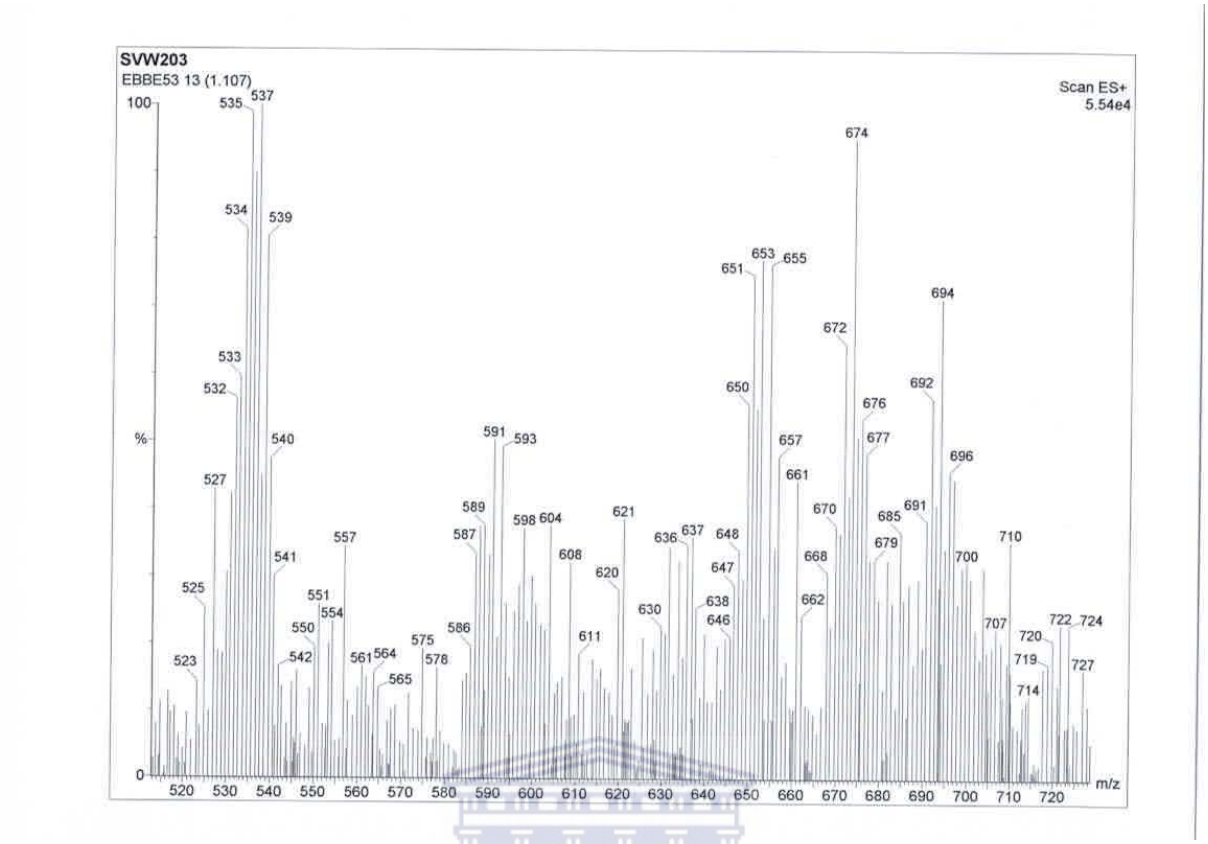

ESI-MS for **C1** enlarged

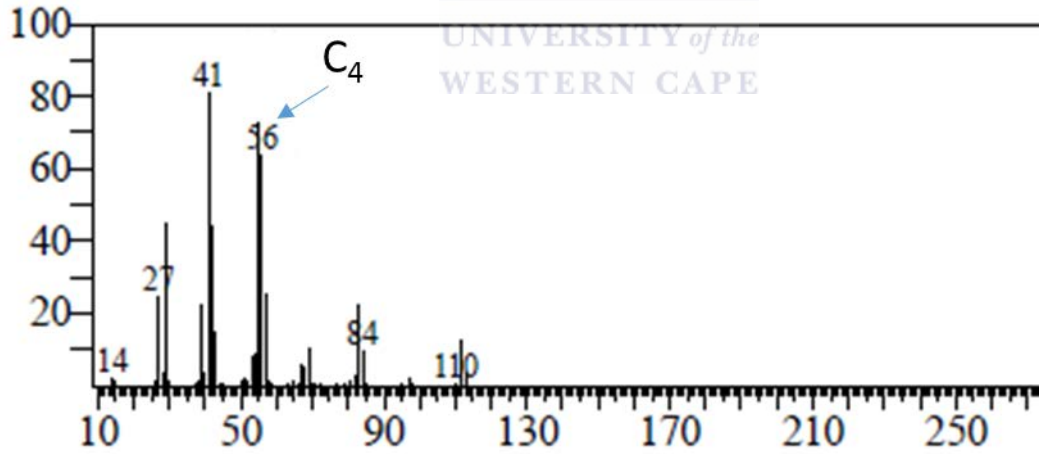

Typical GC-MS spectrum of the product formed using catalyst **3** at 30 °C and 20 bar for 1 h confirming the formation of butene.

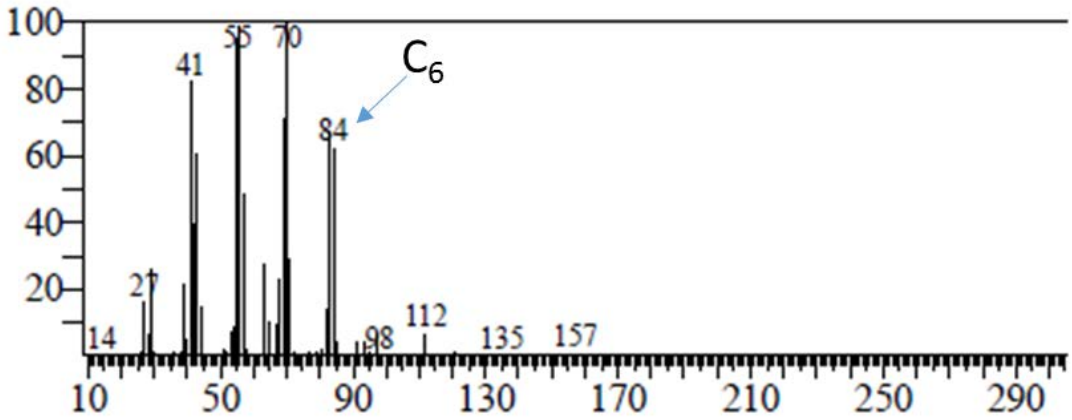

Typical GC-MS spectrum of the product formed using catalyst **5** at 30 °C and 20 bar for 1 h confirming the formation of hexene.